THESIS

ON

AN EXPERIMENTAL INVESTIGATION ON WELDING ASPECTS OF STAINLESS STEEL (SS202 & SS304) DURING GTAW

Submitted in partial fulfillment of the requirement for the award of degree of

MASTER OF ENGINEERING

IN

PRODUCTION AND INDUSTRIAL ENGINEERING

Submitted by

NARENDER BANSAL
ROLL NO. 820982002

Under the guidance of

ANIRBAN BHATTACHARYA
Assistant Professor
Mechanical Engineering Department
Thapar University, Patiala

DEPARTMENT OF MECHANICAL ENGINEERING

THAPAR UNIVERSITY

PATIALA – 147004, INDIA

DECEMBER – 2012

DECLARATION

I hereby declare that work done in this Thesis Report entitled, "**AN EXPERIMENTAL INVESTIGATION ON WELDING ASPECTS OF STAINLESS STEEL (SS202 & SS304) DURING GTAW**" submitted towards partial fulfillment towards partial fulfillment of requirement for the award of **Master of Engineering** degree in **Production and Industrial Engineering** in **Mechanical Engineering Department** of **Thapar University, Patiala,** is an authentic record of work carried out by me under the supervision and guidance of **ANIRBAN BHATTACHARYA, Assistant Professor** of **Mechanical Engineering Department, Thapar University, Patiala.**

The matter embodied in this report has not been submitted in part or full to any other university or institute for the award of any degree.

Narender

NARENDER BANSAL

This is to certify that above declaration made by the student concerned is correct to the best of my knowledge and belief.

07/01/2013

ANIRBAN BHATTACHARYA

Assistant Professor, M.E.D.,

Thapar University, Patiala

Countersigned by:

DR. AJAY BATISH

Professor & Head, M.E.D.,

Thapar University, Patiala

DR. S.K. MOHAPATRA

Senior Professor & D.O.A.A.,

Thapar University, Patiala

ACKNOWLEDGEMENT

I am highly grateful to the authorities of Thapar University, Patiala for providing this opportunity to carry out the thesis work.

I express my sincere gratitude and respects from bottom of my heart to my guide **Anirban Bhattacharya, Assistant Professor, Mechanical Engineering Department, Thapar University, Patiala,** for his keen interest, valuable guidance, strong motivation and constant encouragement during the course of the work. I thank him for his great patience, constructive criticism and myriad useful suggestions apart from invaluable guidance to me.

I thank our head of department **Dr. Ajay Batish**, whose excellent leadership and administration made this research project very convenient in term of required stuff and nice working conditions. I am extremely thankful to member of distinguished faculty.

I am also thankful to authorities of **Chanderpur Works Pvt. Ltd. (CPW), Yamunanagar** and **Oriental Engineering Works Pvt. Ltd. (OEW), Yamunanagar** for providing me the raw material for my research work.

I express my sincere thanks to principal **Dr. Kuldeep Singh** and management of **Haryana Engineering College, Jagadhri** for allowing me to use the infrastructure of the college to carry out my research work.

A very special thanks and regards to non-teaching staff members **Mr. M. Suri, Mr. Surender, Mr. Rath, Mr. Roshan, Mr. Rajinder, Mr. Narender, Mr. Sukhbir, Mr. Ram Naval Yadav** (Biotech deptt.) of Thapar University, Patiala and **Mr. Hism Singh, Mr. Mela Singh and Mr. Pawan Kumar Rana** of H.E.C., Jagadhri for their help during this period of research work.

A special thanks to my friend **Mr. Gianender Kajal** for his various help and cooperation.

Narender

NARENDER BANSAL
ROLL NUMBER – 820982002

ABSTRACT

The aim of present study was to investigate the welding aspects like weld bead geometry, bulk hardness, surface cracks using dye penetrant test, impact strength, microhardness, joint quality and chemical composition of stainless steel (SS202 & SS304) during GTAW using the three levels of welding current, shielding gas, gas flow rate and grove angle and to optimize the process following Taguchi experimental design. Bead geometry of the welded specimens was measured and bead width was mainly dependent on welding current and nature of shielding gas used. Bead height for SS202 was dependent on shielding gas and gas flow rate whereas the same for SS304 was depending on gas flow rate and grove angle. Rockwell hardness test showed that there was no significant variation in hardness value in weld metal and heat affected zone (HAZ) in comparison to base materials for both grades of steel. Dye penetrant test showed that welding was of very good quality and there were negligible amount of defects at corners. Charpy impact test results for SS202 steel showed that toughness at room temperature mainly depends on the value of current used and shielding gas chosen. Maximum value of toughness (71.1225 Joules) was obtained in the welded joint of parameters 180 A, Ar, 12 l/min. & 90^0. For SS304 maximum value of toughness is 93.195 Joule and was observed when welded with parameters 180 A, Ar+He mixture, 9 l/min. & 75^0. Toughness is higher for 180 A and for shielding gas Ar and also at 9 l/min. At -20 ^{0}C Charpy test showed that SS202 is having negligible strength making it unsuitable for use in colder places and that for SS304 showed that it mainly depends on the welding current followed by gas flow rate. Highest value of toughness (63.765 Joule) at this temperature was when welded with 220 A, He gas, 9 l/min. & 90^0. Toughness value is maximum on and after 180 A of current and also highest for gas flow rate of 9 l/min. Microhardness test showed that for SS202 the value of HVN was mainly dependent on welding current and grove angle and it was observed that HVN is mainly influenced by the value of welding current for SS304 grade. Joint quality result showed that for both the materials in welded region there were no major flaws and inclusion except a crack observed in a particular sample of SS202 steel. Chemical composition analysis showed that there was a decrease in the value of chromium for both grades of steel in the welded region which may be because of formation of any compound in the welded region.

TABLE OF CONTENTS

LIST OF TABLES

LIST OF FIGURES

ABBREVIATIONS

S. N.	ABBREVIATION	DESCRIPTION
1	GTAW	Gas tungsten arc welding
2	TIG	Tungsten inert gas welding
3	GMAW	Gas metal arc welding
4	SAW	Submerged arc welding
5	ANOVA	Analysis of variance
6	HVN	Vickers hardness number
7	HRC	Rockwell hardness number (C-Scale)
8	S/N	Signal to noise
9	DPT	Dye penetrant test
10	AWS	American welding society
11	ISO	International organization for standardization
12	DC	Direct current
13	AC	Alternating current
14	DCEN	Direct current with negatively charged electrode
15	DCEP	Direct current with positively charged electrode
16	HAZ	Heat affected zone
17	WM	Weld metal
18	BM	Base metal

CHAPTER – 1
INTRODUCTION

1.1. INTRODUCTION

In industry most of the materials are fabricated into the desired shape mainly by one of the following methods viz. casting, forming, machining and welding. The selection of a particular technique depends upon different factors which may include shape and size of the component, precision required, cost, material and its availability. Sometimes one specific process may be used to achieve the desired object. However, more often it is possible to have a choice between the processes available for making the end product. Among the available options economy plays the decisive role in making the final choice.

1.2. WELDING

Amongst the manufacturing processes welding is primarily used for joining metal parts and is required when larger lengths of standard sections are required or when several pieces are to be joined together to fabricate a desired structure.

Welding is the technique of joining metals and plastics by such methods which do not employ fasteners and adhesives.

1.2.1. Definition: -

"Welding is a process of joining two similar or dissimilar metals by fusion, with or without the application of pressure and a filler metal may be used if required." [1]

The fusion of metal takes place by means of heat and is obtained from electric arc, electric resistance, chemical reaction, friction or radiant energy. The result of welding process is a homogeneous material (weld pool) of the composition and characteristics of two parts which are being joined together.

1.2.2. Weldability: -

It is defined as the capability of being welded into inseparable joints having specified properties such as weld strength, proper microstructure etc. [1]

Weldability of a metal is decided by the weld quality and the ease with which it can be obtained.

Weldability depends on the following major factors:

- Melting point
- Thermal conductivity
- Thermal expansion
- Surface condition
- Microstructure after welding

By proper shielding atmosphere, proper fluxing material, proper filler metal, proper welding procedure and in some cases by proper heat treatment of the metal before and after deposition we can correct the metallurgical, chemical, physical and thermal characteristics of a metal if these are considered undesirable and unfavorable with respect to weldability.

1.3. GAS TUNGSTEN ARC WELDING

Figure 1.1: Gas Tungsten Arc Welding [2]

1.3.1. Definition

Gas tungsten arc welding (GTAW) or tungsten inert gas (TIG) welding is an arc welding process that uses a tungsten (non consumable) electrode to produce the weld. Shielding gas (usually an inert gas such as argon) is used to protect the weld area from atmospheric contamination, and a filler metal is normally used whereas some autogenous welds do not require it. Energy produced

is supplied by a constant-current welding power source which is conducted across the arc through a column of highly ionized gas and metal vapors known as plasma. [2]

“It is a metal arc welding process wherein coalescence is produced by heating the job with an electric arc struck between a job and tungsten electrode. A shielding gas (argon, helium, nitrogen or a mixture of gases etc.) is used to avoid atmospheric contamination of the molten weld pool. A suitable filler metal may be added, if required.” [3]

Thin sections of stainless steel and non-ferrous metals such as aluminum, magnesium, and copper alloys are commonly welded by GTAW. The process gives the operator greater control over the weld than competing processes such as shielded metal arc welding and gas metal arc welding, allowing for stronger and higher quality welds. However, GTAW being significantly slower than most other welding techniques is comparatively more complex, hazardous and difficult to master.

1.3.2. Development

Arc welding developed slowly after the discovery of the electric arc in 1800 by Humphry Davy. In the early 20th century, welding non-ferrous materials like aluminum and magnesium remained difficult, because these metals reacted rapidly with the air, resulting in porous and dross-filled welds even after C. L. Coffin had the idea of welding in an inert gas atmosphere in 1890. Weld area was not protected satisfactorily from contamination even by processes using flux covered electrodes. Bottled inert gases were used in the beginning of the 1930s to solve this problem. A direct current, gas-shielded welding process emerged in the aircraft industry for welding magnesium after a few years later.

In 1941, this process was perfected and became known as heliarc or tungsten inert gas welding, because it utilized helium as a shielding gas and a tungsten electrode. Initially, the electrode overheated quickly and particles of tungsten were transferred to the weld in spite of tungsten's high melting temperature. The polarity of the electrode was changed from positive to negative to address this problem, but it became unsuitable for welding many non-ferrous materials. Finally, it became possible to stabilize the arc and produce high quality aluminum and magnesium welds with the development of alternating current units.

Water-cooled torches were developed by Linde Air Products that helped to prevent overheating when welding with high currents. Additionally, some users turned to carbon dioxide as an alternative to the more expensive weld shielding consisting of argon and helium, during the 1950s, as the process continued to gain popularity. However it reduced weld quality when used in welding aluminum and magnesium, and as a result, this proved unacceptable and is rarely used with GTAW today. [2]

1.3.3. GTAW setup

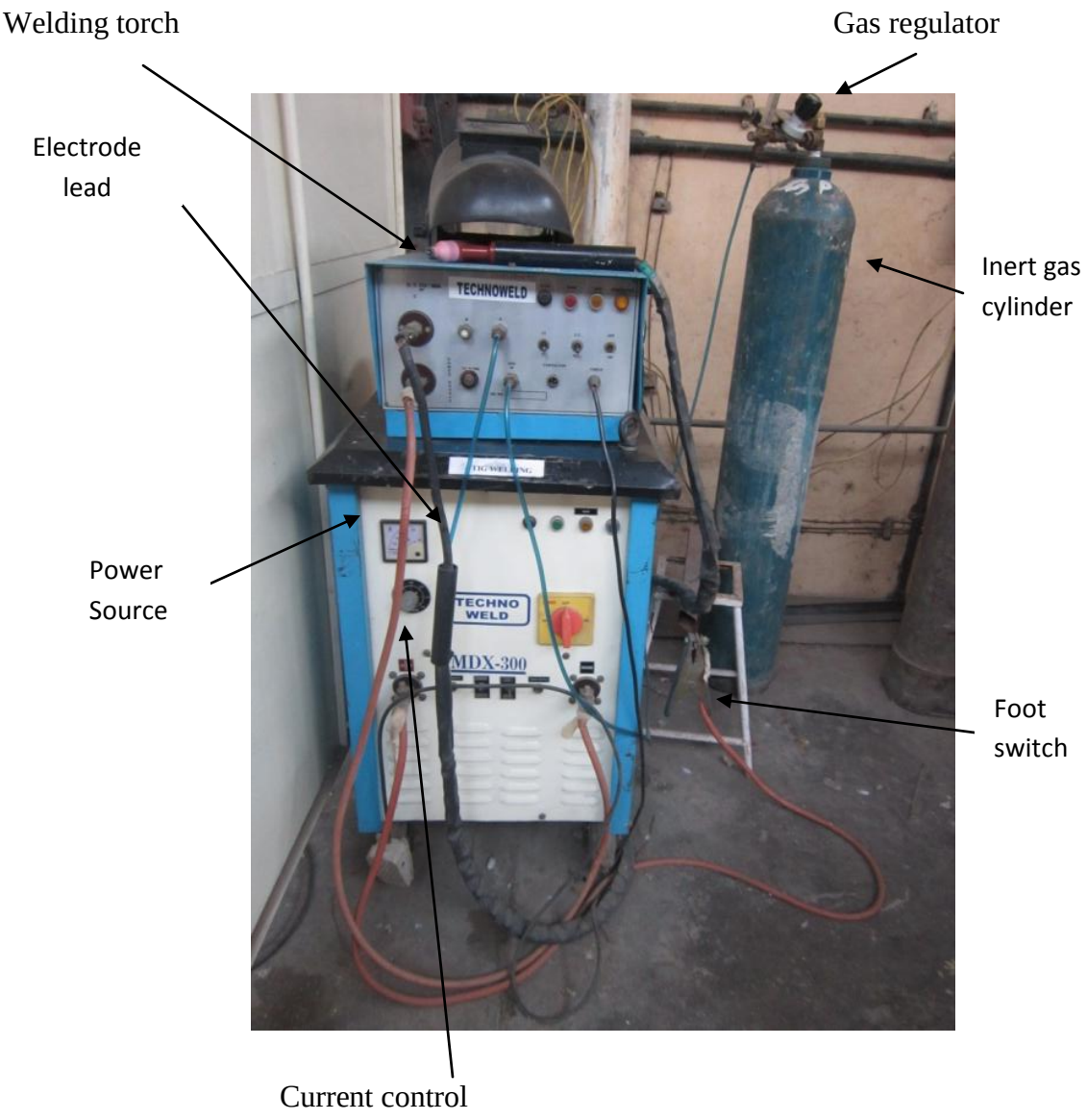

Figure 1.2: GTAW set up (**Courtesy:** Central Workshop, Thapar University, Patiala)

1.3.3.1. Equipment

The gas tungsten arc welding (GTAW) equipment includes a welding torch utilizing a non consumable tungsten electrode, a constant-current welding power supply, and a shielding gas source is also required.

1.3.3.2. Power supply

A constant current power source is used in gas tungsten arc welding uses, meaning that the current and obviously heat remains relatively constant, even if the electrode to workpiece gap and voltage change. This is important because operator holds the torch in manual or semiautomatic applications of GTAW. Maintaining a suitably steady electrode to workpiece gap is difficult in a constant voltage power source, since it can cause dramatic heat variations and make welding more difficult.

The type of metal being welded effect the preferred polarity of the GTAW system. When welding steels, nickel, titanium, and other metals a direct current with negatively charged electrode (DCEN) is often employed. Same can also be used in automatic GTAW of aluminum or magnesium when shielding gas used is Helium. Thermal ionization of the shielding gas and consequently increased temperature of the base material is achieved by the negatively charged electrode which generates heat by emitting electrons which travel across the arc. The ionized positively charged shielding gas flows toward the negatively charged electrode and this can allow oxides to build on the surface of the weld. Direct current with a positively charged electrode (DCEP) is used primarily for shallow welds since less heat is generated in the base material. Electrode reaches very high temperatures in this case because instead of flowing from the electrode to the base material, as in DCEN, electrons go the other direction. A larger electrode is often used to help it maintain its shape and prevent softening. As the electrons flow toward the electrode, ionized shielding gas flows back toward the base material, cleans the weld by removing oxides, impurities and thereby improves its quality and appearance.

Alternating current combines the two direct currents by making the electrode and base material alternate between positive and negative charge and is commonly used when welding aluminum and magnesium manually or semi-automatically. This prevents the tungsten electrode from

overheating while maintaining the heat in the base material as the electron flow to switch directions constantly. Base metal is heated more deeply during the electrode-negative portion of the cycle and the surface oxides are still removed during the electrode-positive portion of the cycle. Some power supplies enable operators to use an unbalanced alternating current, giving them more control over the amount of heat and cleaning action supplied by the power source, by modifying the exact percentage of time that the current spends in each state of polarity. In addition operators must be wary of rectification (in which the arc fails to reignite as it passes from straight polarity (negative electrode) to reverse polarity (positive electrode)). To overcome the problem, a square wave power supply can be used, as can high-frequency voltage to encourage ignition.

1.3.3.3. Welding torch

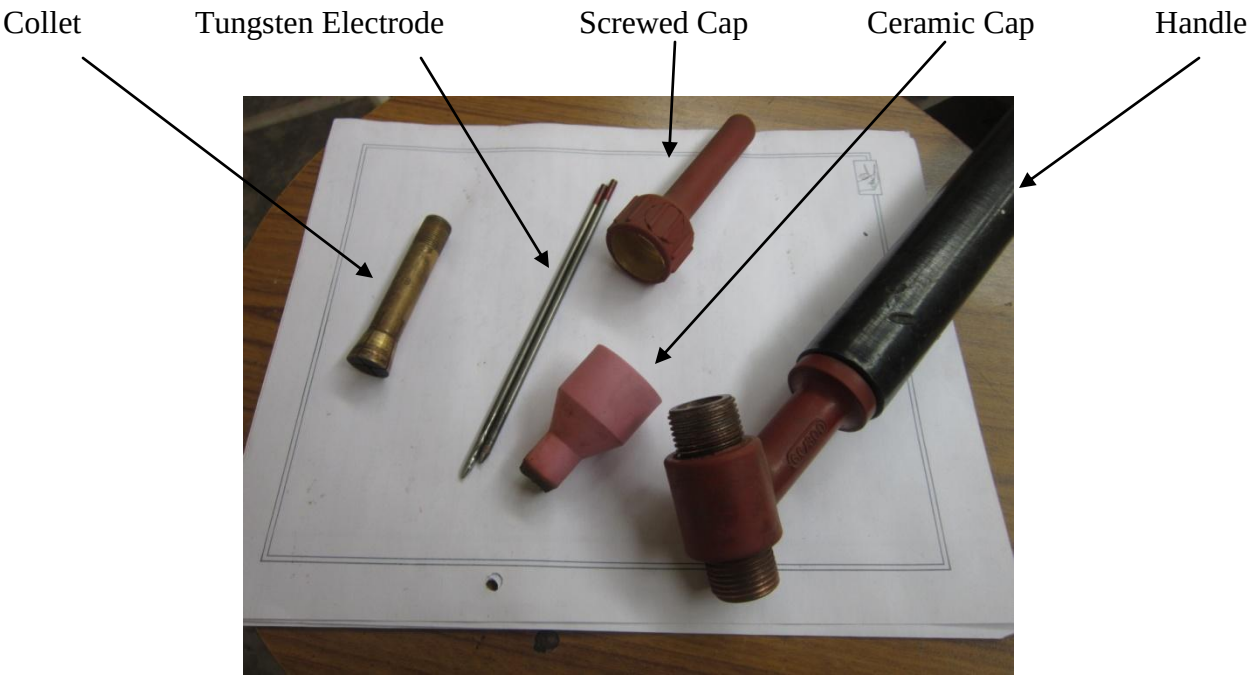

Figure 1.3: GTAW torch with handle, electrode, ceramic cap, screwed cap and collet (**Courtesy:** Central Workshop, Thapar University, Patiala)

GTAW welding torches are designed for both automatic and manual operation and are equipped with cooling systems using air or water. The automatic and manual torches are similar in construction, but automatic torch normally comes with a mounting rack and the manual torch has

a handle. Head angle i.e. the angle between the centerline of the handle and the centerline of the tungsten electrode can be varied on some manual torches according to the preference of the operator. Water cooling is required for high-current welding (up to 600 A), while air cooling systems are most often used for low-current operations (up to about 200 A). The torches are connected with cables to the power supply, with hoses to the shielding gas source and where used, with pipe to the water supply.

The internal metal parts of a torch are made of copper or brass (of hard alloys) in order to transmit current and heat effectively. The tungsten electrode must be held strongly in the center of the torch with an appropriately sized collet, and ports around the electrode provide a regular flow of shielding gas. The diameter of the tungsten electrode decides the collet size as it holds the electrode. The body of the torch is made of heat-resistant, insulating plastics covering the metal components, providing insulation from heat and electricity to protect the operator.

The size of the welding torch nozzle depends on the extent of shielded area desired. The size of the gas nozzle will depend upon the joint configuration, the diameter of the electrode and the availability of access to the joint by the welder. The inside diameter of the nozzle is preferably at least three times the diameter of the electrode, but there are no hard and fast rules. The welder will judge the effectiveness of the shielding and increase the nozzle size to increase the area protected by the external shielding gas according to needed. The nozzle must be heat resistant and thus is normally made of alumina or a ceramic material, but fused quartz (a glass-like substance) offers greater visibility. Some devices can be inserted into the nozzle for special applications, such as gas lenses or valves to improve the control shielding gas flow to reduce turbulence and introduction of contaminated atmosphere into the shielded area. Hand switches (if possible) to control welding current can be added to the manual GTAW torches.

1.3.3.4. Electrode

The electrode used in GTAW is made of tungsten or tungsten alloy, because tungsten has the highest melting temperature among pure metals, at 3,400 °C. As a result, the electrode is not consumed during welding although some erosion (called burn-off) can occur. Electrodes can have either a clean finish or a ground finish. Clean finish electrodes have been chemically

cleaned, while ground finish electrodes have been ground to a uniform size and have a polished surface, making them effective for heat conduction. The diameter of the electrode can vary between 0.5 and 6.4 millimeters, and their length can vary from 75 to 610 millimeters.

A number of tungsten alloys have been standardized by the International Organization for Standardization and the American Welding Society in code ISO 6848 and AWS A5.12, respectively, for use in GTAW electrodes, and are summarized below.

- Pure tungsten electrodes (classified as WP or EWP) are for general purpose and have low cost. These have poor heat resistance and electron emission. They find limited use in AC welding of magnesium and aluminium.
- Cerium oxide (ceria) as an alloying element improves arc stability and easiness in starting while decreasing burn-off. Cerium addition is not as effective as thorium but works well as it is not radioactive.
- Using an alloy of lanthanum oxide (lanthana) has a similar effect. Addition of 1% lanthanum has the same effect as 2% of cerium on tungsten electrode.
- Thorium oxide (or thoria) alloy electrodes can withstand somewhat higher temperatures while providing many of the benefits of other alloys and were designed for DC applications. However, it is somewhat radioactive in nature. Inhalation of the thorium grinding dust during preparation of the electrode is hazardous to health. As a replacement to thoriated electrodes, electrodes with larger concentrations of lanthanum oxide may be used. Larger additions than 0.6% help with electron emission but do not have additional improving effect on arc starting. Higher percentage of thorium makes tungsten more resistant to contamination.
- Electrodes containing zirconium oxide (zirconia) increase electrode life and also current capacity while improving arc stability and starting. Zirconium-tungsten electrodes melt easier than thorium-tungsten electrodes.
- In addition, electrode manufacturers may create alternative tungsten alloys with specified metal additions in appropriate quantity and these are designated with the classification EWG under the AWS system.

Filler metals are also used in nearly all applications of GTAW (the major exception being the welding of thin materials). Filler metals are in a variety of materials and are available with different diameters. In most cases, the filler metal (in the form of a rod) is added to the weld pool manually, but some applications call for an automatically fed filler metal, which often is stored on spools.

Table 1.1: Tungsten electrode specifications for GTAW [4]

S. N.	AWS classification	Material	Thoria	Zirconia	Tip colour
1	EWP	Pure tungsten	---	---	Green
2	EWTh-1	Tungsten + 1% Thorium	0.8-1.2	---	Yellow
3	EWTh-2	Tungsten + 2% Thorium	1.7-2.2	---	Red
4	EWZr	Tungsten + Zirconium	---	0.15-0.40	Brown

1.3.3.5. Shielding gas

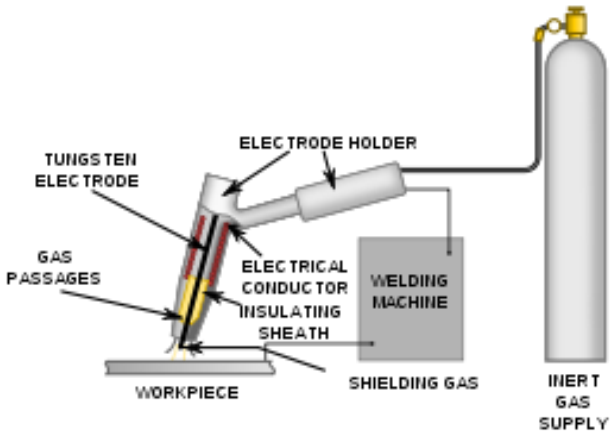

Figure 1.4: GTAW inert gas supply [2]

As with other welding processes such as gas metal arc welding, shielding gases are necessary in GTAW to protect the welding area from atmospheric gases such as oxygen, which can cause fusion defects, porosity and weld metal embrittlement, if they come in contact with the electrode, arc or the welding metal. The gas also transfers heat from the tungsten electrode to the metal and it helps in starting and maintaining a stable arc.

The selection of a shielding gas depends on several factors, including the type of material being welded, joint design and desired final weld. Argon is the most commonly used shielding gas for GTAW since it helps in preventing defects due to a varying arc length. When used with alternating current, the use of argon results in good appearance and higher weld quality. Another common shielding gas (helium) is most often used to increase the weld penetration in a joint, welding speed and to weld metals with high heat conductivity such as copper and aluminum. A significant disadvantage is the decreased weld quality associated with a varying arc length and difficulty of striking an arc with helium gas.

Argon-helium mixtures are also frequently used in GTAW, since they can increase control of the heat input while maintaining the benefits of using argon. Normally, the mixtures are made with helium (about 75% or higher) and a balance of argon gas. These mixtures increase the speed and quality of the AC welding of aluminum and also make it easier to strike arc. Another shielding gas mixture (argon-hydrogen) is used in the mechanized welding of light gauge stainless steel, but as hydrogen can cause porosity, so its uses are limited. Similarly, nitrogen can sometimes be added to argon to help stabilize the austenite in austenitic stainless steels and increase penetration in welding copper. Due to problems of porosity in ferrite steels and limited benefits, however, it is not a popular shielding gas additive.

1.3.4. Operation

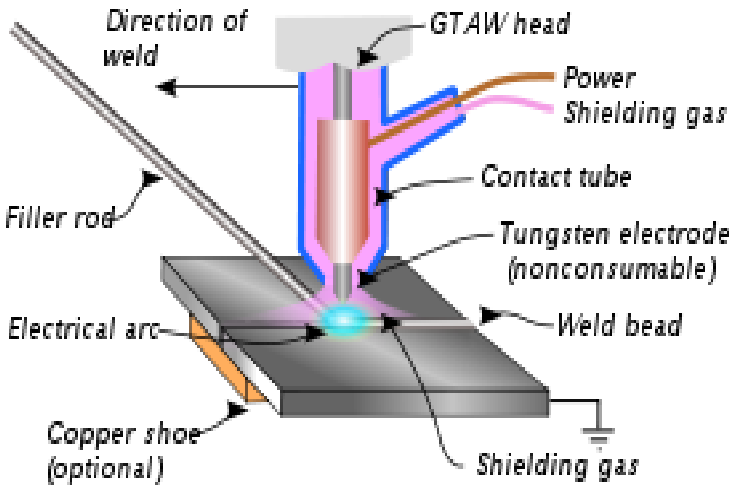

Figure 1.5: GTAW weld area [2]

Manual gas tungsten arc welding is often considered the most difficult amongst all the welding processes commonly used in industry. Great care and skill are required to prevent contact between the electrode and the workpiece during process and the welder must maintain a short arc length. GTAW normally requires two hands, since most applications require that the welder manually feed a filler metal into the weld area with one hand while manipulating the welding torch in the other. However, some welds combining thin materials (known as autogenous welds) can be accomplished without filler metal.

To strike the welding arc, a high frequency generator (similar to a Tesla coil) provides an electric spark. This spark is a conductive path for the welding current through the shielding gas and allows the arc to be initiated while the electrode and the workpieces are separated, typically about 1.5–3 mm apart. This high voltage, high frequency burst can be damaging to some vehicle electrical systems and electronics as induced voltages on vehicle wiring can also cause small conductive sparks in the vehicle wiring or within semiconductor packaging. Vehicle 12V power may conduct across these ionized paths which are driven by the high-current 12V vehicle battery. These currents can be sufficiently destructive as to disable the vehicle. Thus the warning is given to disconnect the vehicle battery power from both +12V and ground before using welding equipment on vehicles.

An alternate to initiate the arc is the "scratch start". Scratching the electrode against the work with the power on also serves to strike an arc, in the same way as SMAW arc welding. However, scratch starting can cause contamination of the electrode. Some GTAW equipment is capable of a mode called "touch start" or "lift arc". Here the equipment reduces the voltage on the electrode to only a few volts, with a current limit of 1-2 amps (well below the limit that causes metal to transfer and contamination of the weld or electrode). When the GTAW equipment detects that the electrode has left the surface and a spark is present, it immediately increases power, converting the spark to a full arc.

Once the arc is struck, the welder moves the torch in a small circle to create a welding pool whose size depends on the size of the electrode and the amount of current. While maintaining a constant separation between the electrode and the workpiece, the welder moves the torch back

slightly and tilts it backward about 10–15 degrees from vertical. Filler metal is added manually to the front end of the weld pool as and when it is needed.

Welders often develop a technique of rapidly alternating between adding filler metal and moving the torch forward (to advance the weld pool). The filler rod is withdrawn from the weld pool when the electrode advances, but it is never removed from the gas shield to prevent oxidation of its surface and contamination of the weld. Filler rods composed of metals with low melting temperature (such as aluminum) require that the operator maintain some distance from the arc while staying inside the gas shield. The filler rod can melt before it makes contact with the weld puddle if held too close to the arc. As the weld nears completion, the arc current is often gradually reduced to allow the weld crater to solidify and prevent the formation of crater and cracks at the end of the weld.

1.3.5. Materials

Gas tungsten arc welding is most commonly used to weld nonferrous materials, such as aluminum and magnesium and stainless steel but it can be applied to nearly all metals, with exceptions being lead and zinc. Its applications involving carbon steels are limited because of the existence of more economical steel welding techniques, such as gas metal arc welding and shielded metal arc welding and not because of process restrictions. Furthermore, GTAW can be performed in a variety of positions, depending on the skill of the welder and the materials being welded.

1.3.5.1. Aluminium and magnesium

Aluminum and magnesium are most often welded using alternating current and the use of direct current is also possible which depends on the properties desired. To improve penetration and increase travel speed the work area should be cleaned and may be preheated to 175 to 200 °C for aluminum or to a maximum of 150 °C for thick magnesium workpieces before welding. Alternating current can provide a self-cleaning effect, removing the thin, refractory aluminium oxide layer that forms on aluminium metal within minutes of exposure to air. This oxide layer must be removed for to do welding. Pure tungsten electrodes or zirconiated tungsten electrodes are preferred over thoriated electrodes, as the latter are more likely to "spit" electrode particles

across the welding arc into the weld when alternating current is used. Blunt electrode tips and pure argon shielding gas should be employed for thin workpieces. Introducing helium allows for greater penetration in thicker workpieces, but can make starting of arc difficult.

Direct current of positive or negative polarity can be used to weld aluminum and magnesium as well. Direct current with a negatively charged electrode allows for high penetration. Argon is commonly used as a shielding gas for DCEN welding of metals like aluminum. Shielding gases with high helium contents are generally used for higher penetration in thicker materials. Thoriated tungsten electrodes are suitable for use in DCEN welding of aluminum. Direct current with a positively charged electrode (DCEP) is used primarily for shallow welds especially joints with a joint thickness of less than 1.6 mm. A thoriated tungsten electrode is used along with a pure argon shielding gas.

1.3.5.2. Steels

For GTAW of carbon and stainless steels, the selection of a filler material is necessary to prevent excessive porosity. Before welding in order to prevent contamination oxides on the filler material and workpieces must be removed, and immediately prior to welding, alcohol or acetone should be used to clean the surface. Preheating is generally not necessary for less than one inch thick mild steels but low alloy steels may require preheating to slow the cooling process and prevent the formation of martensite in the heat-affected zone. Tool steels should be preheated to prevent cracking in the heat-affected zone. Martensitic and ferritic chromium stainless steels require preheating but austenitic stainless steels do not. A DCEN power source is normally used and thoriated electrodes (tapered to a sharp point) are recommended. Pure argon is used for thin workpieces but helium is used as thickness increases.

1.3.5.3. Dissimilar metals

Welding dissimilar metals generally offers new difficulties to GTAW welding, because most materials do not easily fuse to form a strong bond. However, welds of dissimilar materials have numerous applications like in manufacturing, repair work and the prevention of corrosion and oxidation. In some joints, a compatible filler metal is chosen to help form the bond and this filler metal can be the same as one of the base materials (e.g. using a stainless steel filler metal with

stainless steel and carbon steel as base materials) or a different metal (such as the use of a nickel filler metal for joining steel and cast iron). Very different materials may be coated with a material compatible with a particular filler metal and then welded. In addition, GTAW can be used in cladding or overlaying in non-similar materials.

When welding dissimilar metals, the joint must have an accurate fit, with proper bevel angles and gap dimensions. Care should be taken to avoid melting large base material. Pulsed current is particularly useful for these applications as it helps in limiting the heat input. The filler metal should be added rapidly and a large weld pool should be avoided to prevent dilution of the base materials.

1.3.6. Quality

Figure 1.6: GTAW fillet weld [2]

Gas tungsten arc welding can produce high-quality welds when performed by skilled operators because it affords greater control over the weld area than other welding processes. Maximum weld quality is assured by maintaining cleanliness. All equipment and materials used must be free from oil, moisture, dirt and other impurities, as these cause weld porosity and consequently a decrease in weld strength and quality. Alcohol or similar commercial solvents may be used to remove oil and grease, while a stainless steel wire brush or chemical process can remove oxides from the surfaces of metals like aluminum. Rust on steels can be removed by first grit blasting the surface and then using a wire brush to remove any stacked grit. These steps are especially important when negative polarity direct current (DCEN) is used because such a power supply provides no cleaning during the welding process, unlike positive polarity direct current or alternating current. To maintain a clean weld pool during welding, the shielding gas flow should be sufficient so that the gas covers the weld and blocks impurities in the atmosphere. GTAW in

drafty environments increases the amount of shielding gas necessary to protect the weld increasing the cost and making the process unpopular outdoors.

The level of heat input also affects weld quality in different ways. Low heat input (caused by low welding current or high welding speed) can limit penetration and cause the weld bead to lift away from the surface being welded. If there is too much heat input the weld bead grows in width while the likelihood of excessive penetration and spatter increase. Additionally, the shielding gas becomes ineffective if the welding torch is too far from the workpiece causing porosity within the weld. This results in a weld with pinholes which is weaker than a typical weld.

Tungsten inclusions in the weld may result if the amount of current used exceeds the capability of the electrode. Tungsten spitting, can be identified with radiography and prevented by changing the type of electrode or increasing the electrode diameter. In addition, if the electrode is not well protected by the gas shield or the operator accidentally allows it to contact the molten metal, it can become contaminated. This often causes the welding arc to become unstable and requires that electrode should be ground with a diamond abrasive to remove the impurity.

1.3.7. Safety

Like other arc welding processes, GTAW can be dangerous if proper precautions and care is not taken. Welders wear protective clothing including heavy leather gloves and protective long sleeve jackets to avoid exposure to extreme heat. Due to the absence of smoke in GTAW, the electric arc can seem brighter than in shielded metal arc welding making operators especially susceptible to eye and skin irritations like sunburn. Helmets with dark face plates are worn to prevent this exposure to ultraviolet light and new helmets often feature a liquid crystal-type face plate that self-darkens upon exposure to high amounts of UV light. Transparent welding curtains, made of a PVC plastic film, are often used to shield nearby workers and bystanders from exposure to the UV light from the arc.

Welders are also often exposed to very dangerous gases and particulate matter. While smoke is not produced, the brightness of the arc in GTAW can cause surrounding air to break down forming ozone. Similarly, the brightness and heat can cause formation of poisonous fumes from

cleaning and degreasing materials. Cleaning operations using these agents should not be performed near the site of welding, and proper ventilation is necessary to protect the welder.

1.3.8. Applications

While the aircraft industry is one of the primary users of gas tungsten arc welding, the process is used in a number of other engineering areas. Many industries use GTAW for welding thin workpieces like nonferrous metals. It is used extensively in the manufacture of space vehicles, and is also frequently employed to weld small-diameter, thin-wall tubing like those used in the bicycle industry. GTAW is often used to make root or first pass welds for piping of various sizes. In maintenance and repair work the process is commonly used to repair tools and dies especially components made of aluminum, magnesium etc. Because the weld metal is not transferred directly across the electric arc like most open arc welding processes, a large variety of welding filler metal is available to the welding engineer. In fact, no other welding process permits the welding of so many alloys in so many configurations like this. Filler metal alloys (such as elemental aluminum and chromium) can be lost through the electric arc from volatilization. This loss does not occur with the GTAW.

GTAW welds are highly resistant to corrosion and cracking over long time periods because the resulting welds have the same chemical integrity as the original base metal or match the base metals more closely. GTAW is the welding procedure of choice for critical welding operations like sealing.

1.3.9. Advantages of GTAW [5]

- No flux is required
- Increased corrosion resistance
- No slag formation
- Higher deposition rate
- Deeper penetration rate
- Welds all metals including aluminium and stainless steel.

1.3.10. Disadvantages of GTAW [5]

- Equipment used is costlier and less portable
- Difficult to weld in sharp corners
- Less suitable for outdoor work
- Radiations can produce harmful effects to the operator if exposed continuously for long time.
- Non consumable electrode requires frequent grinding

1.4. WELDABILITY

The weldability, also known as joinability, of a material refers to its ability to be welded. Many metals and thermoplastics can be welded but some are easier to weld than others.

The weldability of a material is used to determine the welding process and to compare the final weld quality to other materials.

Weldability is often hard to define quantitatively, so most standards define it qualitatively. The International Organization for Standardization (ISO) defines weldability in ISO standard 581-1980 as: "Metallic material is considered to be susceptible to welding to an established extent with given processes and for given purposes when welding provides metal integrity by a corresponding technological process for welded parts to meet technical requirements as to their own qualities as well as to their influence on a structure they form."

1.5. STAINLESS STEEL [6]

They are also known as Corrosion Resistant Steels. Their principal alloying element is chromium while some other elements like nickel, manganese etc. can also be present in different amounts. They cannot be considered as low alloy steels because substantial amount of chromium is present in them. It is seen that an addition of 4 - 6 percent chromium to low carbon steels renders them fairly required to be highly corrosion resistant with very superior appearance. A very high percentage of chromium (> 12%) is added. The chromium reacts with the oxygen to form a strong layer of Chromium Oxide on the surface of the metal which is responsible for offering the

resistance to corrosion. Stainless steels carrying chromium more than 12 % are known as True Stainless Steels.

1.5.1. Welding of stainless steels

Stainless steels can be classified according to the their matrix structure as

- Austenitic stainless steels
- Ferritic Stainless Steels
- Martensitic stainless steels
- Precipitation hardening stainless steels
- Duplex stainless steels

Heat conductivity of Cr-Ni stainless steels is about 50 percent less than that of mild steel. Henc less heat input is required for a given job. As a general rule about 10-12 per cent less current is used with stainless steel electrodes as compared to mild steel.

Melt off rates of stainless steel electrodes are higher in comparison to that for M.S. electrodes. This is another reason for slightly lower current being used in welding of stainless steels. Thermal expansion of Cr-Ni steels is about 50 percent greater than for mild steel. This will increase the chance of warping and buckling in welded joints so suitable fixture must be used while welding stainless steels. Electrical resistance of stainless steel is 6 to 12 times higher than that of M.S. and hence it may cause over heating in the electrodes. So electrodes of smaller length are used to reduce heating.

We will concentrate our discussion regarding weldability of only austenitic stainless steel which is the object of this experimental work.

1.5.2. Austenitic stainless steels

Standard austenitic stainless steels contain chromium in the range of 15 to 25 percent and nickel 6 to 20 percent. Typical AISI types of stainless steel and their compositions are given in table 1.2.

Table 1.2: Typical AISI type of stainless steels. (wt %) [6]

Type → composition↓	301	302	304	310	316	321	347	201	202
C%	0.15	0.08	0.08	0.25	0.08	0.08	0.08	0.15	0.15
Cr	16-18	17-19	11-20	24-26	16-18	17-19	17-19	16-18	17-19
Ni	6-8	8-10	8-12	19-22	10-14	9-12	9-13	3-6	4-6
N	0.03	0.03	0.03	0.03	0.03	0.03	0.03	0.25	0.25
Ti	-	-	-	-	-	5C	-	-	-
Nb	-	-	-	-	-	-	10C	-	-
Mo	-	-	-	-	2-3	-	-	-	-
Mn	-	-	-	-	-	-	-	6-8	8-10

1.5.3. Difficulty in welding of Stainless steel [6]

- Low thermal conductivity and high electrical resistance: - It is a big problem as overheating of SS may result in diffusion of metal. It may be overcome by using low values of current and using electrode of shorter lengths.
- Carbide Precipitation: - The austenitic grades are non-hardening type and welding normally does not affect the strength and ductility of the deposit. However, one detrimental effect of heating of a Cr – Ni steel is carbide precipitation at the grain boundaries which results in reduced corrosion resistance. A fine film of rich in chromium carbides containing as much as 90 % Cr, taken from the layer of metal next to the grain boundary will get precipitated along the grain boundary. Precipitation of intergranular chromium carbides is accelerated by an increase in time at that temperature and increase in temperature within the sensitized range.

  Carbide precipitation can be controlled by

  - Using stabilized steels by adding columbium and titanium which have greater affinity for carbon than chromium.

- Rapid quench may minimize the carbide precipitation. However, this may not be possible in all cases especially in thick sections.
- Limiting the carbon content to a maximum of 0.03 % can help avoiding the harmful carbide precipitation.
- Post weld solution annealing – it puts carbide back into solution and restores corrosion resistance. Austenitic stainless steel stabilized with niobium plus tantalum or titanium and welded with stabilized filler metal gives good strength and corrosion properties.

- Cracking - Interdendritic cracking in the weld area that occurs before the weld cools to room temperature is known as hot cracking. When metal with a wholly austenitic structure is more susceptible to cracking that weld metal with a duplex structure of delta ferrite in austenite. Susceptibility can be reduced by a small increase in carbon or nitrogen content or by an increase in manganese content.

  Cracking can be avoided: Weld metal should have a ferrite content of atleast 3 to 5 ferrite number (FN) and hence filler metal of suitable composition is to be selected. To determine suitable composition and the corresponding ferrite number the Schaeffler diagram is used which is shown.

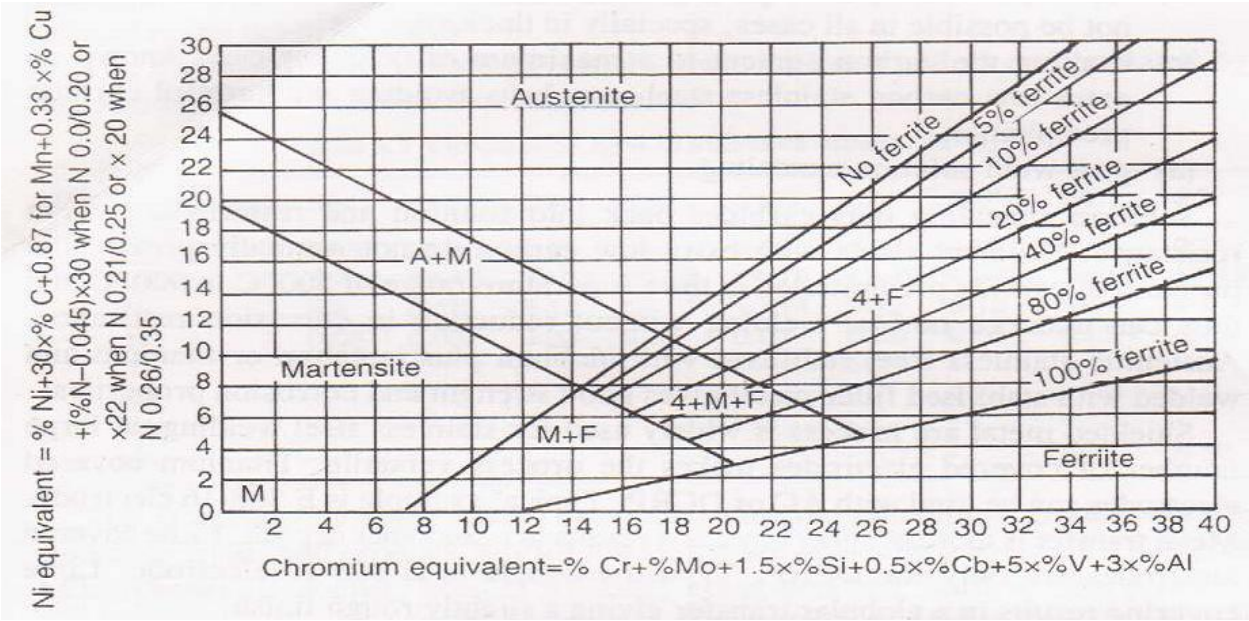

Figure 1.7: Schaeffler Diagram [6]

Nitrogen acts as a solid solution strengthener and increases the annealed yield strength to twice to that of the conventional austenitic steels. Specific attention should be paid to the control of nitrogen when welding these steel grades. A reduction in nitrogen will result in a loss of strength and corrosion resistance. An increase in the nitrogen content results in weld porosity or weld hot cracking.

1.6. EFFECTS OF ALLOYING ELEMENTS IN STEEL

Steel is basically iron alloyed to carbon with certain additional elements to give the required properties to the finished melt. Listed below is a summary of the effects of various alloying elements in steel.

1.6.1. Carbon

The basic metal, iron, is alloyed with carbon to make steel and has the effect of increasing the hardness and strength by heat treatment but the addition of carbon enables a wide range of hardness, strength and other properties.

1.6.2. Manganese

Manganese is added in steel to improve hot working properties and increase strength, toughness and hardenability.

1.6.3. Chromium

Chromium is added to the steel to increase its resistance to oxidation. This resistance increases as more chromium is added. When added to low alloy steels, chromium increases the response to heat treatment, thus improving hardenability and strength.

1.6.4. Nickel

Nickel has a tendency to form austenite (austenite is responsible for a great toughness and high strength at both high and low temperatures). Nickel also improves resistance to oxidation, surface reactions and corrosion. It increases toughness at low temperatures when added in smaller amounts to steels.

1.6.5. Molybdenum

Molybdenum when added to low alloy steel improves high temperature strengths and hardness.

1.6.6. Phosphorus

Phosphorus is usually added with sulphur to improve machinability in low alloy steels. Phosphorus, in small amounts, aids strength and corrosion resistance.

1.6.7. Sulphur

Sulphur improves machinability when added in small amount to alloy steel.

1.6.8. Silicon

Silicon is used as a deoxidizing (killing) agent in the melting of steel. As a result, most steels contain a small percentage of silicon. Silicon contributes to hardening of the ferritic phase in steels.

1.6.9. Copper

Copper is normally present in stainless steels as a residual element and is added to a few alloys to produce precipitation hardening properties. [7]

CHAPTER - 2

LITERATURE REVIEW

2.0. INTRODUCTION

A lot of research work has been carried out throughout the world for predicting the strength and other mechanical properties of different kinds of steel welded by gas tungsten arc welding (GTAW) or tungsten inert gas welding (TIG) process and stainless steels. A brief review of literature is being presented here. The available literature can be categorized in the following broad areas:

- Effect of process parameters on welding properties
- Application of ANSYS modeling
- Effect of Shielding Gas Mixture on Mechanical Properties of Steel
- Application of ANOVA methodology to optimize the parameters
- Effect on Microstructure
- Welding parameter in different welding positions

2.1. LITERATURE REVIEW

2.1.1. Effect of process parameters on welding properties

Kumar and Shahi [8] in the present study applied three levels of heat (2.563 kJ/min., 2.784 kJ/min. and 3.017 kJ/min.) input in the form of welding current (120A, 150A and 180 A) on AISI 304 SS plates of sizes 200 mm X 100 mm X 6 mm by using 308 SS solid electrode of diameter 3.15 mm as filler on GTAW process. Tensile test, microhardness testing and metallographic studies were carried out to study the effect. The results of study shows that

- Good joint strength is exhibited by all the joints which show that for welding 6 mm thick AISI 304 SS the operating envelope of GTAW process offers a wide range of parameters to the welder.

- As the dendrite size in the fusion zone is smaller in low heat input joints than the dendrites in medium and high input joints, it is found that maximum tensile strength and ductility is possessed by the weld joints made using low current.
- Fusion zone and HAZ area also increases as the heat input increases, the. Significant grain coarsening is found in the HAZs of all the joints. It is also observed that increasing heat input increases the extent of grain coarsening.
- Near to the fusion boundary the size of the grains in the HAZ of the joints is found to be coarser at high heat input.

Choi and Choi [9] in the present study used annealed pure titanium of the ASTM B265 grade 2 as the specimen and used the shielding gas flow of 15 l/min., 20 l/min. & 25 l/min., number of passes as 4, 5 and 7, welding current as 130, 140 & 145 A, arc voltage 14.5 – 16 V and welding speed as 4, 5.5 and 8 cm/min. Tension, impact and hardness tests were carried out to study their effect. The results conclude that

- Under the welding condition according to the amount of shielded gas the highest tensile strength and elongation was shown by the 25 l/min. specimen. The cooling time after welding did not affect the tensile strength and elongation significantly. Under the welding condition according to the number of welding passes, highest tensile strength but the longest elongation was shown by the 4-pass specimen.
- The impact absorption energy was high when the number of welding passes was large and the amount of shielded gas was large. With respect to the welding time interval, shorter the cooling time, more the impact absorption energy.
- For each welding condition, the hardness value was high in the 15 l/min. specimen, followed by the one minute specimen, and the 4-pass specimen. The hardness was the highest in HAZ and the difference in the hardness between HAZ and other zones was a major cause of the reduction of fatigue life of the welded zone.

Sivashanmugam et al. [10] in the present study have compared the microstructure and mechanical properties (tensile strength, hardness and impact strength) on the joints of AA7075 aluminum alloy welded by GTAW and GMAW processes. They found that

- Higher strength was found in welded joints by GTAW in comparison that of GMAW and the improvement in strength value is approximately 28%.
- Hardness is lower in the weld metal (WM) region in comparison to the HAZ and BM regions. High hardness is reported in the GTAW (HAZ) and the maximum hardness of 157 VHN was observed in the HAZ as compared to 153 VHN in base metal. In GMAW (HAZ) also high hardness of 133 VHN was observed in comparison to 100.5 VHN in parent metal.
- In GTAW and GMAW, the values of impact strength (Charpy method) were 6J and 4J respectively as compared to 12J of base metal.
- Fine equiaxed grains were formed in the welding zone and were uniformly distributed in the microstructure.
- Brittle, in nature, mode of fracture was observed as studied by SEM image.

Wang et al. [11] in the present study used Ni-base superalloy plates, grade GH99, of thickness 1.2 mm & 1.5 mm and TIG welding was employed to process butt weld of the plates with equal thickness. Welding parameter selected were: welding current 55-165 A, welding speed 19-29 cm/min, impulse frequency 2-5 Hz. Twenty three experiments were conducted and tensile test of the specimens was carried out along with SEM of fracture surface and microstructure of welded joint through metalloscope. Results of experiments showed that

- The decrease of welding speed and the increase of welding current resulted in the heat input. It can induce the widening and deepening of the welding pool, the decrease of columnar crystals and increasing of free dendritic crystals in the seam. Moreover, it can cause that the strength and the elongation of welded joints goes up first and then fall down.
- The increment of the impulse frequency may lower the strength (tensile) and the elongation. The tensile fracture is ductile and the dimples scatter on fracture surface.
- The optimized process parameters for the process on the said material are welding current as 80-90 A, welding speed as 25 cm/min. and impulse frequency as 3Hz.

Gulenc et al. [12] in the present study used austenitic stainless steel AISI 304L of size 140 mm X 75 mm and 10 mm thick as specimen and carried GMAW process with the gas composition of pure argon, 1.5 % H + 98.5 % Ar and 5 % H + 95 % Ar at different current values of 140, 180

and 240 A, welding speed of 50 cm/min. and a gas flowing rate of 10 l/min. They carried out tensile test, impact test, hardness test, bending test and microscopic investigations. They found that

- Highest tensile strength of 630 N/mm^2 was obtained with the welding that was carried out under 1.5 % Hydrogen-argon shielding and a welding current of 240 A.
- Welding parameters with 5 % hydrogen – argon mixture shielding gas and a welding current of 240 A gave the best toughness value.
- Visual examination of the bended specimens did not show any tearing, cracking or other defect. The base metal always gave the highest hardness value for all the welding parameters followed by that of heat affected zone and weld metal.
- The heat input increased and resulted in larger grains of the weld metal with increasing hydrogen addition into the shielding media.
- Increasing hydrogen content in argon as a shielding medium increased penetration profile depth and width.

Bang et al. [13] in the present study carried out submerged arc welding (SAW) and hybrid CO_2 laser-gas metal arc welding on austenitic stainless steel (STS304L) of 13 mm thickness and 600 mm x 500 mm size. They found that that the residual stress in the welding line direction, which affects the service characteristics of welded structures, in hybrid welding is less (13-15%) than that of the submerged arc welds because of lower heat input, faster cooling rate and smaller volume of the weld metal than SAW process. Because of sufficiently large cooling rate weld metal of both hybrid and SA welded joints exhibited over fine dendritic structure. However, as a result of larger heat input of SAW process, the HAZ of SA welded joints became more than two times thick in comparison to that of hybrid welded joints.

- Thermal behavior of the SAW showed ellipsoid isothermal distribution, however, thermal behavior of the hybrid welding showed combination of ellipsoid and line distribution that characterized the heat source of both arc and laser welding.
- Authors confirmed that it was more reasonable to replace hybrid CO_2 laser – GMA welding with SAW for butt joint of STS304L thick steel.

Cao et al. [14] in the present study carried out MAG and TIG welding on the 8% Ni 980 MPa high strength steel (10 mm thick) of following composition:

Table 2.2: Main chemical composition of used steel (wt %) [14]

Material	Ni	Mn	Cr	Mo	C
980 MPa steel	8.00	0079	0.62	0.61	0.03

The shielding gases and welding currents for TIG and MAG were chosen as Ar and Ar + 5% CO_2 and 300 A and 280 A respectively. They carried out microstructure analysis of welded joint, Charpy toughness test of specimens and observation of the fracture surface of weld metal. They found that

- The weld metal with inferior toughness, even in a fraction as low as 20%, caused remarkable deterioration on the toughness of the welding joint once it appears in front of the notch tip. The weld metal with comparable toughness has minor effect on the property of the welding joint.
- High content of Ni increased the hardenability of the weld metal and produced fine lath bainite microstructure. 6% Ni increases the residual austenite in the weld metal, which increases the crack resistance and promotes ductile fracture in the same.
- The microstructures and facture surfaces were observed to analyze the mechanism of the inferior toughness in a MAG weld metal.

Li and Liu [15] in the present study have used four welding methods, including laser welding, gas tungsten arc (GTA) welding, laser–GTA hybrid welding, and laser–GTA hybrid welding with cold welding wire to investigate the weldability of T-joints of magnesium alloy thin sheet. Magnesium alloy AZ31B sheets were used as base metal with the dimensions of the strengthening rib and the wall panels were 100 mm X 30 mm X 1.4 mm and 100 mm X 40 mm X 1.4 mm respectively. The effect of heat source type on weldability of T-joints was analyzed. The microstructures and mechanical properties (microhardness) were investigated and reported. Experimental results indicated that comparing with three welding methods, laser–GTA hybrid welding with cold welding wire was the most effective process for T-joints of magnesium alloy

thin sheet. In this process, in T-joints there was full penetration, the toes were smooth and round, and besides reinforcement forms on the upside of weld bead by the filled wire. The mechanical properties of T-joints made with laser–GTA hybrid welding with cold welding wire achieved 90 % of that of base metal and were better to that without welding wire.

Balasubramanian et al. [16] in the present study have employed four welding processes namely continuous current GTAW (CCGTAW), pulsed current GTAW (PCGTAW), continuous current GMAW (CCGMAW) and pulsed current GMAW (PCGMAW) on pure aluminum of size 300 mm X 150 mm X 6 mm to study their effect on mechanical properties of the same. Single V butt joint welding was carried out with argon as shielding effect. Tensile testing and microhardness tests were carried out. Results of research showed that

- Of the four types of welded joints, the joints fabricated by PCGTAW exhibited very high strength values and the increase in strength value is approximately 25% compared to CCGMAW joints, 15% compared to PCGMAW joints and 8% compared to CCGTAW joints.
- PCGTAW joints exhibited relatively higher joint efficiency (57%) and the improvement in joint efficiency is 25%, 16% and 8% in comparison to that of CCGMAW joints, PCGMAW joints and CCGTAW joints respectively.
- Hardness is lower in the weld metal (WM) region in comparison to the PMZ, HAZ and BM regions irrespective of welding technique. Minimum hardness is recorded in the CCGMAW joints (70 VHN) and the maximum hardness is recorded in the PCGTAW joints (100 VHN).
- The PCGTAW technique produced very fine grains (20 μm) in the weld metal region in comparison to another techniques and the reduction in grain diameter was 75% compared to CCGMAW joints, 66% compared to PCGMAW joints and 50% compared to CCGTAW joints.

Lakshminarayanan et al. [17] in the present study have welded AA6061 aluminium alloy of size 300 mm X 150 mm X 6 mm by using gas tungsten arc welding (GTAW), gas metal arc welding (GMAW) and friction stir welding (FSW) and carried out tensile test, microhardness test, microstructure and fracture surface analysis. It can be concluded from the results that

- Of the three welded joints, the joints fabricated by FSW process exhibited higher strength values and the increase in strength values is approximately 34% in comparison to GMAW joints and 15% in comparison to GTAW joints.
- Hardness is lower in the weld metal (WM) region in comparison to the HAZ and BM regions irrespective of welding technique. Minimum hardness is recorded in the GMAW joints (58 VHN) and the maximum hardness is recorded in the FSW joints (85 VHN).
- The formation of fine (equiaxed grains and uniformly distributed) very fine strengthening precipitates in the weld region are the reasons for superior tensile properties of FSW joints compared to GTAW and GMAW joints.

2.1.2. Application of ANSYS modeling

Teng et al. [18] in the present study examined the effects of the temperature field on the sensitization of Alloy 690 butt welds fabricated using the gas tungsten arc welding (GTAW) method and the laser beam welding (LBW) method, respectively. The welding thermal cycles of the two welding methods are simulated using ANSYS based upon a moving heat source model and the high-temperature thermal physical property data maintained in the JMatPro database. Base metal for study was alloy 699 (Ni base) and size of the plate chosen was 60 mm X 150 mm and 3 mm thick. Welding parameter for GTAW process were welding current as 90 A, voltage as 15 V and welding speed as 84 and 108 mm/min. and that of LBW were PW waveform, 1750 W average power and welding speed of 80 mm/min. The validity of numerical model is confirmed by comparing the simulation results with corresponding experimental findings. It is found that agreement between the numerical results for the temperature field and the experimental temperature measurements by utilizing the value of the thermal diffusivity in the thermal model for the GTAW and LBW weldments. In addition, it is shown that the LBW weldment experiences a rapid heating and cooling effect than the GTAW weldment and therefore has both a smaller heat affected zone (HAZ) and a narrower sensitization region. Overall, the simulation results presented in this study were found to be in good agreement with the experimental findings. Thus, the validity and general applicability of the thermal welding models are confirmed.

2.1.3. Effect of Shielding Gas Mixture on Mechanical Properties of Steel

Durgutlu [19] in this study has investigated the effect of hydrogen in argon as shielding gas for tungsten inert gas welding of 316L austenitic stainless steel. The microstructure, penetration and mechanical properties were examined. Stainless steel plates of size 200 mm X 80 mm X 4 mm taken as specimen were chamfered at 30^0 and welding was carried out with 2.4 mm tungsten electrode, gas flow rate of 10 l/min., welding current 115 A, welding speed as 100 mm/min. and pure argon, 1.5%H_2–Ar and 5%H_2–Ar were used as shielding gas. Bending test, tensile test and microstructure analysis was carried out to know the effect of shielding effect. Results of above tests showed that

- For tensile strength, the best result is obtained from 1.5% H_2–Ar as gas shielding.
- Cracks, tearing and surface defects were not observed with naked eye after bending the samples welded under all three shielding media.
- For all shielding media, hardness of weld metal is lower than that of the HAZ and base metal.
- Penetration profile examinations for all three different shielding gases show that penetration depth and weld bead width increases with increasing hydrogen content.
- Mean grain size in the weld metal increases with increasing hydrogen content. More hydrogen content caused deviations in the grain orientation of weld metal.

2.1.4. Application of ANOVA methodology to optimize the parameters

Sittichai et al. [20] studied the effect of welding current (80, 90 & 100 A), welding speed (250, 300 & 350 mm/min.) and shielding gas mixture (75% Ar + 25% CO_2, 70% Ar + 25% CO_2 + 5% O_2 and 69.5% Ar + 25% CO_2 + 5% O_2 + 0.5% He) on the mechanical properties like ultimate tensile strength and elongation of the steel AISI 304. Statistical data of mean, standard error of mean and analysis of variance (ANOVA) were applied to identify the significant factors. The raw material for the study was AISI 304 (Austenitic stainless steel grade 304) of dimensions 65 mm x 80 mm x 3 mm. They found that the shielding gas had the major effect on UTS and best results of 954.81 N/mm^2 was obtained with a combination of 70% Ar + 25% CO_2 + 5% O_2 against other combinations of 75% Ar + 25% CO_2 and 69.5% Ar + 25% CO_2 + 5% O_2 + 0.5%

He. Best result in elongation (47.94%) was obtained with the combination of 69.5% Ar + 25% CO_2 + 5% O_2 + 0.5% He shielding gas at a welding speed of 250 mm/min.

Kumar et al. [21] have studied the influences of pulsed current parameters such as peak current, base current, pulse frequency and pulse on time on tensile properties of pulsed current TIG welded AA 6061 aluminium alloy and following conclusions were obtained.

- Factorial experimentation technique was more convenient to predict the effect of pulsed current welding parameters on tensile properties of TIG welded aluminium alloy joints.
- ANOVA method is more appropriate to find out the significant main and interaction factors of pulsed current TIG welding process. In general, peak current and pulse frequency are having directly proportional relationship with the tensile properties of the welded joints i.e. if the peak current is increased then the tensile strength is increasing and similar effect is observed when frequency is increased.
- However, base current and pulse on time is having inverse proportional relationship with the tensile strength i.e. if the base current is raised then the tensile strength is decreasing and similar influence is noticed when pulse on time is increased further.

Tarng and Yang [22] in the present study optimized the GTAW process parameters for weld bead geometry by Taguchi Method. Pure aluminium plates of 1.6 mm thickness were used as specimens. Various process parameters such as arc gap (2.4-3.2 mm), the alternative current polarity ratio in the range of 30-70%, the welding speed (24-26 cm/min.), filler speed (1.5-2.5 mm/min.) and welding current (80-110A) were taken as variables in the design of experiment and three levels of each were used. L18 orthogonal array was used as design of experiments. Front width, front height, back width and back height were taken as objective of measurement. The investigation showed that

- Taguchi Method provides a systematic and efficient methodology for searching the welding process parameters with optimal weld bead geometry.
- The optimal weld bead geometry has a smaller-the-better quality characteristic for the front height, front width, back height and back width of the weld bead.
- Through the ANOVA, it is seen that welding speed, welding current, and polarity ratio are the most important parameters for the determination of the weld bead geometry. The

confirmation experiments were conducted and verified the optimal welding process parameters.

- It was shown that the front height, front width, back width and back height of the weld bead in the gas tungsten arc welding process are improved by using this approach.

Giridharan and Murugan [23] in the present study have carried out the pulsed gas tungsten arc welding on stainless steel (304L), developed a mathematical model and optimized the parameters like welding current and welding speed for weld bead geometry. It can be concluded from the present study that

- Mathematical models correlating weld bead parameters to pulsed GTAW process parameters were developed for predicting the bead parameters for welding thin stainless steel sheets of 3 mm thickness with high accuracy.
- Pulsed GTAW process parameters have shown significant influence on weld bead geometry parameters.
- Welding speed (S) is the most important and pulse current (I_p) the next most important influencing process variable on bead parameters while pulse current duration is the least important among the three process parameters.
- Quasi-Newton numerical optimization technique was used to find the optimum pulsed GTAW process and optimum weld bead parameters for welding of 3 mm thick stainless steel (304L) sheets. The results were confirmed using conformity test and found to have good accuracy.

Kumar and Sundarrajan [24] have studied the effect of pulsed TIG welding process parameters on dilution and mechanical properties such as notch tensile strength, hardness, and impact toughness in welded condition on Al-Mg-Si alloy of 250 mm × 150 mm × 3.14 mm. Pulsed TIG welds exhibited lower notch tensile strength and impact toughness than the parent metal because of interdendritic network microstructure features. Taguchi method was used to optimize the pulsed TIG welding process parameters of heat treatable (Al-Mg-Si) aluminum alloy weldments for maximizing the mechanical properties. An inverse relationship has been observed between the notch tensile strength and impact toughness.

2.1.5. Effect on Microstructure

Nakata et al. [25] have studied re-weldability of neutron irradiated stainless steel (SS 304) plates, size 60 mm X 100 mm X 10 mm by TIG welding using filler of Type 308 L stainless steel, simulating the repair-welding of reactor components. Specimens were submerged arc welding (SAW) joint of Type 304 SS containing 0.5 appm helium (1.8 appm in the SAW weld metal). Sound welding could be obtained by 1-3 pass welding on the plates at weld heat inputs less than 1 MJ/m in the irradiated 304 SS base metal. In the case of the build-up welding of a groove, no visible defects appeared in the specimen at a heat input as low as 0.4 MJ/m. However, build-up welding at a high heat input of 1 MJ/m was prone into weld cracking, owing weld metal in the area within 0.6 mm from the fusion line.

Gharibshahiyan et al. [26] in the present study used low carbon steel of size 10 mm x 10 mm x 55 mm as raw material and GMAW with parameters voltage 20, 25 & 30 V, current 130 & 180 A, filler wire diameter 1 mm, welding speed 40 cm/min. and shielding gas CO_2. The results of experiment showed that by increasing the voltage from 20 to 30 V the grain size number decreased from 12.4 to 9.8. It was also observed that high heat input and rapid cooling rates in the weld metal produced fine grain austenite at high temperature resulting in the formation of fine grained polygonal ferrites at ambient temperature. High heat input led to grain coarsening which was more pronounced in the HAZ as well as reducing the impact energy and toughness. Elevation of heat input reduced the hardness in the HAZ raising the heat input from 5 to 8 KJ/cm decreased the hardness from 160 to 148 HBN. This is considered to be because of reduction in the density of dislocations and microstructural coarsening.

2.1.6. Welding parameter in different welding positions

Lothongkum et al. [27] studied the TIG pulse welding parameters of 304L stainless steel sheet of 3 mm thickness in flat, vertical and overhead positions were investigated. Specimens were of size 100 mm X 125 mm X 3 mm and the shielding gases were Ar, and Ar + N_2. The base and pulse currents in all welding positions were adjusted to achieve a weld bead contour corresponding to DIN 8563 class AS at 3.4 mm/s welding speed, 1 pulse/s pulse frequency and 55% on-time. The weld bead aspect ratios (W/D) are 2.7-2.8. Increasing welding speed to 5 and 6.8 mm/s whilst simultaneously increasing the pulse frequency, the base and pulse currents, at

constant 55% on-time was not successful in achieving weld bead contours to satisfy DIN 8563. In the vertical and overhead positions, gravitational force made the weld pool fall down, leading to undercut after solidification. With the appropriate welding parameters, the gravitational effect could be eliminated. The δ-ferrite content in the weld metals was in the acceptable range when the nitrogen content in the Ar shielding gas was between 3-5% v/v.

2.2. SUMMARY OF LITERATURE REVIEW

After going through the literature it can be reviewed that a lot of work was done in the field of gas tungsten arc welding in one way or another. Some investigators had studied the effect of various parameters on the mechanical properties of the base metal and a some of them have also go through the microstrutural changes and their effect. Some investigators have optimized the gas tungsten arc welding process by using optimization techniques like Taguchi Design of Experiments and Analysis of Variance (ANOVA). Some of the research work is carried out in the direction of looking in the metallurgical aspects and microstructural properties of the base metal before and after welding in the base metal, weld metal and heat affected zone (HAZ). One of the researcher has employed ANSYS software tool and has compared the results of actual testing with those of theoretical ones from the software. Research work has also been carried out by varying the shielding gas composition like mixture of hydrogen and helium in argon and so during the gas tungsten arc welding process and studying its effect on the various mechanical properties and microstructure of base metal. It can be concluded from literature review that the main process parameter which affect the properties of welded joints are welding current, shielding gas, gas flow rate, electrode chosen composition of base metal and filler metal.

2.3. GAPS IN LITERATURE

1. AISI/SAE 202 grade (Austenitic stainless steel) is being commonly used in routine structural work because of economic consideration but research work carried on this material is very less. In the present thesis work it is proposed to optimize process parameter to achieve best welded joints using gas tungsten arc welding (GTAW) process.

2. AISI/SAE 304 grade stainless steel has been analyzed and tested by many researchers but that of AISI/SAE 202 grade stainless steel has not been reported yet. In the present thesis work it is proposed to do so and a comparison will be made between the two grades of stainless steels.

3. Dye penetrant test and joint quality are very important test for stainless steels which are being used in the routine structural work but very less such tests have been reported yet. In the present study it was proposed to carry out the above tests along with other mechanical tests like Bulk (Rockwell C-Scale) hardness, impact tests (Charpy) at room temperature and -20 ^{0}C, Microhardness (Vickers), weld bead geometry (bead width and bead height), chemical composition analysis (spectrometry) of the base metal and weld metal.

4. Effect of argon and its mixture with Hydrogen and nitrogen has been reported by many but that of argon and helium is rare to find. In the proposed study effect of pure helium, argon-helium mixture (50-50) and pure helium on the mechanical properties and bead geometry was carried out.

2.4. OBJECTIVE OF THE STUDY

The objective of the present study is to investigate effect of parameter like welding current, shielding gas nature, gas flow rate and grove angle on weld bead geometry, bulk hardness, surface cracks and porosity, impact strength at room temperature and -20 ^{0}C, microhardness and chemical composition of the weld metal on AISI/SAE 202 grade (Austenitic stainless steel) and AISI/SAE 304 grade stainless steel using gas tungsten arc welding (GTAW) or tungsten inert gas welding (TIG) process. Taguchi Design of experiments and analysis of variance (ANOVA) was used to optimize the process parameters. In the present work GTAW process was carried out by using three levels of welding current, shielding gas, gas flow rate and grove angle. SS202 and SS304 grade wires of 2.5 mm diameter were used as filler wire. Shielding gas combinations of pure Argon, Argon-Helium (50-50) and pure Helium were used. Following tests and analysis work were carried out

- Bead geometry (Bead width and bead height)
- Bulk Hardness test
- Dye Penetrant test for identification of surface cracks
- Impact test (at room temperature and -20 ^{0}C)

- Microhardness (Vickers) test
- Joint Quality (cracks, flaws etc.) and
- Chemical composition analysis of weld metal

CHAPTER – 3

DESIGN OF EXPERIMENTAL STUDY

The literature review showed that any change in the parameters of gas tungsten arc welding or TIG welding affects the properties of welding. So in this study it was proposed to find out the effect of changing different parameters like welding current, shielding gas composition, groove angle and gas flow rate on hardness, impact strength, chemical composition, microhardness, weld bead geometry and joint quality. The stainless steel specimens of grades SS 202 (100 mm X 50 mm X 6 mm) and SS 304 (120 mm X 50 mm X 5 mm) were used as test materials.

Figure 3.1: Samples for spectroscopy of SS304 and SS202 grade stainless steel

Table 3.1: Chemical composition of base metals

Metal	MAIN CHEMICAL CONSTITUENTS									
	Fe	C	Si	Mn	P	S	Cr	Mo	Ni	Cu
SS 202	72.6	0.0813	0.434	10.7	0.600	0.0082	15.0	0.0050	0.153	0.707
SS 304	70.1	0.0474	0.272	1.11	0.0446	0.0050	19.1	0.169	8.26	0.388

TIG welding was carried out on tungsten inert gas welding machine (Make: TECHNO WELD MDX – 300, INDIA) available at Central Workshop, Thapar University, Patiala as shown in the figure 3.2. The main parts of the machine are control box panel, electrode gun, gas regulator, gas cylinder. The welding current can be regulated and displayed on control box panel of the welding machine and has a range of 0-500 A. The function of electrode gun is to carry the tungsten electrode and direct the supply of shielding gas in the welding region. Gas regulator is used to control the shielding gas flow into the welding area. The machine is totally manual and requires a skilled operator to operate it.

Figure 3.2: TIG Welding setup

(**Courtesy:** Central Workshop, Thapar University, Patiala)

Table 3.2: Main technical parameters of welding machine

S.N.	WELDING PARAMETER	RANGE
1	Welding current	0-500 A
2	Electrode diameter	3 mm
3	Gas flow rate	0-25 L/min.

3.1. SELECTION OF VARIOUS FACTORS AFFECTING WELDING

The determination of contributing which needs to be investigated depends on the responses of interest. Theoretical studies and literature review suggested that when doing welding with TIG welding machine on steel plates of 5-6 mm thickness the values of different parameters should be

Welding current 100-300 A

Gas flow rate 9-15 L/min.

Grove angle $60\text{-}90^0$

3.1.1. Welding current

Pilot study was carried out to identify the value of welding current as it is the most important parameter during TIG welding (because TIG welding works on the constant current characteristics). It shows that there was start of the arc and a weld bead was formed at 100 A and then current was raised in the steps of 50 A each and later on at 250 A it was found that metal fused completely and deposited at the back of the plate (as shown in figure 3.3) because of high heat generated at this temperature in case of SS304 grade stainless steel. Similar study was also carried on SS202 grade stainless steel and results are shown in the figure 3.3. On the basis of this study values of current were chosen as 140, 180 and 220 A for the present research work.

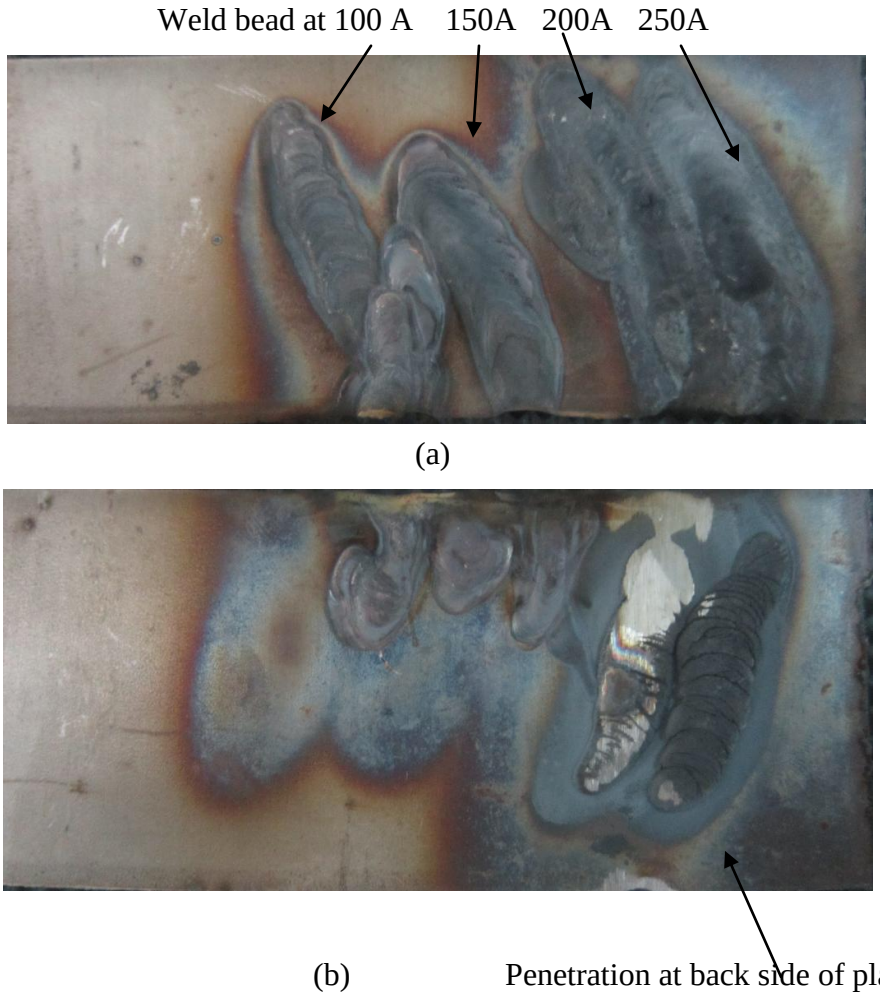

Figure 3.3: Result of pilot study on SS304 grade stainless steel showing (a) up & (b) down side

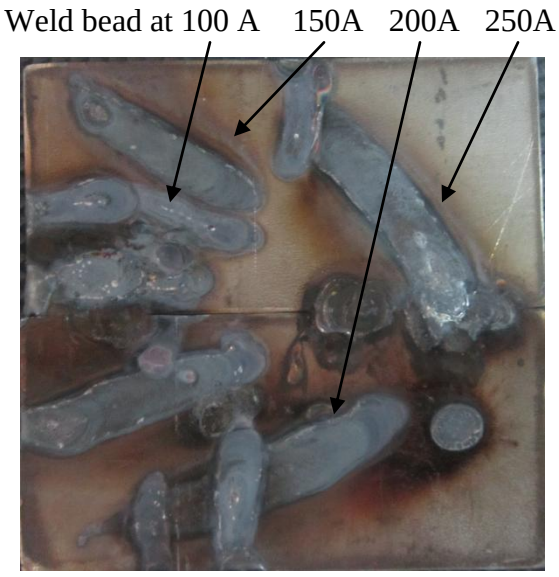

Figure 3.4: Result of pilot study on SS202 grade stainless steel

3.1.2. Welding Speed

Pilot study for welding speed was also carried out to know the effect of different gas composition on it. SS304 stainless steel plates of size 125 mm X 50 mm X 5 mm were used as the test specimen. Welding current for pilot study was chosen as 180 A and gas flow rate as 12 l/min. No edge preparation was done and accordingly no filler metal was used as shown in the figure 3.5 and results of pilot study are given in table 3.3.

Figure 3.5: Pilot study for welding speed a) specimens, b) after welding, c) after cleaning

Table 3.3: Results of pilot study

Gas used	Time used in welding (seconds)	Welding speed (mm/sec.)	Time consumed as Percentage w.r.t. argon gas
Argon	35.99	3.4732	100
Argon-Helium (50-50)	31.48	3.9708	87.469
Helium	26.04	4.8003	72.437

Results of pilot study shows that by using Helium gas and a mixture of argon-helium (50-50) we can save time upto 27.5% and 12.5% (approximately) respectively. Since welding speed cannot be controlled in manual TIG welding so it is not considered as a parameter.

3.1.3. Filler Wire

Filler wires chosen for welding the two grades of stainless steel are of grade SS202 and SS304 (ER304L) of size Ø2.5 mm X 1000 mm long as shown in the figure 3.6.

Figure 3.6: ER 304L grade filler wire

Non-consumable tungsten electrode = EWTh-2 (Thoriated tungsten) of 3 mm diameter, electrode to work angle 45^0 and DCEN electrode polarity was used for welding of specimens.

Table 3.4 shows the chemical composition of filler wire metal used for welding purpose.

Table 3.4: Chemical composition of filler metals

Metal	MAIN CHEMICAL CONSTITUENTS									
	Fe	C	Si	Mn	P	S	Cr	Mo	Ni	Cu
SS 202	Bal.	0.12	0.9	9.0	0.06	0.008	16.0	0.2	1.0	0.707
SS 304 (ER304L)	Bal.	0.03	1.0	2.0	0.0446	0.0050	18.2	0.05	8.5	0.40

3.1.4. Shielding gases for TIG welding of stainless steel

Three shielding gases namely pure argon, pure helium and a mixture of argon and helium gas in the equal amount were used in the present study to have variations in the welding joints. Gas cylinders of 10 litre capacity containing helium and argon-helium (50-50) mixture were obtained from Dwarka Mai Gases, Jalandhar.

Figure 3.7: Cylinder of Argon Gas, Helium Gas and Argon - Helium (50-50) mixture gas

In the present experimental setup, there are four factors varied at 3-level. Taguchi design has been used for the design of experiments, because it reduces the number of iterations and used to optimize the known parameters. The values of the input process parameters and their three levels for the TIG welding are as given below in Table 3.5.

Table 3.5: Process parameters and three levels for the TIG welding

S.N.	PARAMETER	UNITS	SYMBOL	LEVELS		
				1	2	3
1.	Welding current	Ampere	I	140	180	220
2.	Grove angle	Degree	Ɵ	60^0	75^0	90^0
3.	Shielding Gas	--------	G	Pure Argon	Pure Helium	50% Ar + 50%He
4	Gas flow rate	Litre/minute	F	9	12	15

3.2. ORTHOGONAL ARRAY

To select an appropriate orthogonal array for experiments, the total degrees of freedom must be computed. The degrees of freedom are defined as the number of comparisons between process parameters that must be made to determine which level is better and, specially, how much better it is. For example, a two-level process parameter counts for one degree of freedom. The degrees of freedom associated with interaction between two process parameters are given by the product of the degrees of freedom for the two process parameters. In the present study, once the degrees of freedom are known, the next step is to select an appropriate orthogonal array to fit the specific task. The degrees of freedom for the orthogonal should be greater than, or at least equal to, those for the process parameters. In this study, Taguchi L9 orthogonal array with four columns and four rows was used. Each welding parameter was assigned to a column and nine welding parameter combinations were tested. Therefore, only nine experiments were required to study the entire welding parameter space using the L9 orthogonal array. The experimental layout for the welding parameters using the L9 orthogonal array is shown in Table 3.6.

Table 3.6: Orthogonal array for experimentation on both SS202 and SS304 grade stainless steel

Experiment no.	Current (ampere)	Gas	Gas flow rate (L/min.)	Groove angle (Θ^0)	Parameters abbreviation
1	140	Ar	9	60	I1,G1,F1,Θ1
2	140	He	12	75	I1,G2,F2,Θ2
3	140	Ar+He	15	90	I1,G3,F3,Θ3
4	180	Ar	12	90	I2,G1,F2,Θ3
5	180	He	15	60	I2,G2,F3,Θ1
6	180	Ar+He	9	75	I2,G3,F1,Θ2
7	220	Ar	15	75	I3,G1,F3,Θ2
8	220	He	9	90	I3,G2,F1,Θ3
9	220	Ar+He	12	60	I3,G3,F2,Θ1

3.2.1. Selection of Orthogonal Array and Factor Assignment

In this experimental study, four factors were varied to three levels each. The degree of freedom (DOF) to a three level parameter is 2 (because DOF = number of levels-1), hence total DOF for the experiment is 8. So the Orthogonal Array (OA) which could be used was L9. Degree of freedom allocated to various factors is given in Table 3.7.

Table 3.7: DOF allocated to various factor combinations

Serial No.	Parameter	Units	DOF
1	Welding current	Ampere	2
2	Shielding gas	----	2
3	Gas flow rate	L/min.	2
4	Grove angle	degrees	2
	Total		**8**

3.3. WELDING OF SPECIMENS

3.3.1. Edge preparation of stainless steel specimen

Stainless steel plates of grade SS 202 and SS 304 grades were obtained from Oriental Engineering Works Pvt. Ltd. Yamunanagar and Chanderpur Works Pvt. Ltd., Yamunanagar respectively in the form of plates of sizes 100 mm X 50 mm X 6 mm and 120 mm X 50 mm X 5 mm respectively as shown in the figure 3.8.

Figure 3.8: Specimens of SS 304 (120 mm X 50 mm X 5 mm) & SS 202 (100 mm X 50 mm X 6 mm)

The specimens were machined in the longitudinal direction on milling machine (Make: Highway Engg. Works, Ludhiana) as shown in the figure 3.9.

Figure 3.9: Longitudinal sides being machined on the milling machine

(**Courtesy:** Workshop, HEC, Jagadhri)

Figure 3.10: Sides of specimens after milling the edges and ready for marking

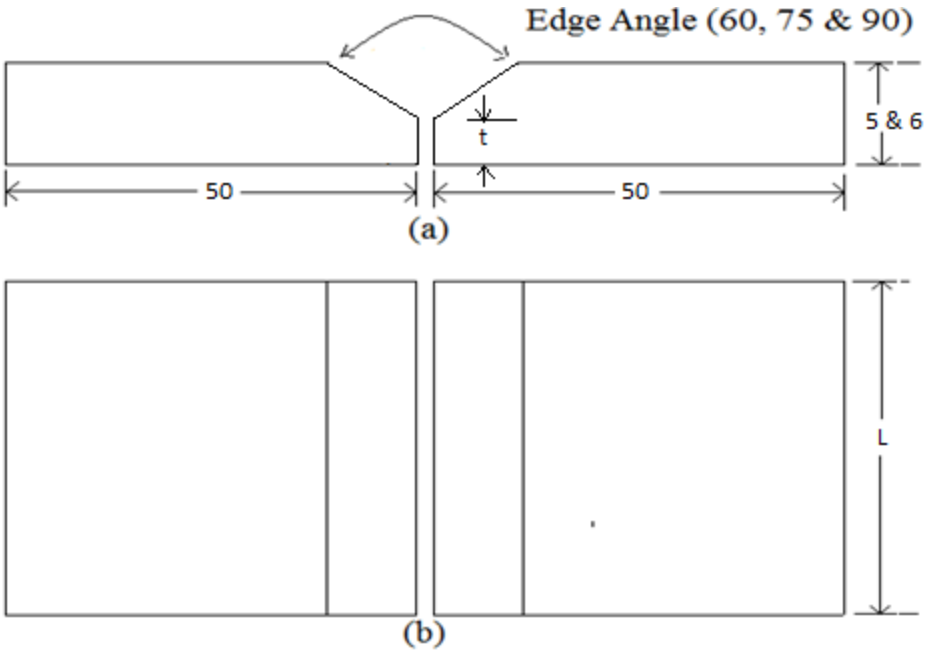

Where t = 2.5 mm for SS304 and 3 mm for SS202

Figure 3.11: Grove geometry (a) front view and (b) top view (all dimensions are in mm)

Thereafter marking was done on various specimens according to the groove angle decided previously (as shown in the figure 3.11 above). Grinding and filing was done to make the grove as shown in the figure 3.12 and 3.13.

Figure 3.12: Grinding the bulk material after marking on grinder/polisher machine (**Courtesy:** Workshop, H.E.C., Jagadhri)

Figure 3.13: Preparation of V-grove by filing on bench vice

Groves in the specimens were now ready for welding as shown in the figure 3.14.

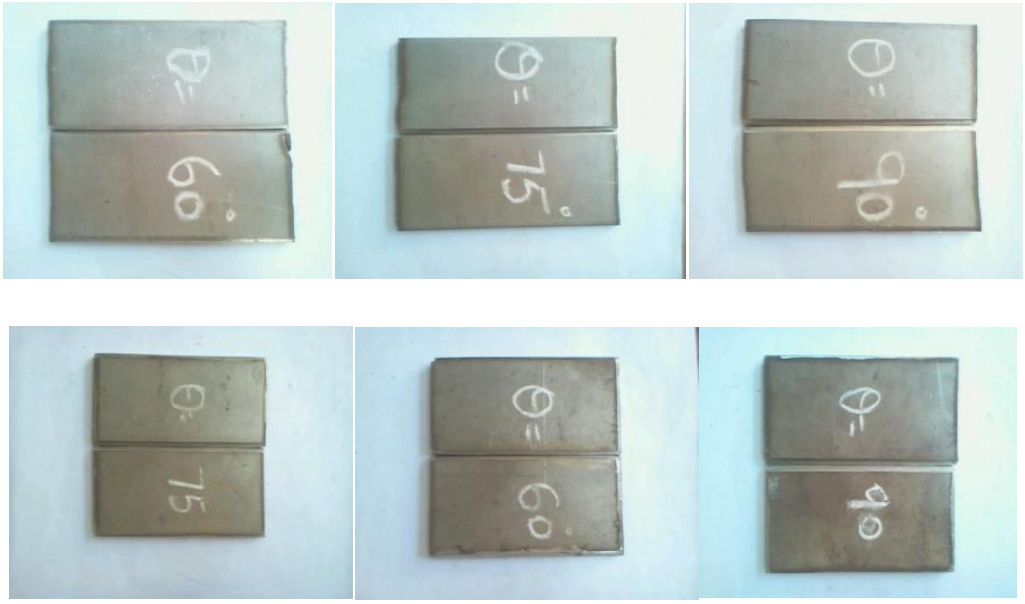

Figure 3.14: Grove angles on SS304 & SS 202 stainless steel specimens

3.3.2. Tacking of welding specimens

After edge preparation tacking was done at three points on the specimens using TIG welding by properly clamping in the jaws to ensure their proper alignment and no mismatch. Figure 3.15 shows the specimens after tacking on the backing side.

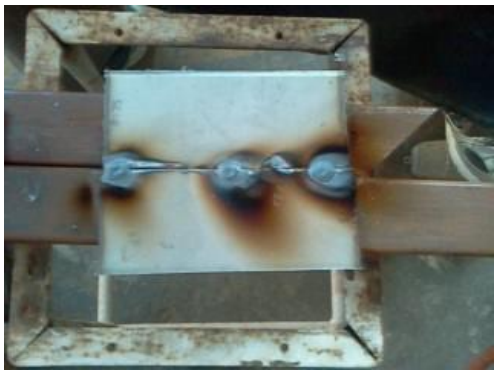

Figure 3.15: Tacking of the welding specimen using TIG welding

3.3.3. Welding of specimens

As previously decided L9 orthogonal array was chosen and welding on specimens was carried out by using TIG welding machine (Make: TECHNO WELD, INDIA, model MDX-300) available at central workshop Thapar University, Patiala, according to the nine experimental parameter combinations previously decided. All necessary precautions for the operator like hand gloves, helmet with shield, apron etc. were used as shown in the figure 3.16.

Figure 3.16: TIG welding on the specimens

All welded specimens immediately after welding are shown in the figure 3.17 and 3.18 to have an idea of weld bead.

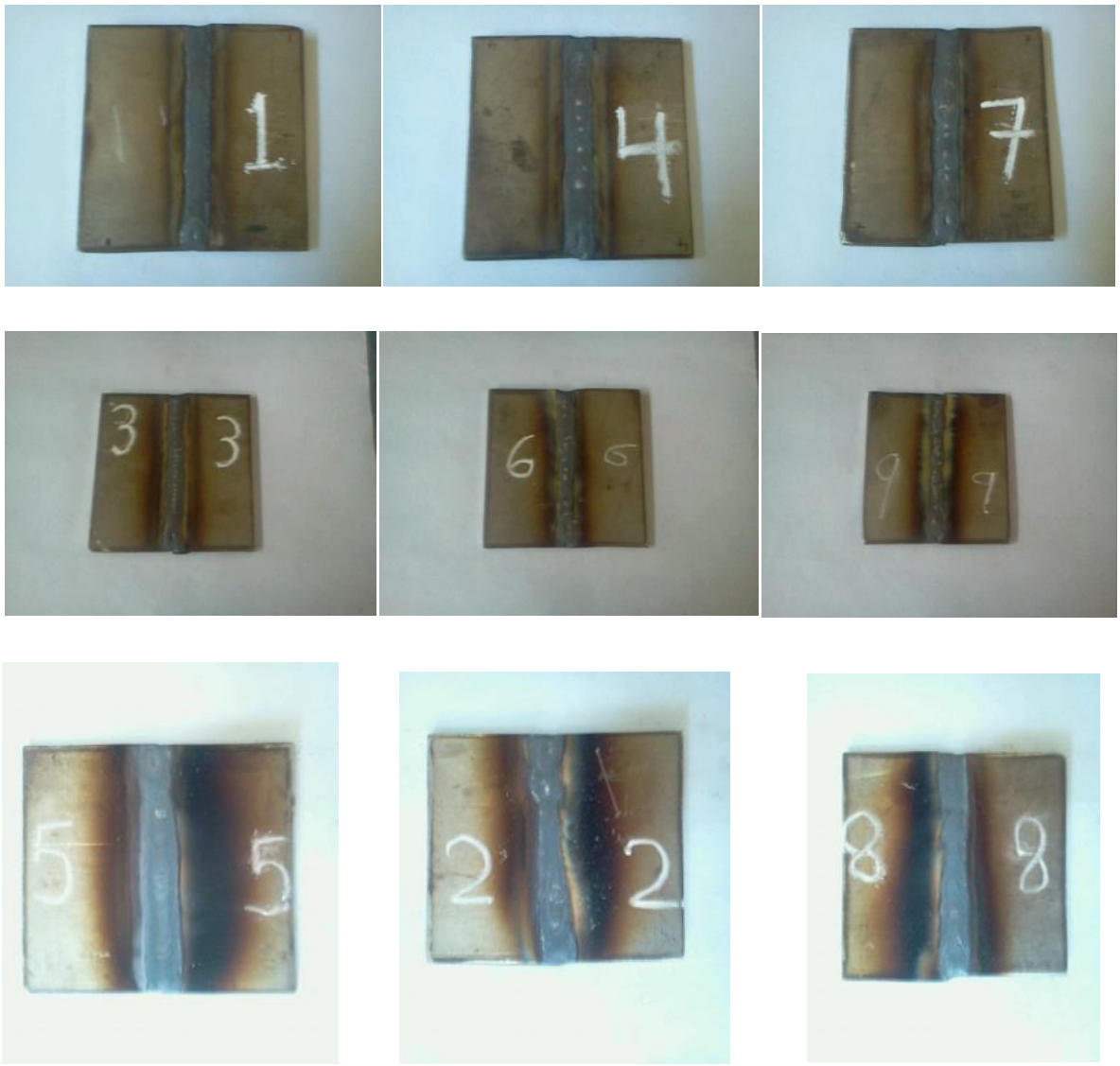

Figure 3.17: Specimens of SS 202 grade stainless steel immediately after welding

Dark regions on the sides of the weld bead of specimen numbers 2, 5 & 8 are because of the Helium gas.

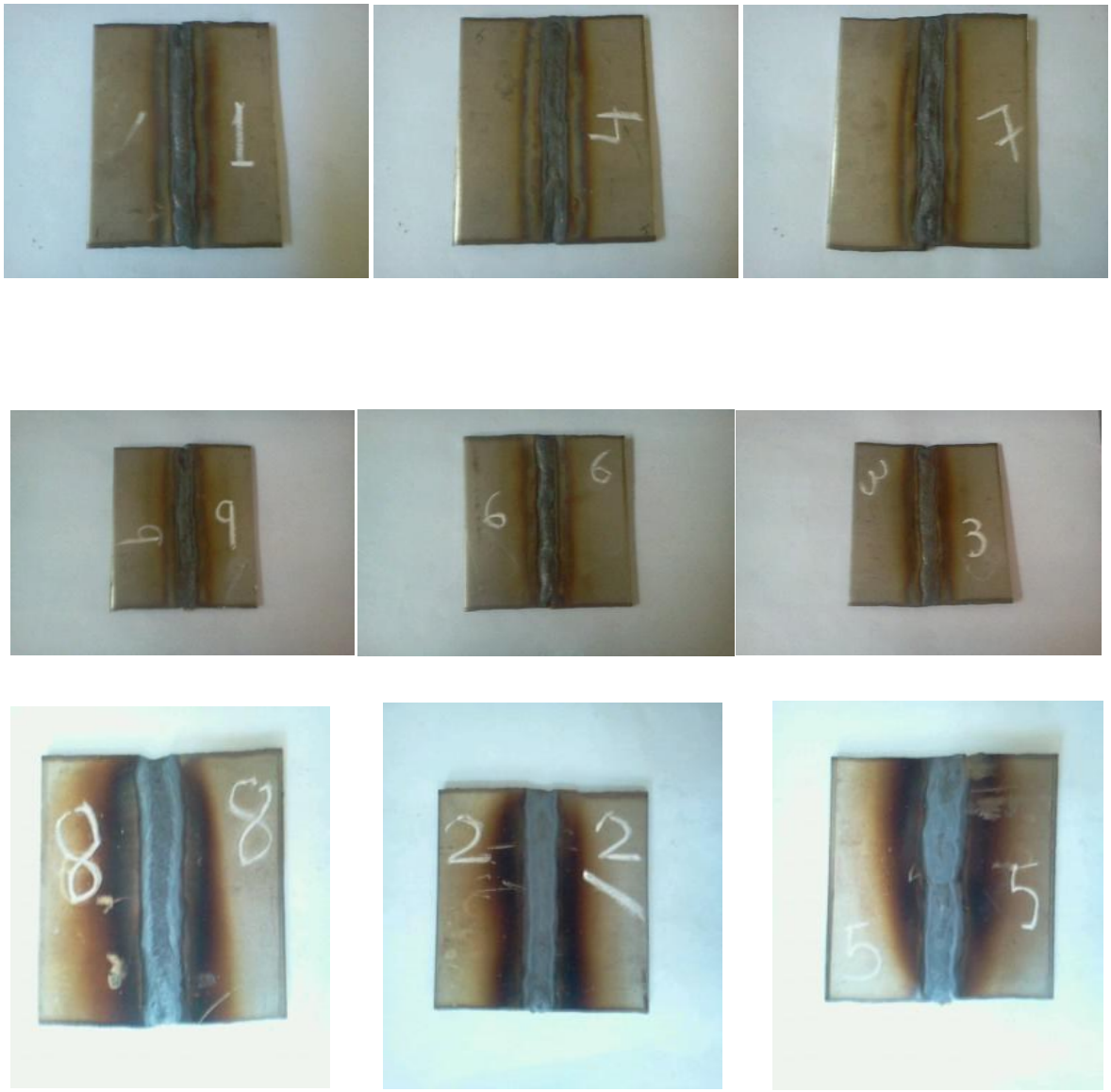

Figure 3.18: Specimens of SS 304 grade stainless steel immediately after welding

3.3.4. Cleaning of specimens

After welding the weld bead was cleaned thoroughly with clean cloth, acetone and a light buffing was done to have a clear look at the weld bead. Figure 3.19 & 3.20 shows the various specimens after cleaning the surface.

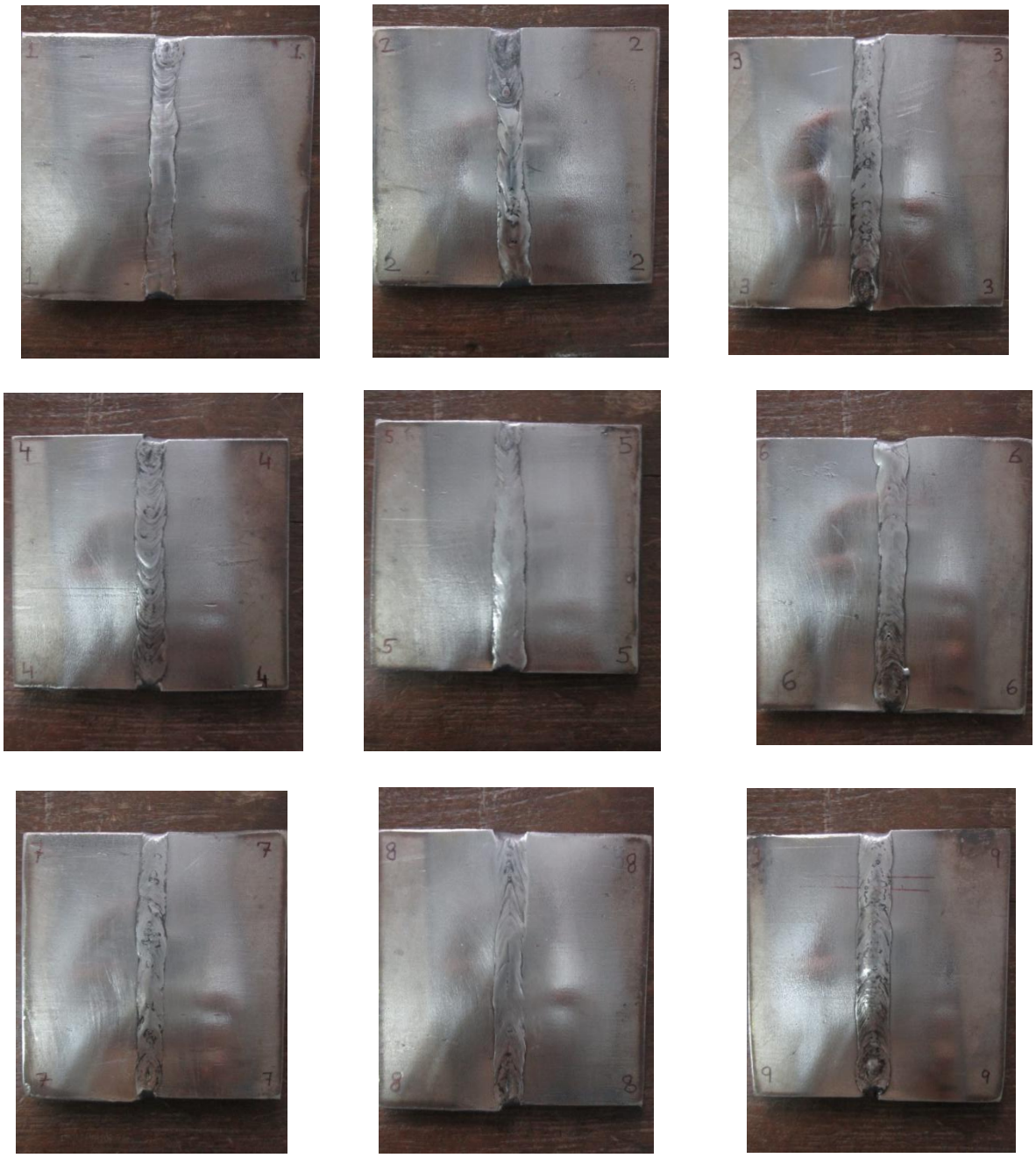

Figure 3.19: Specimens of SS 202 grade stainless steel after cleaning and buffing

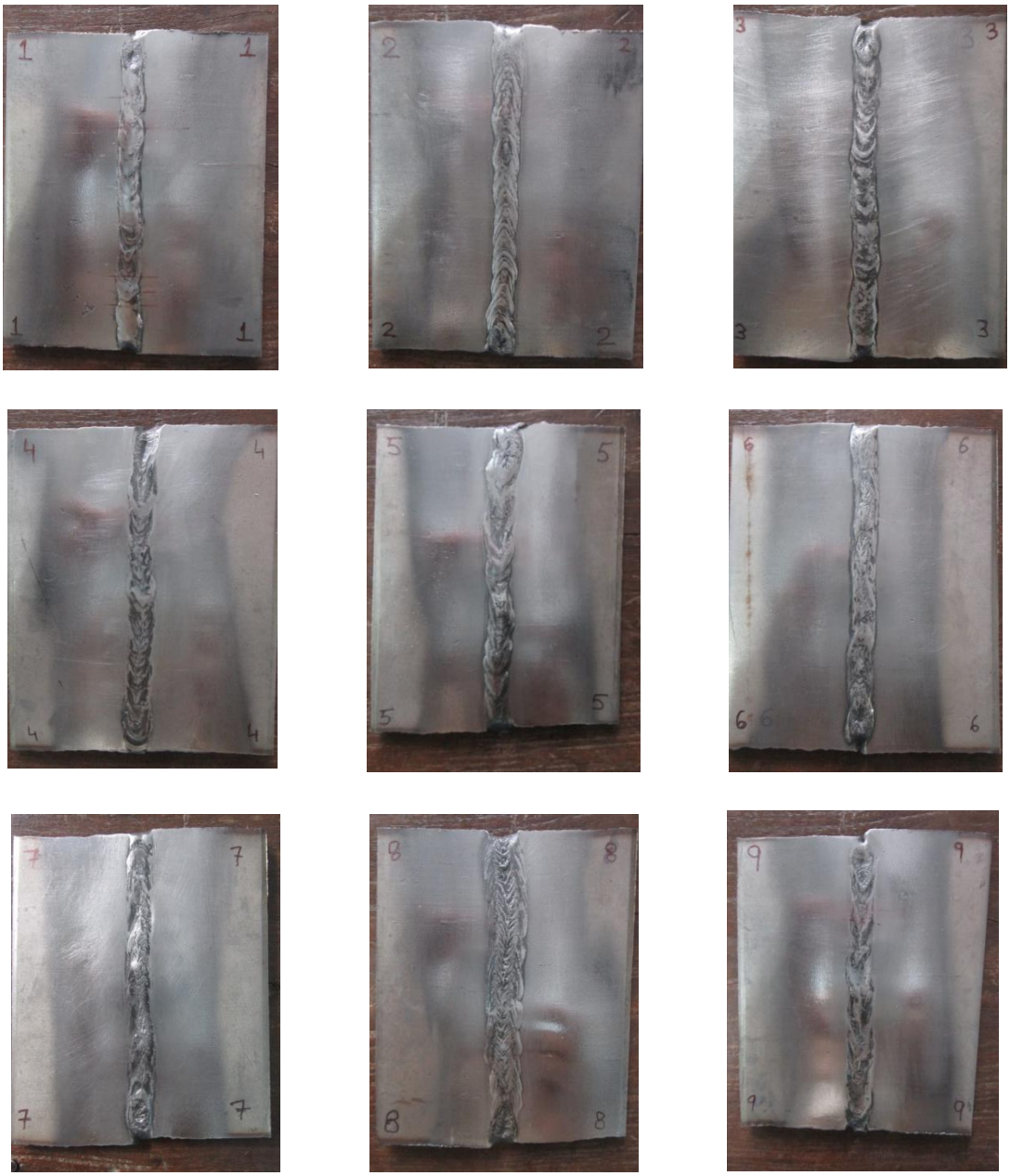

Figure 3.20: Specimens of SS 304 grade stainless steel after cleaning and buffing

3.4. CUTTING OF WELDED SPECIMENS FOR MECHANICAL TESTING AND CHEMICAL COMPOSITION

For the purpose of testing (mechanical, chemical and optical) of welded joints, weld bead was removed on the surface grinder machine (Make: Arvinder Engg. Works, India) as shown in the figure 3.21.

Figure 3.21: Weld bead removal on Surface Grinder Machine

(**Courtesy:** Workshop, H.E.C., Jagadhri)

Welded plates were marked for various tests (mechanical, chemical and optical) as shown in the figure 3.22. A margin of 3 mm was left for cutting of the specimens on Chop-Saw machine.

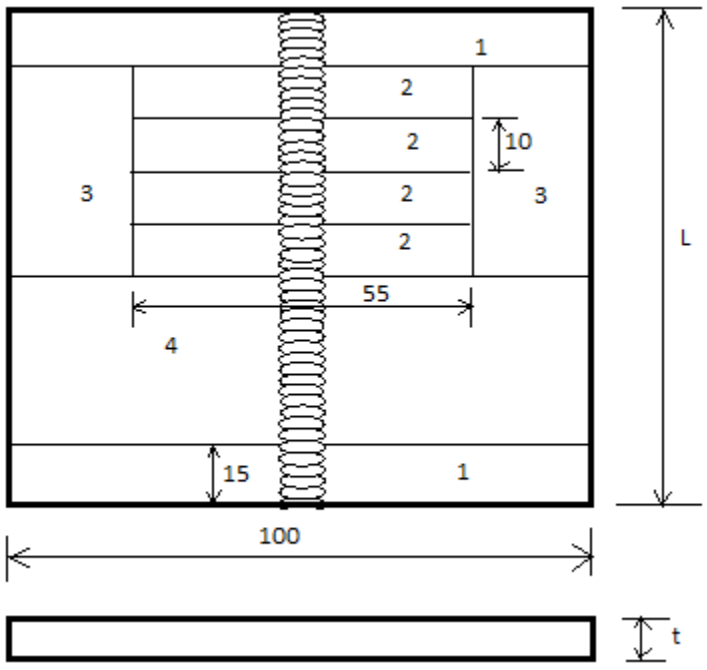

Where t = 3 mm for SS202 and 2.5 mm for SS304, L = 100 mm for SS202 and 120 mm for SS304

Figure 3.22: Marking and Cutting of plates after welding

Table 3.8: Description of various marked portions in the welded specimens (refer figure 3.22)

Part number	Use
1	Rejection at the start and end of welded region
2	Specimen for impact test
3	Rejection at the sides of plates
4	Specimen for bulk hardness test, microstructure analysis, microhardness test, chemical composition of welded region

Figure 3.23: Marking on welded specimens and cutting on Chop Saw machine (**Courtesy:** Workshop, H.E.C., Jagadhri)

Cutting of welded specimens as per the sizes mentioned above was done on Chop Saw Machine (Make: Dewalt Industrial tool co.) as shown in the figure 3.23. Water was used as coolant during cutting to ensure that temperature of specimens do not raises high. After cutting, specimens were grinded on the surface grinder machine (Make: Arvinder Engg. Works, India) to make them of exact sizes (especially for impact test) and V-notch was prepared on Shaper Machine (Make: J.A.Machine Tools, India) as shown in the figure 3.24.

Figure 3.24: Grinding and V-notch preparation for impact testing specimens (**Courtesy:** Workshop, H.E.C., Jagadhri)

3.5. TESTING OF WELD SPECIMENS

As proposed in this thesis work, following tests and measurements were conducted on the weld specimens:

- Weld bead geometry
- Bulk hardness test
- Dye penetrant test
- Impact test
- Microhardness test
- Joint quality
- Chemical composition

3.5.1. Weld bead geometry

Bead width and bead height of all the specimens were measured in the metrology lab of Thapar University by keeping all the specimens on the surface plate as shown in the figure 3.25. Five readings at different points were taken to take a better overall average. Bead width was measured using digital vernier caliper (Make: Starrett No. 723, American and least count = 0.01 mm) and bead height was measured using vernier height gauge (Make: Mitutoyo, Japan and least count = 0.02 mm).

Figure 3.25: Surface plate

(**Courtesy:** Metrology lab, Thapar University, Patiala)

Figure 3.26: Measurement of bead width using digital vernier caliper and bead height using vernier height gauge

(**Courtesy:** Metrology lab, Thapar University, Patiala)

3.5.2. Dye Penetrant Test

DPT (dye penetration test) test was performed on the welded region to detect the surface cracks and porosity. For performing test, three solutions namely Cleaner CL-96, Penetrant PT-97 and Developer DV-98 (Make: Checkmate India, Haryana) were used as shown in the figure 3.27.

Figure 3.27: Checkmate's cleaner, penetrant & developer used for DPT test of specimens

Steps while performing DPT test were as under:

- Cleaned the test surface for removing the dust, oil, grease, oxide etc. by using the cleaner
- Application of penetrant on the test surface/welded region and allowed penetrant to enter into the weld bead (approximately 15 minutes waiting)
- Cleaned the surface with a dry and clean cloth
- Applied of developer on the test surface and allowed the developer to dry out
- Defect/porosity (if any) appeared on the test surface in the form of colored spot.

Step by step DPT test is shown by the figures 3.28.

Figure 3.28: Application of penetrant and developer in the welded region on the test surface

3.5.3. Bulk hardness test

Hardness is defined as the resistance offered by any material to the applied load in the form of indentation/scratch. Bulk hardness of the weld specimen was found using Rockwell Hardness Testing Machine (Make: Avery, England, **Courtesy:** Solid Mechanics Lab, Thapar University, Patiala) on C – scale which uses a diamond cone indenter and a load of 150 Kg was applied for 10 seconds before release.

Figure 3.29: Rockwell Hardness Testing Machine

(**Courtesy:** Solid Mechanics Lab, MED, Thapar University, Patiala)

Observations were made at the centre (0 or mean position) of weld bead, 2 mm away from mean position and 5 mm away from mean position thereafter in both the directions so that all regions like weld region, heat affect zone and base metal could be covered. 3-4 readings were taken at mean position, weld region and heat affected zone to nullify the error and finding a better average value as shown in the figure 3.30.

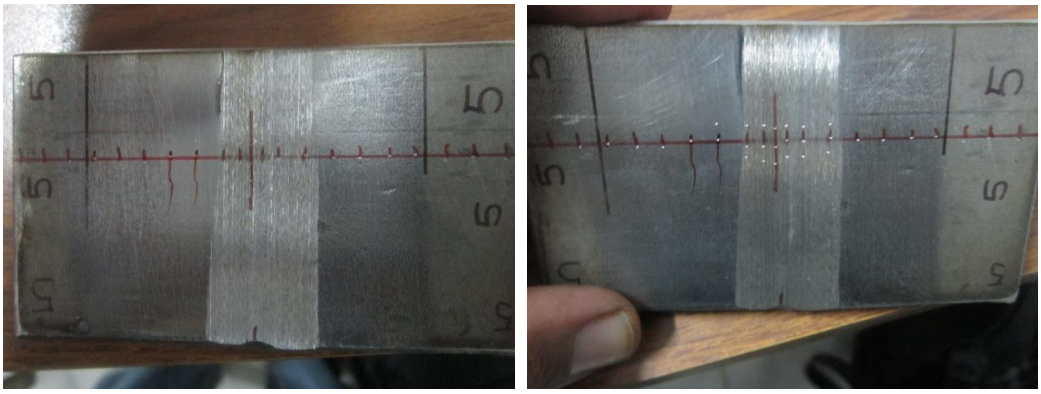

Figure 3.30: Bulk hardness samples for Rockwell hardness (C-Scale) testing machine (a) Marked points showing mean position and other points (b) Indentation marks on the surface of specimen after measuring bulk hardness

3.5.4. Impact Test

Impact strength of a material is defined as the resistance offered by the material against the suddenly applied load. It is also defined as the maximum amount of energy absorbed by the material when subjected to sudden load. Impact test on the weld specimen is performed on the impact testing machine (Make: Alfred J. Amsler & Co., Switzerland) having a range of 0-30 Kgm or 0-300 joules as shown in the figure 3.31. For impact test initial energy to the hammer was given as 15 Kg-m or 147.15 Joules.

Figure 3.31: Impact testing machine (**Courtesy:** Solid Mechanics Lab, MED, Thapar University, Patiala)

Specimens were prepared according to ASTM standards A-370 (2010) and having size as cross – section of 10 mm X 5 mm (SS 202) and 10 mm X 6 mm (SS 304) and length 55 mm.

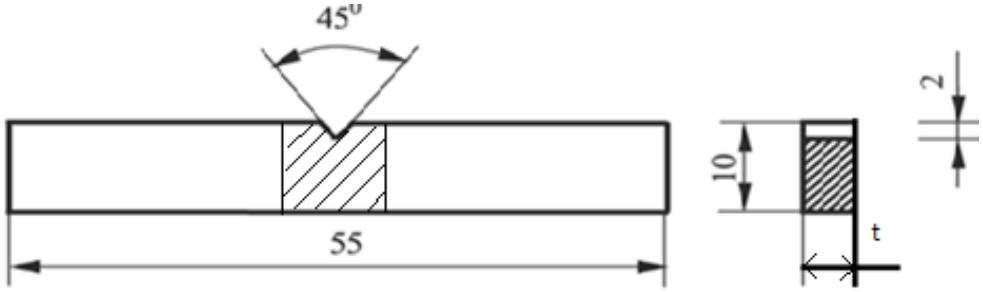

(Where t = 5 mm for SS304 & 6 mm for SS202)

Figure 3.32: Standard size of impact test specimen according to ASTM standard A-370 [28]

Figure 3.33 shows the actual sample ready for impact test.

Figure 3.33: Samples prepared for impact strength showing the notch angle and all sizes

The temperature of specimens below room temperature (i.e.-20 ^{0}C) was generated by using liquid nitrogen and the specimens were put in the same for 5 minutes as shown in the figure 3.34. An infrared thermometer (shown in the figure 3.35) was used for the measurement of temperature of test specimens.

Figure 3.34: Vacuum flask being used for generating a temperature of -20 ^{0}C

Figure 3.35: Infrared thermometer used for the measurement of temperature

3.5.5. Microhardness (VHN) Test

The samples measuring for microhardness were firstly ground on the belt grinder, then rubbed with emery paper size no. 400, 600, 800, 1000, 1500 & 2000 and then polished on polishing wheel (Make: Scientific, India) as shown in Figure 3.36 (a,b,c). Microhardness of the weld region was measured by using the computer interfaced microhardness tester (Make: Metatech Industries, Pune, India) as shown in Figure 3.38. The measurement was dependent on the size of indentation on the samples. The diagonals of the indents formed by a pyramid- shaped diamond indenter were measured with the help of Quantimet software at 40X magnification, which gave a direct hardness Vickers number (HVN) for microhardness. The hardness values obtained were useful indicators of material properties. The load applied on the indenter was 500 gms and the dwell time was 20 sec. Figure 3.39 shows the specimen which were used for microhardness test.

(a) **(b)** **(c)**

Figure 3.36: (a) Belt grinder (**Courtesy:** Machine Tool Lab, Thapar University, Patiala), (b) Apparatus with emery paper of grit size 400, 600, 800 and 1000, (c) Polisher (**Courtesy:** Material Science Lab, Thapar University, Patiala)

Figure 3.37 shows the suface finish on the specimens finally achieved to carry out the microhardness test.

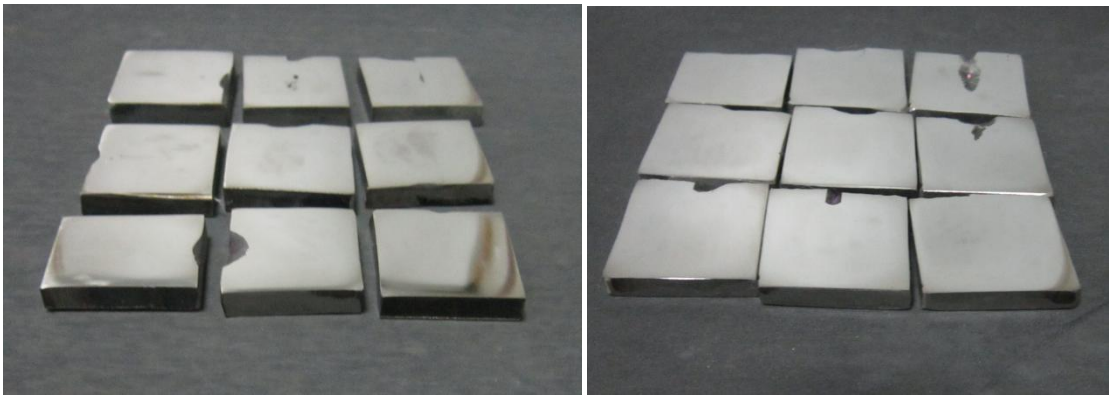

Figure 3.37: SS202 & SS304 specimens for microhardness testing

FIGURE 3.38: Microhardness test machine

(**Courtesy:** Central Workshop, Thapar University, Patiala)

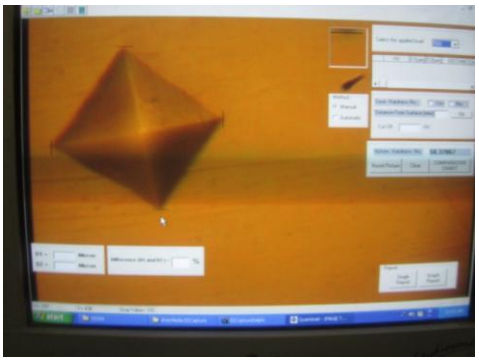

Figure 3.39: Diamond indent shown at 40X on the screen and its measurement

3.5.6. Joint Quality

All the polished specimens prepared above for microhardness testing were seen under optical (which uses a light beam to view the object) microscope at 100X to find the joint quality in terms of internal defects like crack, porosity, blow hole etc.

Figure 3.40: Leica optical microscope (**Courtesy:** Metrology lab, Thapar University, Patiala)

3.5.7. Chemical Composition of Weld Metal

The composition of base metal and welded metal was found by using atomic absorption spectrometer (Figure 3.41) in which Argon gas pressure was maintained at 60 litre/min and the software used for finding chemical composition was Worldwide Analytical System (WAS). Figure 3.42 shows the specimen for composition test.

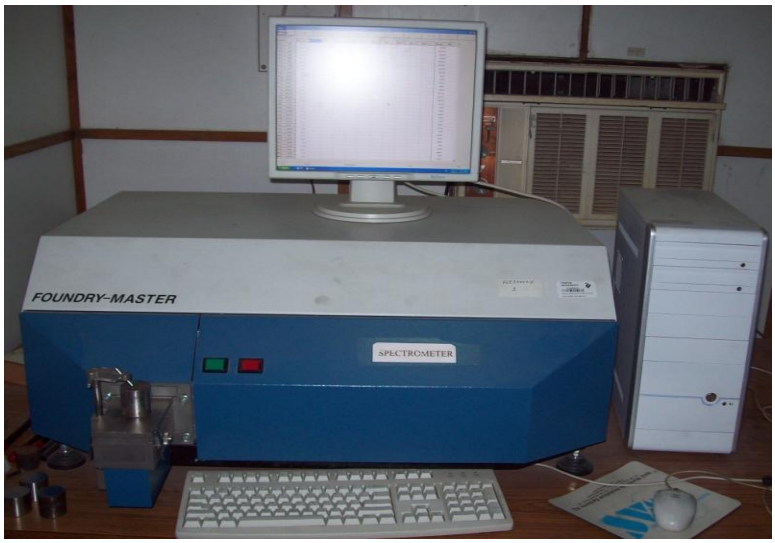

Figure 3.41: Atomic absorption spectrometer

(**Courtesy:** Central Workshop, Thapar University, Patiala)

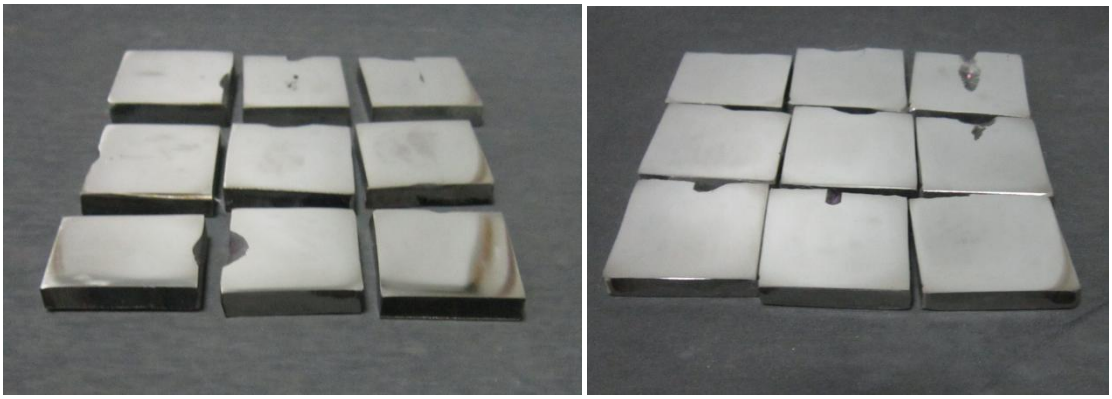

Figure 3.42: Samples for chemical composition testing

3.6. ANALYSIS OF RESULTS

Analysis of the results was to be done by using ANOVA for Mean.

3.6.1. Analysis of Variance

ANOVA is a statistical technique which can infer some important conclusions based on analysis of the experimental data. The method is very useful for revealing the level of significance of influence of factor(s) or interaction of factors on a particular response. It separates the total variability of the response (sum of squared deviations about the grand mean) into contributions rendered by each of the parameter/ factor and the error. Thus

$\mathbf{SS_T = SS_F + SS_E}$

Where, $SS_T = \sum_{J=1}^{P} \left(\gamma_j - \gamma_m\right)^2$

Where, SS_T = Total sum of squared deviations about the mean.

γ_j = Mean response for j^{th} experiment.

γ_m = Grand mean of the response.

SS_F = Sum of squared deviations due to each factor.

SS_E = Sum of squared deviations due to error.

In the ANOVA table mean square deviation is defined as:

MS = Mean Square

$$\mathbf{MS = \frac{SS\ (Sum\ of\ squared\ division)}{DOF\ (Degree\ of\ Freedom)}}$$

F-value of Fisher's F ratio (Variance ratio) is defined as:

$$\mathbf{F = \frac{MS\ for\ a\ term}{MS\ for\ the\ error\ term}}$$

Depending on F value, PC value (percentage contribution) is then calculated. F (critical) value is drawn from the table. If F-value for a term appears greater than its F(critical) then it can be concluded that the effect of the factors is significant on the selected response. Significance of all the dependent variables has been completed using statistical software MINITAB 15. The dependent variables studied in this study are (1) Bead Geometry (Bead width and height) (2) Toughness at room temperature (3) Toughness at -20 ^oC (4) Microhardness (HVN).

In the ANOVA table, the degrees of freedom are used to calculate the mean square (MS). In general, the degrees of freedom measure how much "independent" information is available to calculate each sum of squares (SS).

Total DOF = DOF for all factors + DOF for all interactions + DOF for error

Where n is the total number of observations and,

DOF for factor = $k-1$

Where k is the number of the factor levels.

DOF for Interaction = $(k_1-1) \times (k_2-1)$

Where k_1 is the number of levels of factor one, and k_2 is the number of levels of factor two. The same rule applies to interactions of more than two factors. In the present study, the interaction of factors has not been studied. The sequential sum of squares for each term in the model (factor or interaction) measures the amount of variation in the response that is explained by adding each term to the model sequentially in the order listed under. Thus, the sequential sums of squares for terms are specific to the order of the terms specified in the linear model. The adjusted sum of squares for a term in the model (factor or interaction) measures the amount of additional variation in the response that is explained by the term, given that all the other terms are already in the model. Thus, the values for the adjusted sums of squares do not depend on the order of the terms listed under source. The adjusted mean square for a term is simply the adjusted sum of squares (Adj. SS) divided by the degrees of freedom.

For this experimental work, the following response characteristics have been studied-

1. Response Name	:	Bead width
Response type	:	Smaller-the-better
Units	:	mm
2. Response Name	:	Bead Height
Response type	:	Smaller-the-better
Units	:	mm
3. Response Name	:	Toughness at room temperature (18 ^{o}C)
Response type	:	Higher-the-better
Units	:	Joule

4. Response Name	:	Toughness at -20 ^{o}C
Response type	:	Higher-the-better
Units	:	Joule
5. Response Name	:	Microhardness at weld region
Response type	:	Higher-the-better
Units	:	HVN

CHAPTER - 4

RESULTS OF BEAD GEOMETRY

Bead width and bead height measurement of the various welding specimens was done as explained earlier and the results of the measurement are shown as in the table 4.1.

4.1. RESULTS OF BEAD GEOMETRY FOR SS202 GRADE STAINLESS STEEL

Table 4.1 shows the different observations made for calculating the average bead width and height. On an average five reading for bead width and height were taken as explained earlier and average of all was taken as the final value.

Table 4.1.: Results of bead geometry for SS 202 grade stainless steel

Exp. n.	Parameters	Bead width observations	Bead height observations	Avg. Bead width (mm)	Avg. Bead height (mm)
1	I1,G1,F1,Θ1	9.72,7.33,8.87,8.95,9.68	0.44,0.30,0.68,0.50,0.54	8.91	0.492
2	I1,G2,F2,Θ2	10.76,10.73,8.83,7.92,10.41	1.22,1.12,0.90,1.06,0.84	9.73	1.028
3	I1,G3,F3,Θ3	9.96,10.70,10.20,9.30,9.28	0.96,0.94,0.46,0.60,1.02	9.888	0.796
4	I2,G1,F2,Θ3	9.93,9.91,9.27,10.12,9.37	0.50,0.34,0.40,0.36,0.34	9.72	0.388
5	I2,G2,F3,Θ1	8.13,9.87,11.55,11.51,11.32	0.82,1.12,1.32,1.24,1.28	10.476	1.156
6	I2,G3,F1,Θ2	10.09,10.11,9.57,9.83,10.01	0.42,0.38,0.40,0.48,0.50	9.922	0.436
7	I3,G1,F3,Θ2	10.03,10.46,9.47,9.69,9.40	0.70,0.74,0.58,0.52,0.52	9.81	0.612
8	I3,G2,F1,Θ3	10.81,10.50,10.89,11.17,10.96	0.36,0.52,0.40,0.44,0.74	10.866	0.492
9	I3,G3,F2,Θ1	12.18,12.76,12.87,12.52,12.11	0.36,0.58,0.68,0.76,1.22	12.488	0.72

Figure 4.1 & 4.2 shows the variation of bead width and bead height for the different experiments performed on SS 202 grade stainless steel materials.

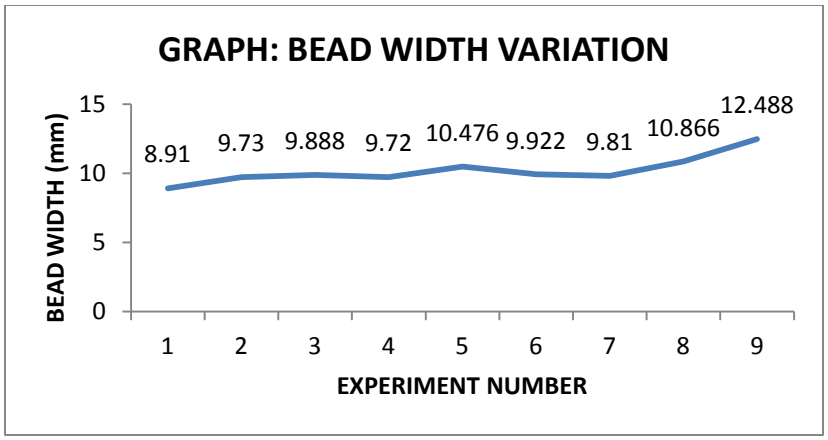

Figure 4.1: Graph showing variation of bead width for different experiments conducted on SS 202 grade stainless steel material

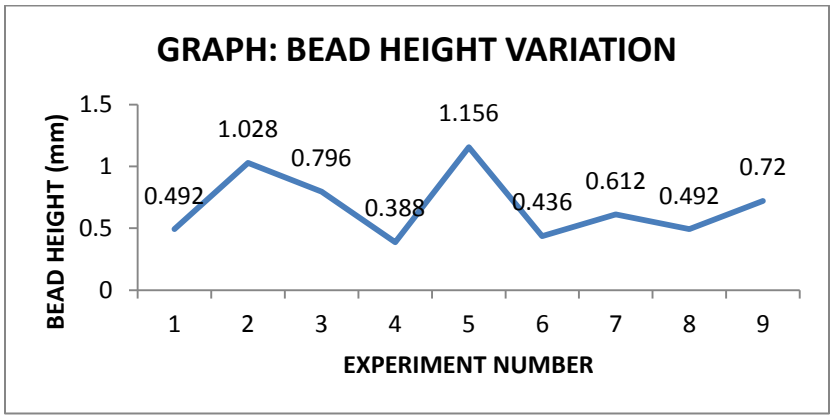

Figure 4.2: Graph showing variation of bead height for different experiments conducted on SS 202 grade stainless steel material

4.1.1. ANOVA table for the variation of bead width on SS202 steel

Column no. 5 of table 4.1 gives the average values of bead width for the different specimens. It is clear from the ANOVA table that current is the significant factor in affecting bead width statistically. Minimum value of bead width in Table 4.1 is 8.91 mm (140 A, Ar, 9l/min. & 60^0). After current shielding gas has the major effect on bead width. It is also clear from figure 4.3 that with the increase of current value of bead width increases and amongst the gases argon gives the minimum values of bead width. Main effects are plotted in figure 4.3 and show the variation in bead width with all the four parameters. It is clear from the figure that current and shielding gas has the major effect on bead width and gas flow rate has minor effect on bead width.

Table 4.2: Analysis of variance for SN ratio of Weld Bead Width for SS202 material

Source	Units	DOF	SS	Variance	F	F(critical)	PC
Current	Ampere	2	2.48752	1.24376	4.582	19.0	46.044
Gas	--------	2	1.79824	0.89912	3.313	19.0	33.286
Gas flow rate	L/min.	2	0.57383	0.28692	1.057	19.0	10.622
Grove angle	Degrees	2	0.54284	0.27142	1.0	19.0	10.048
Total		8	5.40243				100
Pooled Error		2	0.54284	0.27142			10.048

(SS= Sum of Square, F= F factor, PC = percent contribution, factor with least variance value is considered for error pooling)

Table 4.3: Response table for SN ratio of Weld Bead Width for SS202 material

LEVEL	CURRENT	GAS	GAS FLOW RATE	GROVE ANGLE
1	-19.55	-19.53	-19.88	-20.44
2	-20.03	-20.30	-20.48	-19.84
3	-20.83	-20.59	-20.05	-20.13
DELTA	1.27	1.06	0.60	0.60
RANK	1	2	4	3

Table 4.4: Analysis of variance for means of Weld Bead Width for SS202 material

Source	Units	DOF	SS	Variance	F	F(critical)	PC
Current	Ampere	2	3.69986	1.84993	3.985	19.0	45.138
Gas	--------	2	2.59052	1.29526	2.791	19.0	31.604
Gas flow rate	L/min.	2	0.92843	0.46422	1.0	19.0	11.327
Grove angle	Degrees	2	0.97799	0.48899	1.0533	19.0	11.931
Total		8	8.19679				100
Pooled Error		2	0.92843	0.46422			11.327

(SS= Sum of Square, F= F factor, PC = percent contribution, factor with least variance value is considered for error pooling)

Table 4.5: Response table for means of Weld Bead Width for SS202 material

LEVEL	CURRENT	GAS	GAS FLOW RATE	GROVE ANGLE
1	9.509	9.480	9.899	10.625
2	10.039	10.357	10.646	9.821
3	11.055	10.766	10.058	10.158
DELTA	1.545	1.286	0.747	0.804
RANK	1	2	4	3

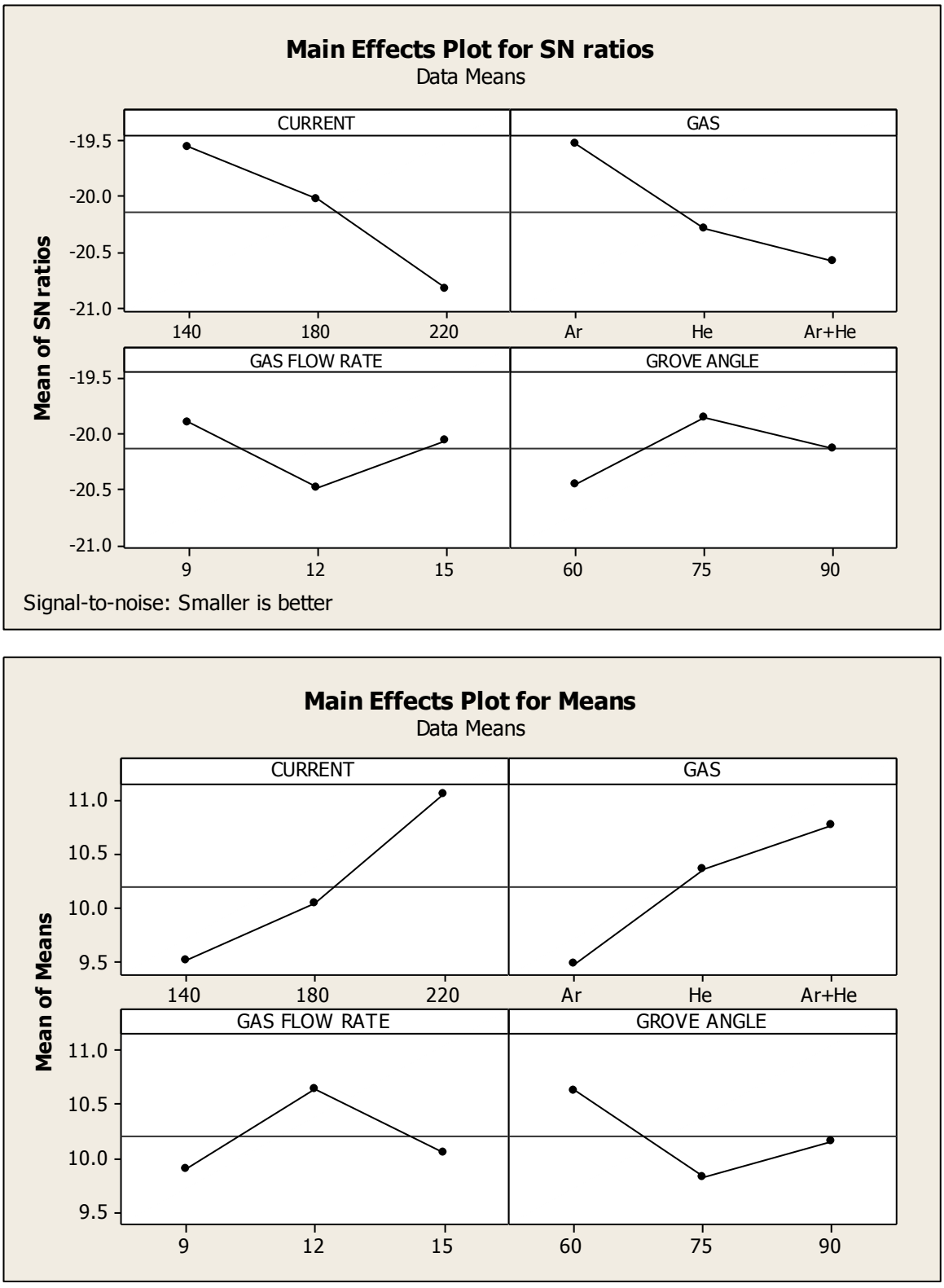

Figure 4.3: Main effects plot for SN ratios and means for Weld Bead Width of SS202

4.1.1.1. Optimal design for bead width of SS202 steel

It is clear from ANOVA for means (table 4.3) that F value of not even a single factor is greater than F (critical) so we can say statistically that there is no optimum value of bead width.

4.1.2. ANOVA table for the variation of Weld Bead Height on SS202 steel

Table 4.1 and column no. 6 gives the values of average bead height for the various specimens of SS202 steel. The results of bead width are analysed using ANOVA and are given from table 4.6 to 4.9. It is clear from table 4.6 and table 4.8 that gas and gas flow rate has major impact on bead height and equally affect the same. It is clear from table 4.6 and 4.8 that no factor's F value is greater than the critical value so we can conclude that no factor is most significant statistically and we cannot give any optimum value statistically. Minimum value of bead height is obtained in experiment no. 4 (180 A, Ar, 12l/min. & 90^0). From main effects diagram we can conclude that bead height is minimum for argon gas in comparison to others and similar is the case with a gas flow rate of 9 l/min. in comparison to others. Current and grove angle does not play any significant role for the above response.

Table 4.6: Analysis of variance for SN ratio of Weld Bead Height for SS202 material

Source	Units	DOF	SS	Variance	F	F(critical)	PC
Current	Ampere	2	7.6716	3.8358	1.0	19.0	8.666
Gas	--------	2	32.6415	16.3207	4.255	19.0	36.872
Gas flow rate	L/min.	2	35.7050	17.8525	4.654	19.0	40.332
Grove angle	Degrees	2	12.5092	6.2546	1.631	19.0	14.130
Total		8	88.5274				100
Pooled Error		2	7.6716	3.8358			8.666

(SS= Sum of Square, F= F factor, PC = percent contribution, factor with least variance value is considered for error pooling)

Table 4.7: Response table for SN ratio of Weld Bead Height for SS202 material

Level	Current	Gas	Gas flow rate	Grove angle
1	2.634	6.216	6.511	2.585
2	4.725	1.554	3.612	3.745
3	4.426	4.015	1.663	5.455
DELTA	2.091	4.662	4.848	2.870
RANK	4	2	1	3

Table 4.8: Analysis of variance for means of Weld Bead Height for SS202 material

Source	Units	DOF	SS	Variance	F	F(critical)	PC
Current	Ampere	2	0.042144	0.021072	1.0	19.0	7.231
Gas	--------	2	0.237515	0.118757	5.636	19.0	40.751
Gas flow rate	L/min.	2	0.222731	0.111365	5.285	19.0	38.214
Grove angle	Degrees	2	0.080459	0.040229	1.909	19.0	13.804
Total		8	0.582848				100
Pooled Error		2	0.042144	0.021072			7.231

(SS= Sum of Square, F= F factor, PC = percent contribution, factor with least variance value is considered for error pooling)

Table 4.9: Response table for means of Weld Bead Height for SS202 material

LEVEL	CURRENT	GAS	GAS FLOW RATE	GROVE ANGLE
1	0.7720	0.4973	0.4733	0.7893
2	0.6600	0.8920	0.7120	0.6920
3	0.6080	0.6507	0.8547	0.5587
DELTA	0.1640	0.3947	0.3813	0.2307
RANK	4	1	2	3

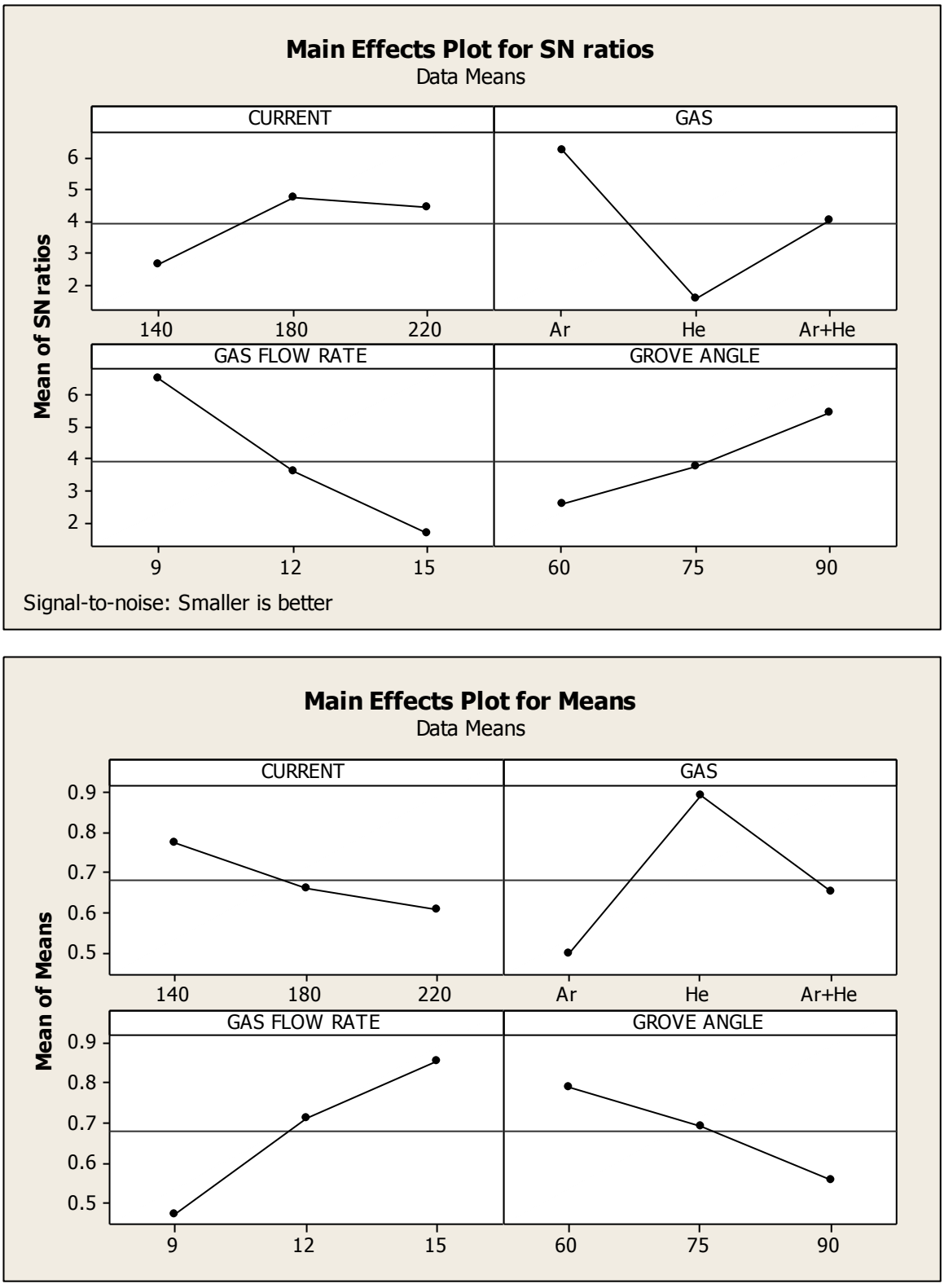

Figure 4.4: Main effects plot for SN ratios and means for Weld Bead Height of SS202 steel

4.2. RESULTS OF BEAD GEOMETRY FOR SS304 GRADE STAINLESS STEEL

Table 4.10 shows the different observations made for calculating the average bead width and height. On an average five reading for bead width and height were taken as explained earlier and average of all was taken as the final value.

Table 4.10: Results of Bead Geometry for SS 304 Grade Stainless Steel Specimens

Exp. N.	Parameters	Bead width observations	Bead height observations	Avg. bead width (mm)	Avg. bead height (mm)
1	I1,G1,F1,Θ1	8.04,7.70,8.27,9.10,7.91	1.3,0.48,1.02,0.88,0.74	8.204	0.884
2	I1,G2,F2,Θ2	9.98,9.08,8.63,8.09,7.96	1.32,0.90,0.82,0.92,1.0	8.748	0.992
3	I1,G3,F3,Θ3	9.13,8.31,8.08,7.67,7.06	1.00,0.54,0.50,0.70,0.84	8.05	0.716
4	I2,G1,F2,Θ3	8.40,8.67,9.70,8.48,9.00	0.40,0.08,0.36,0.08,0.18	8.85	0.22
5	I2,G2,F3,Θ1	10.22,12.00,9.85,10.40,9.15	1.42,1.04,1.62,1.78,1.42	10.324	1.456
6	I2,G3,F1,Θ2	9.29,8.11,8.27,8.35,8.44	1.14,0.80,0.86,0.92,1.38	8.492	1.02
7	I3,G1,F3,Θ2	8.88,10.44,8.92,10.17,9.16	1.52,1.42,1.02,1.5,1.56	9.514	1.404
8	I3,G2,F1,Θ3	12.25,12.64,12.13,12.47,13.69	0.94,0.90,0.58,0.50,0.36	12.636	0.656
9	I3,G3,F2,Θ1	9.18,9.42,10.25,11.83,10.92	0.14,0.18,0.62,0.36,0.08	10.32	0.276

Figure 4.5 & 4.6 shows the variation of bead width and bead height for the different experiments performed on SS 304 grade stainless steel materials.

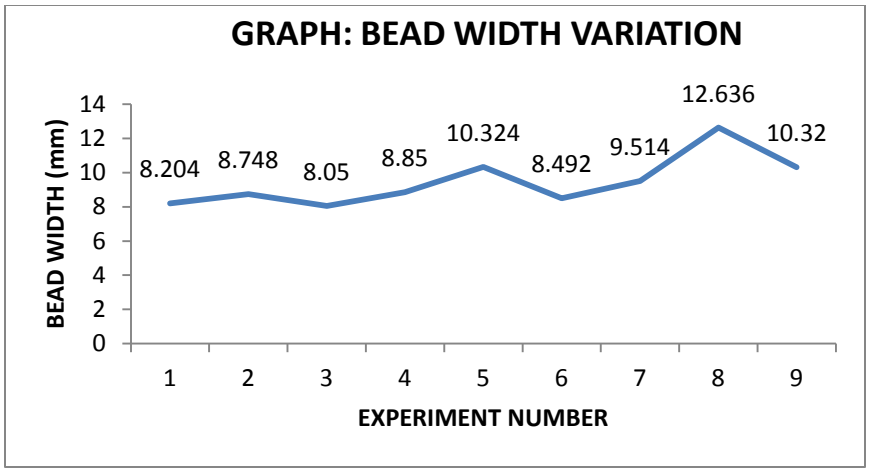

Figure 4.5: Graph showing variation of bead width for different experiments conducted on SS 304 grade stainless steel material

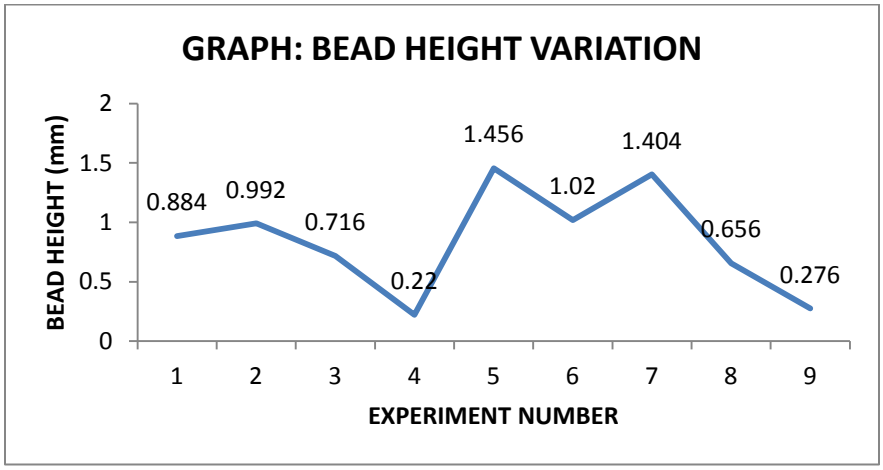

Figure 4.6: Graph showing variation of bead height for different experiments conducted on SS 304 grade stainless steel material

4.2.1. ANOVA table for the variation of bead width on SS304 steel

Table 4.10 and column no. 5 gives the values of bead width for the various experiments on SS304 steel. The results are analysed using ANOVA and are shown in the form of tables from table 4.11 to table 4.14. It is clear from the tables that current is the most significant factor effecting bead width and then is the shielding gas whereas gas flow rate and grove angle have almost negligible effect on the same. Minimum value of bead width is for experiment no. 3 (140 A, Ar-He, 15 l/min. and 90^0). It is clear from main effects plot in figure 4.7 that increase in current increases the value of current and among the gases except pure helium other gases keeps the bead width to minimum value.

Table 4.11: Analysis of variance for SN ratio of Weld Bead Width for SS304 material

Source	Units	DOF	SS	Variance	F	F(critical)	PC
Current	Ampere	2	7.47244	3.73622	42.3653	19.0	59.395
Gas	--------	2	4.05573	2.02787	22.9917	19.0	32.237
Gas flow rate	L/min.	2	0.17641	0.08820	1.0	19.0	1.402
Grove angle	Degrees	2	0.87630	0.43815	4.9677	19.0	6.965
Total		8	12.5809				100
Pooled Error		2	0.17641	0.08820			1.402

(SS= Sum of Square, F= F factor, PC = percent contribution, factor with least variance value is considered for error pooling)

Table 4.12: Response table for SN ratio of Weld Bead Width for SS304 material

LEVEL	CURRENT	GAS	GAS FLOW RATE	GROVE ANGLE
1	-18.41	-18.93	-19.63	-19.61
2	-19.27	-20.38	-19.35	-19.00
3	-20.62	-18.99	-19.32	-19.70
DELTA	2.21	1.45	0.31	0.70
RANK	1	2	4	3

TABLE 4.13: Analysis of variance for means of Weld Bead Width for SS304 material

Source	Units	DOF	SS	Variance	F	F(critical)	PC
Current	Ampere	2	9.54959	4.77480	21.037	19.0	56.314
Gas	--------	2	5.55442	2.77721	12.236	19.0	32.755
Gas flow rate	L/min.	2	0.45394	0.22697	1.0	19.0	2.677
Grove angle	Degrees	2	1.39974	0.69987	3.084	19.0	8.254
Total		8	16.9577				100
Pooled Error		2	0.45394	0.22697			2.677

(SS= Sum of Square, F= F factor, PC = percent contribution, factor with least variance value is considered for error pooling)

Table 4.14: Response table for means of Weld Bead Width for SS304 material

LEVEL	CURRENT	GAS	GAS FLOW RATE	GROVE ANGLE
1	8.334	8.856	9.777	9.616
2	9.222	10.569	9.306	8.918
3	10.823	8.954	9.296	9.845
DELTA	2.489	1.713	0.481	0.927
RANK	1	2	4	3

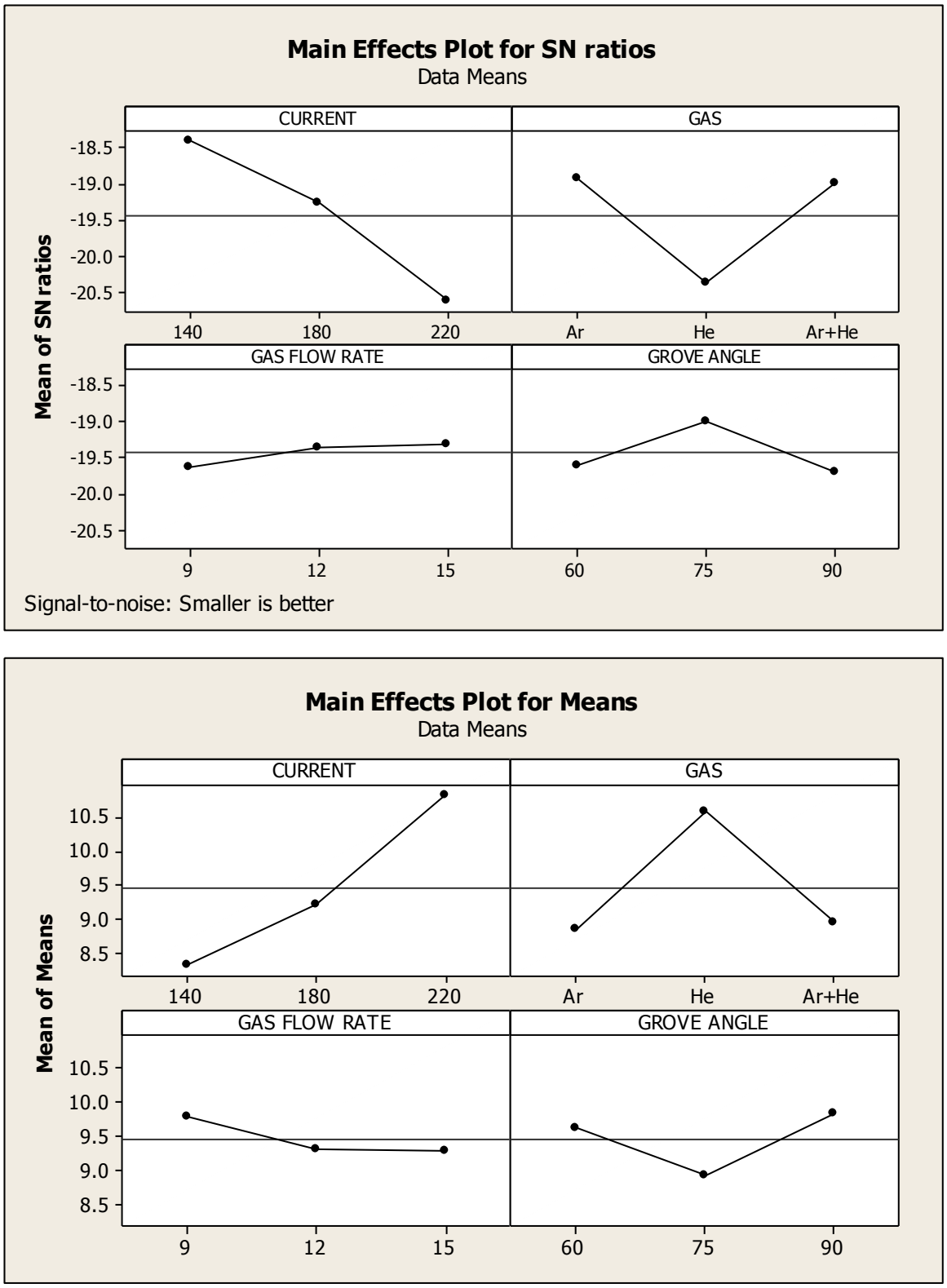

Figure 4.7: Main effects plot for SN ratios and means for Weld Bead Width of SS304 steel

4.2.1.1. Optimal design for bead width of SS304 steel

It is clear from ANOVA for means (table 4.13) that F value of only current is greater than F (critical) and the main effect plot shows that bead width is minimum for 140 A current. So from response table of means we can conclude that mean value of bead width is 8.334 mm.

4.2.2. ANOVA table for the variation of bead Height on SS304 steel

The results of bead height are given in column no. 6 of table 4.10. The results are being analysed using ANOVA and are compiled from table 4.15 to table 4.18. It is clear from the results that gas flow rate and grove angle are the most significant factors for bead height. Minimum value of bead height is obtained for experiment no. 4 (180 A, Ar, 12l/min. & 60^0). It is clear from mains effect plotted in figure 4.8 that bead height is minimum for a gas flow rate of 12 l/min. among the three values and grove angle of 90^0 gives the minimum value of bead height. Welding current has negligible effect on the bead height. Amongst the gases Ar-He mixture provides the desired results.

Table 4.15 Analysis of variance for SN ratio of Weld Bead Height for SS304 material

Source	Units	DOF	SS	Variance	F	F(critical)	PC
Current	Ampere	2	10.959	5.4794	1.0	19.0	4.101
Gas	--------	2	33.828	16.9140	3.087	19.0	12.66
Gas flow rate	L/min.	2	135.956	67.9778	12.406	19.0	50.88
Grove angle	Degrees	2	86.468	43.2342	7.890	19.0	32.359
Total		8	267.211				100
Pooled Error		2	10.959	5.4794			4.101

(SS= Sum of Square, F= F factor, PC = percent contribution, factor with least variance value is considered for error pooling)

Table 4.16: Response table for SN ratio of Weld Bead Height for SS304 material

LEVEL	CURRENT	GAS	GAS FLOW RATE	GROVE ANGLE
1	1.3475	3.7584	1.5203	2.9965
2	3.2388	0.1562	8.1344	-1.0165
3	3.9655	4.6372	-1.1029	6.5717
DELTA	2.6180	4.4810	9.2373	7.5883
RANK	4	3	1	2

Table 4.17: Analysis of variance for means of Weld Bead Height for SS304 material

Source	Units	DOF	SS	Variance	F	F(critical)	PC
Current	Ampere	2	0.022884	0.011442	1.0	19.0	1.519
Gas	--------	2	0.199300	0.099650	8.709	19.0	13.231
Gas flow rate	L/min.	2	0.726798	0.363399	31.760	19.0	48.252
Grove angle	Degrees	2	0.557284	0.278642	24.353	19.0	36.998
Total		8	1.50626				100
Pooled Error		2	0.022884	0.011442			1.519

(SS= Sum of Square, F= F factor, PC = percent contribution, factor with least variance value is considered for error pooling)

Table 4.18: Response table for means of Weld Bead Height for SS304 material

LEVEL	CURRENT	GAS	GAS FLOW RATE	GROVE ANGLE
1	0.8640	0.8360	0.8533	0.8720
2	0.8987	1.0347	0.4960	1.1387
3	0.7787	0.6707	1.1920	0.5307
DELTA	0.1200	0.3640	0.6960	0.6080
RANK	4	3	1	2

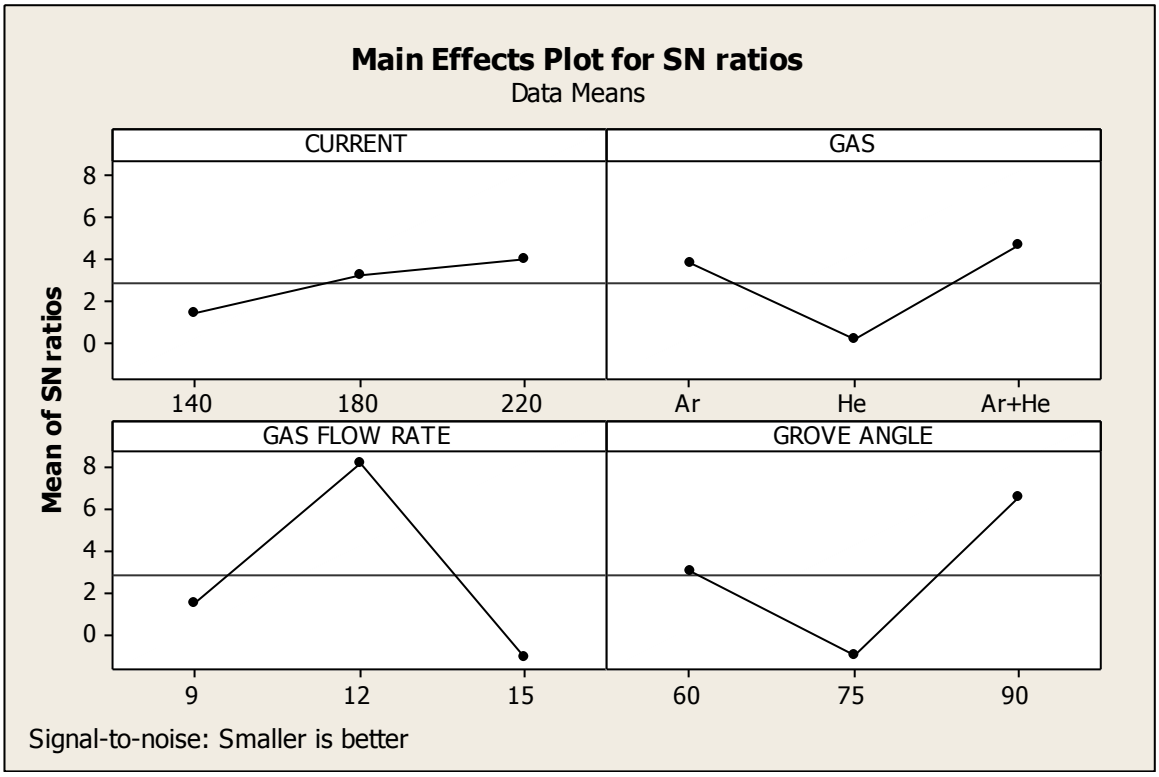

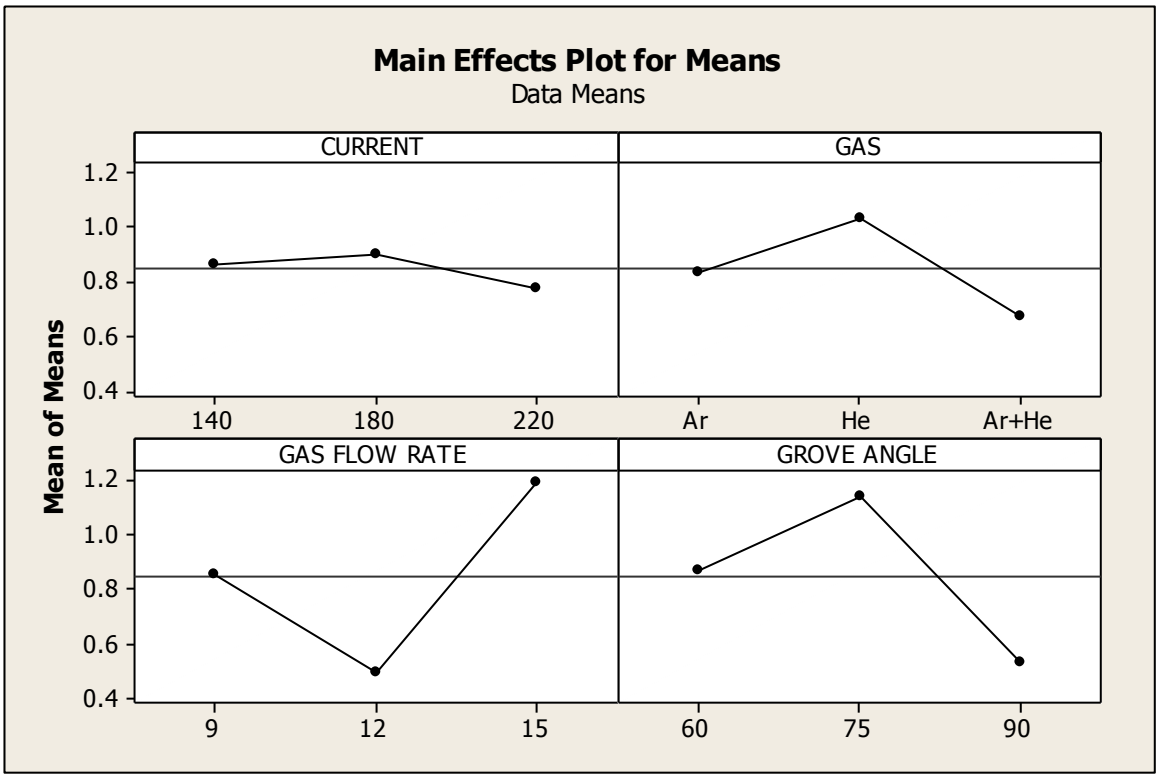

Figure 4.8: Main effects plot for SN ratios and means for Weld Bead Height of SS304 steel

4.2.2.1. Optimal design for bead height of SS304 steel

It is clear from ANOVA for means (table 4.13) that F value of gas flow rate and grove angle is greater than F (critical) and the main effect plot shows that bead height is minimum for second level of gas flow rate (i.e. 12 l/min.) and third level of grove angle (i.e. 90^0). Confidence interval predict with 95 % confidence so that value of bead height for SS304 steel would be 0.1796 ± 0.10697 mm.

Mean value of bead height is given by-

$\mu_{F2\theta3} = \overline{F_2} + \overline{\theta_2} - \overline{T}$

= 0.4960 + 0.5307 – 0.8471 (where $\overline{T}$ = average bead height calculated from table)

= 0.1796 mm

Confidence Interval around the estimated mean toughness

$C.I. = \sqrt{\frac{f\alpha:v1:v2\ X\ Ve}{neff}}$

v2 = DOF for error = 2

Where $f\,\alpha: v1:v2 = f\,0.05:1:2 = 18.5$

Variance of error = $Ve = 0.011442$

$n_{eff} = \frac{9}{1+\mathrm{DOF}_{F2\theta3}} = 1.40$

C.I. = 0.10697

So, the confidence interval for bead width is given by 0.1796 ± 0.10697 mm.

CHAPTER - 5

RESULTS OF HARDNESS TEST

As discussed earlier, hardness of the specimens was measured at the centre of the weld (mean position), 2 mm away from mean position, 5 mm away from mean position and then 5 mm away from last point till the end as shown in the figure 5.1. 3-4 readings were taken at main position like weld metal and heat affected zone.

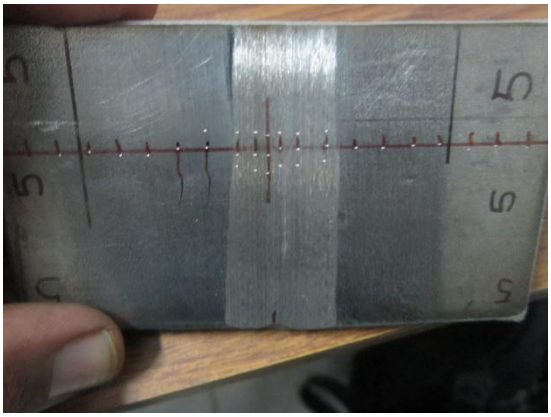

Figure 5.1: Specimen showing indentation marks after hardness test

5.1. ROCKWELL (C-SCALE) HARDNESS TEST RESULTS FOR SS202 STEEL

The summary of the hardness test is shown in the form of Table 5.1. The results of hardness test are plotted as graph in figure 5.2 (a-i). It is clear from the results that there is no significant variation in hardness of the weld region, HAZ and base metal. It may be because of the chromium oxide layer formed on the surface of the metal.

Table 5.1: Rockwell Hardness Test Values for SS 202 Grade Stainless Steel Specimens

EXP. NO	PARAMETERS	ROCKWELL HARDNESS (C-SCALE) TEST VALUE DISTANCE FROM MEAN '0' POSITION																				
		-45	-40	-35	-30	-25	-20	-15	-10	-5	-2	0	+2	+5	+10	+15	+20	+25	+30	+35	+40	+45
1	I1,G1, F1,Θ1	60	61	60	61	62	62	61	60	60.5	60	59.3	60	61	60	61	61	61	62	62	60	60
2	I1,G3, F2,Θ2	62	62	59	63	64	61	61	60.5	62	61.7	61.7	61.3	61.7	61.5	62	62	62	61	62	62	61
3	I1,G2, F3,Θ3	61	61	62	63	61	62	62	62	61	58	59	60	60	60	60	60	63	62	60	60	60
4	I2,G1, F2,Θ3	60	59	62	60	61	60	62	62	62	62	61	60	62	63	62	63	61	62	62	62	62
5	I2,G3, F3,Θ1	59	61	60	60	61	60	61	60.5	59.7	60.7	60.7	61	59.7	62	62	62	61	61	59	61	62
6	I2,G2, F1,Θ2	61	60	61	62	62	62	62	62	62	61.7	61.7	60.3	60.7	61	61	61	61.5	61	62	61	60
7	I3,G1, F3,Θ2	60	60	62	62	61	61	60	60	58	60.3	61	60	60.7	61.5	63	62	62	61	60	60	60
8	I3,G3, F1,Θ3	59	60	59	62	62	62	63	63	61	63	63	63	63	64	62	62	63	61	60	60	59
9	I3,G2, F2,Θ1	60	61	61	61	61	61	60	60	60	60	61	60.7	60.7	61	61	62	62	61	60	60	60

Variation of hardness values from mean position (centre of weld) for the SS202 grade stainless steel for different experiments is shown in the form of graphs in figure 5.2.

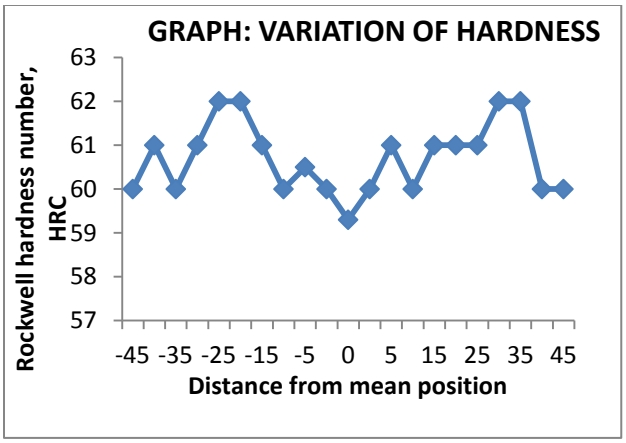

(a) For experiment no. 1

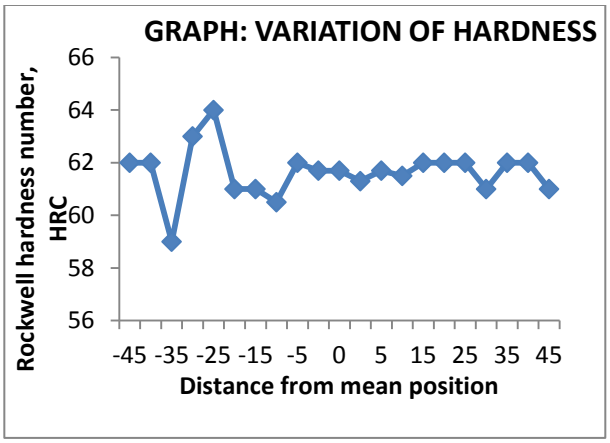

(b) For experiment no. 2

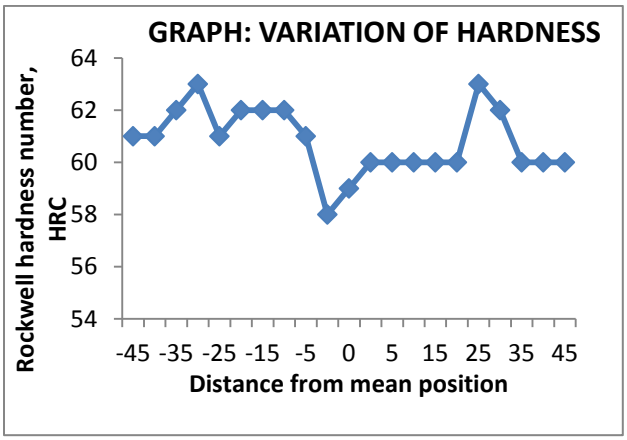

(c) For experiment no. 3

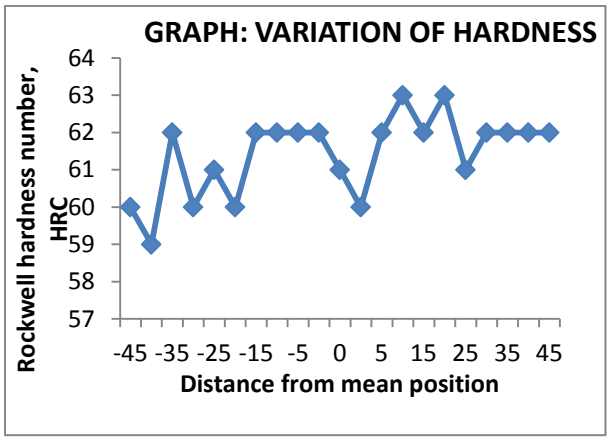

(d) For experiment no. 4

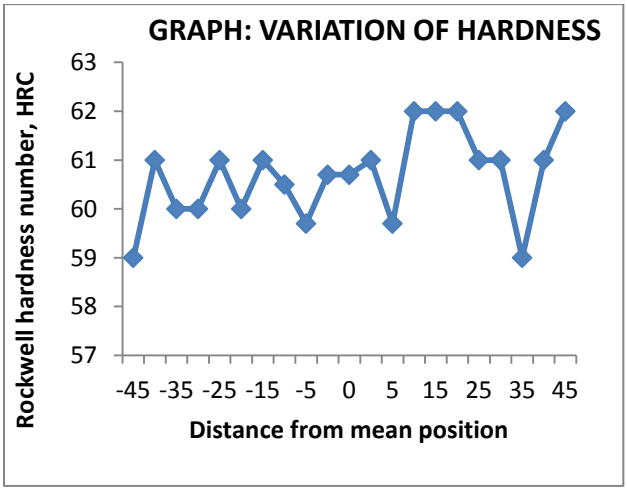

(e) For experiment no. 5

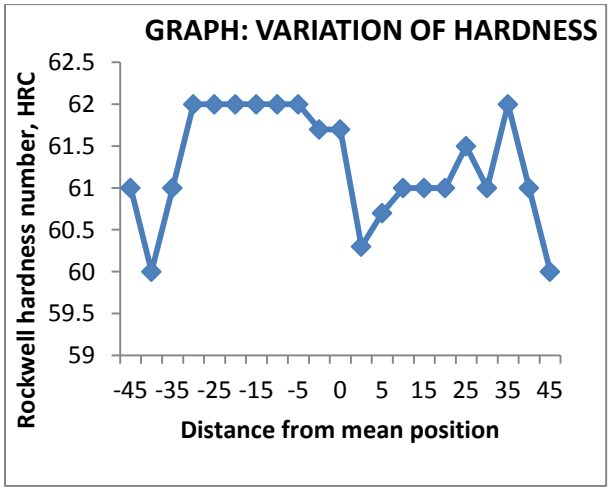

(f) For experiment no. 6

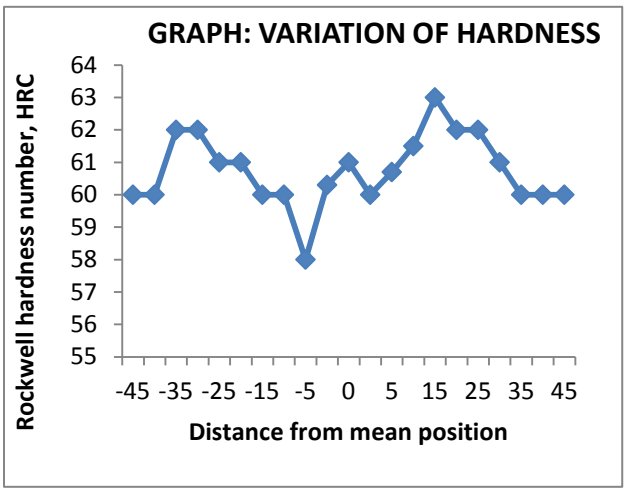

(g) For experiment no. 7

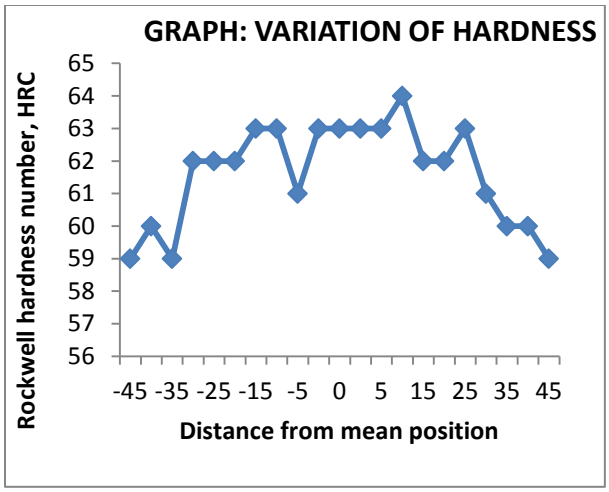

(h) For experiment no. 8

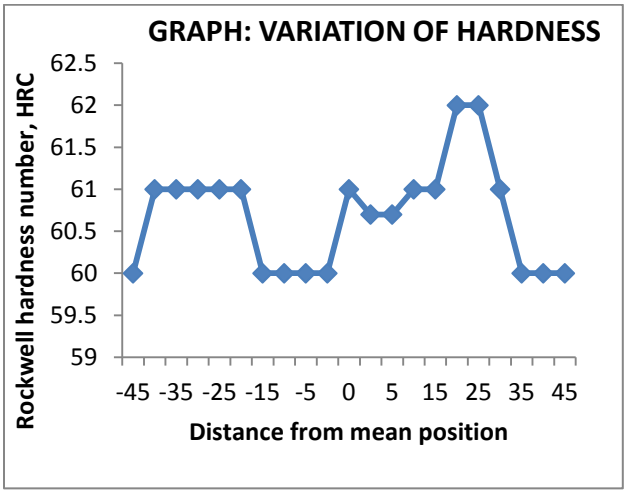

(i) For experiment no. 9

Figure 5.2 (a-i): Graphs for Rockwell hardness number (HRC) vs distance from mean position of experiments nos. 1-9 for SS202 grade steel

5.2. ROCKWELL (C-SCALE) HARDNESS TEST RESULTS FOR SS304 STEEL

The summary of the hardness test is shown in the form of Table 5.2. The results of hardness test are plotted as graph in figure 5.3 (a-i). It is clear from the results that there is no significant variation in hardness of the weld region, HAZ and base metal. It may be because of the chromium oxide layer formed on the surface of the metal.

Table 5.2: Rockwell Hardness Test Values for SS 304 Grade Stainless Steel specimens

EXP NO	PARAMETERS	ROCKWELL (C-SCALE) HARDNESS TEST VALUE DISTANCE FROM MEAN '0' POSITION																				
		-45	-40	-35	-30	-25	-20	-15	-10	-5	-2	0	+2	+5	+10	+15	+20	+25	+30	+35	+40	+45
1	I1,G1, F1,Θ1	58	57	57	58	60	60	60	60.5	60	59.7	60	59.7	60.7	61	59	60	60	58	58	56	57
2	I1,G3, F2,Θ2	56	57	58	58	58	59	59	58	57.7	58	59.7	58	58.3	60	60	60	60	58	58	59	57
3	I1,G2, F3,Θ3	59	60	58	59	59	59	60	59	58	58	58	59	57	60	59	58	59	60	58	59	56
4	I2,G1, F2,Θ3	57	57	58	59	59	59	59	57	57	58	57	57	57	58	59	59	59	58	59	60	59
5	I2,G3, F3,Θ1	61	61	61	58	58	59	60	59.5	60	60.3	59.7	59	59.7	59	60	59	59	59	58	57	57
6	I2,G2, F1,Θ2	59	59	58	59	57	59	60	59.5	58.7	60	59	59.7	58.7	58.5	59	59	58	58	58	59	60
7	I3,G1, F3,Θ2	60	59	60	60	59	59	59	60.5	59	59	58.7	58.7	59	61.5	63	57	58	57	59	60	60
8	I3,G3, F1,Θ3	60	60	60	60	60	60	59	57	58	59	59	60	58	58	59	58	60	61	59	60	62
9	I3,G2, F2,Θ1	57	56	59	58	59	59	59	59.5	57.7	60	59	59.7	58.7	59.5	59	59	58	58	58	57	58

Variation of hardness values from mean position (centre of weld) for the SS304 grade stainless steel for different experiments is shown in the form of graphs in figure 5.3.

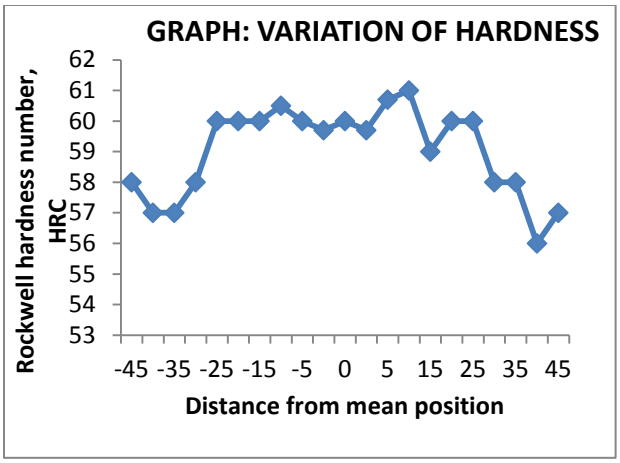

(a) For experiment no. 1

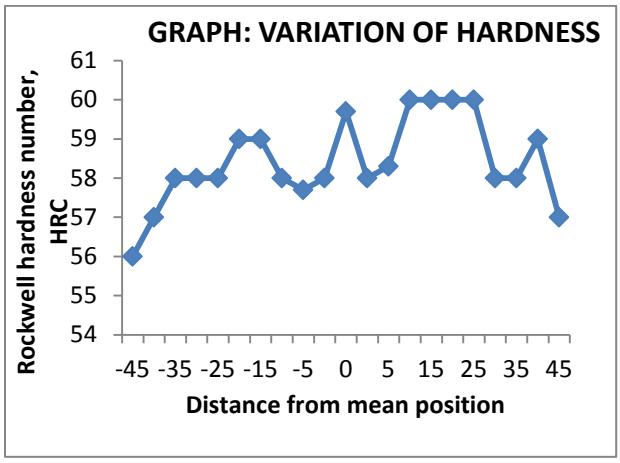

(b) For experiment no. 2

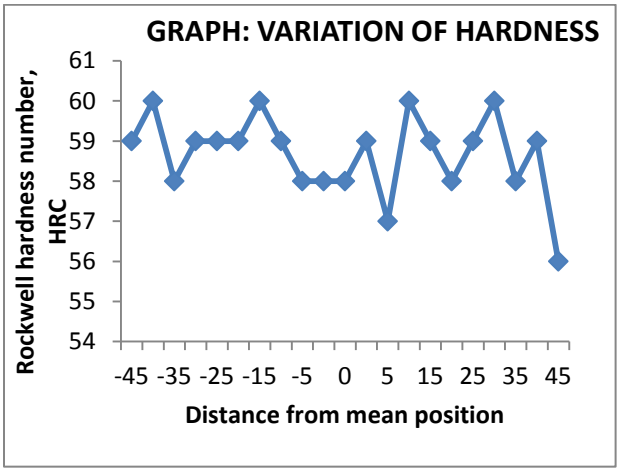

(c) For experiment no. 3

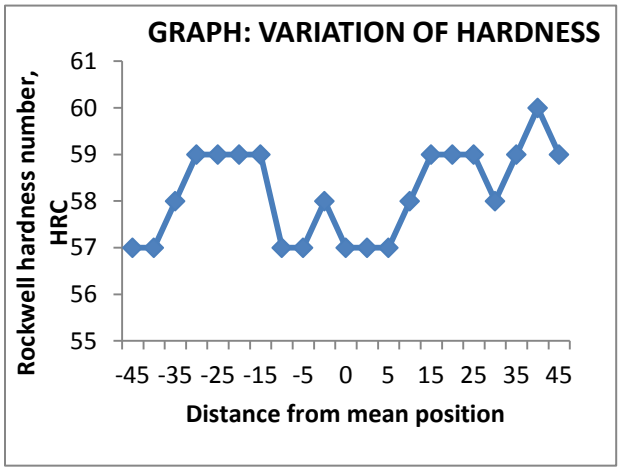

(d) For experiment no. 4

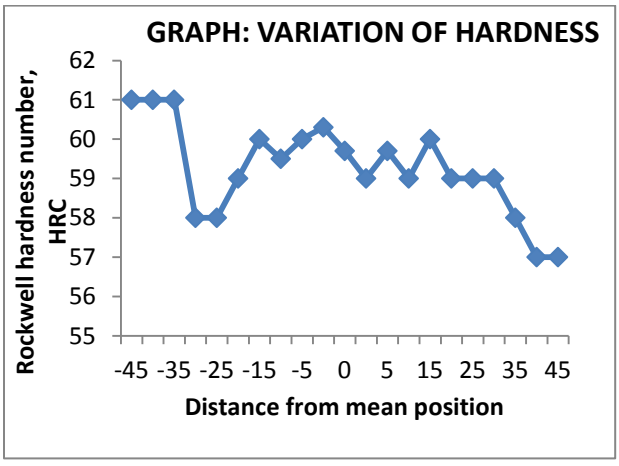

(e) For experiment no. 5

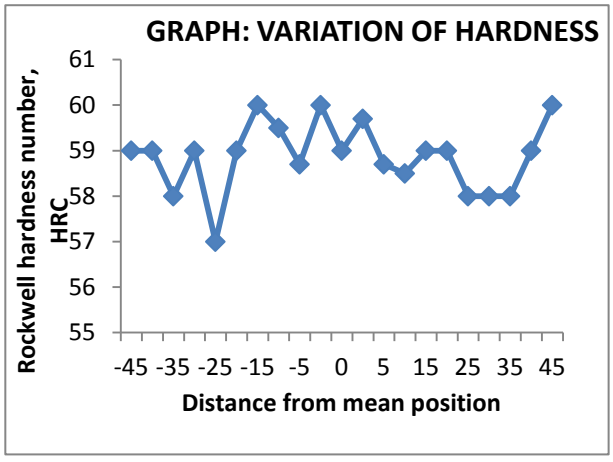

(f) For experiment no. 6

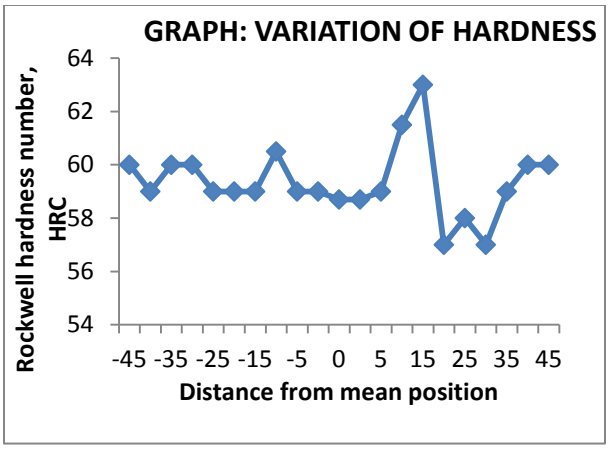

(g) For experiment no. 7

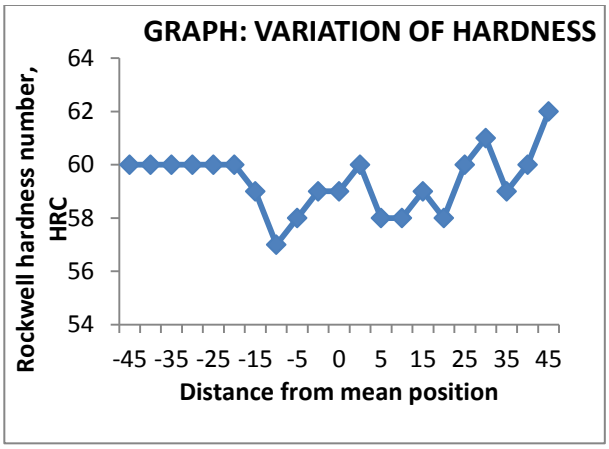

(h) For experiment no. 8

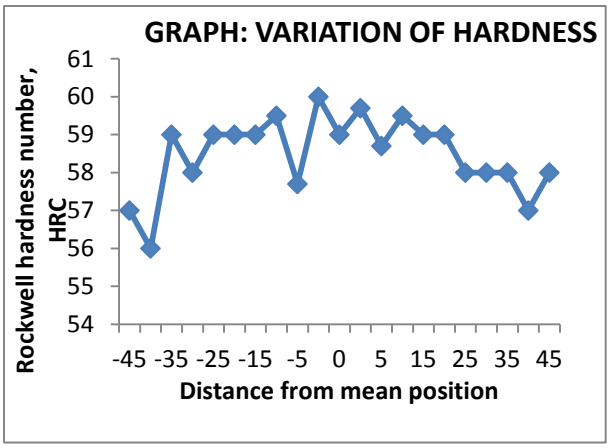

(i) For experiment no. 9

Figure 5.3 (a-i): Graphs for Rockwell hardness numbers (HRC) vs distance from mean position of experiments nos. 1-9 for SS304 grade steel

CHAPTER - 6

RESULTS OF DYE PENETRANT TEST (DPT)

Dye penetrant test was performed on the various specimens as discussed earlier and the results of the same are reported.

6.1. RESULTS OF DYE PENETRANT TEST (DPT) FOR SS304 STAINLESS STEEL

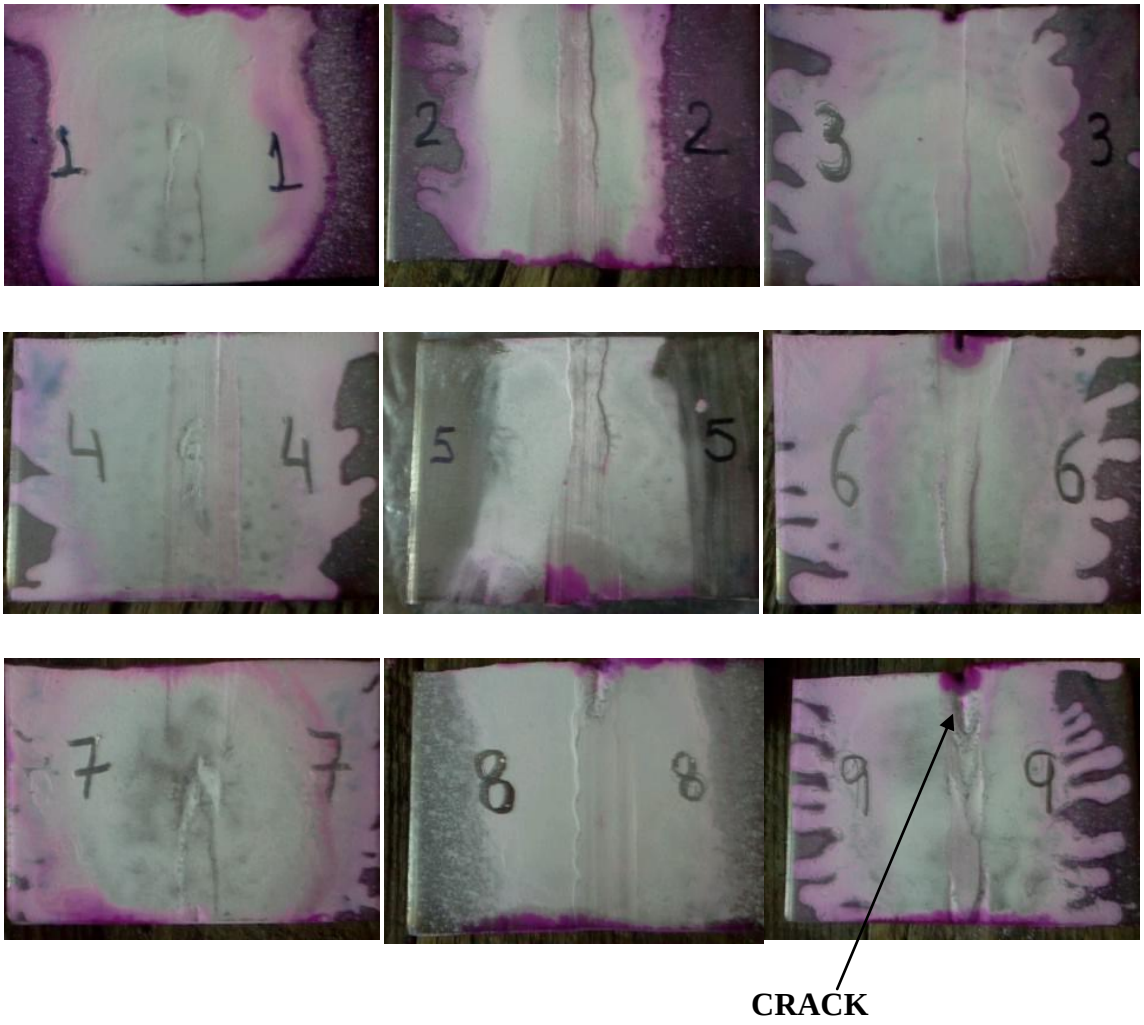

Figure 6.1: Results of Dye Penetrant Test (DPT) carried on SS304 specimens

Above figures shows that welded joints have no surface defect except specimen no. 9 which is having a minor surface defect at the extreme end of the plates. Last end of plate (nearly 10-15 mm) would be rejected while cutting the plates for various mechanical testing. In overall we can conclude that welded region have no surface cracks and porosity for the effective portion of the welded plates.

6.2. RESULTS OF DYE PENETRANT TEST (DPT) FOR SS202 STAINLESS STEEL

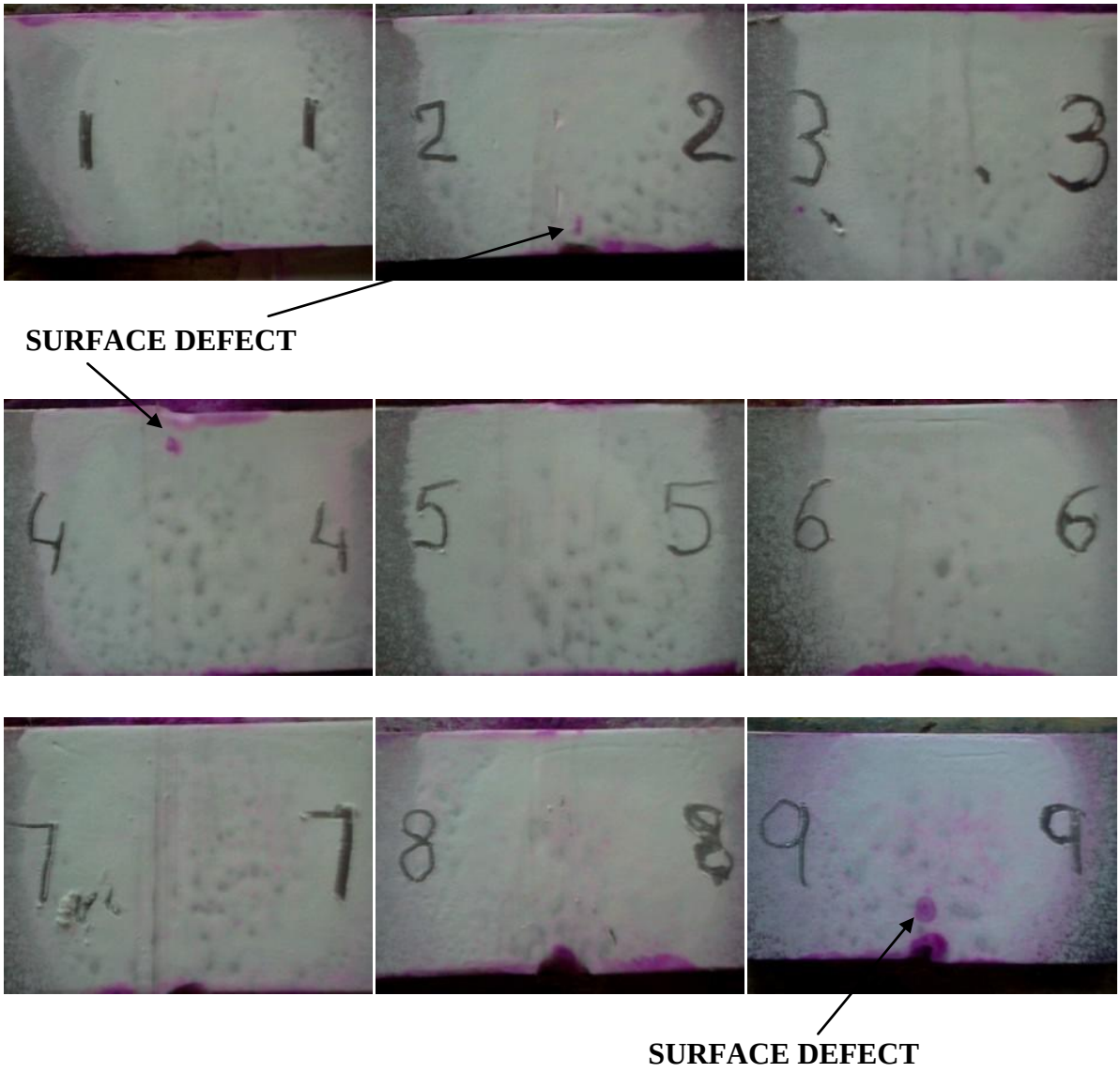

Figure 6.2: Results of Dye Penetrant Test (DPT) carried on SS202 specimens

Above figures shows that welded joints have no surface defect except specimen nos. 2, 4 & 9 which are having a minor surface defect at the extreme end of the plates. Last end of plate (nearly 10-15 mm) would be rejected while cutting the plates for various mechanical testing. In overall we can conclude that welded region have no surface cracks and porosity for the effective portion of the welded plates.

CHAPTER - 7

RESULTS OF TOUGHNESS TEST

As discussed earlier toughness is defined as the failure of a material when subjected to suddenly applied load. The tested specimens after toughness test are shown in the figure 7.1 to 7.3.

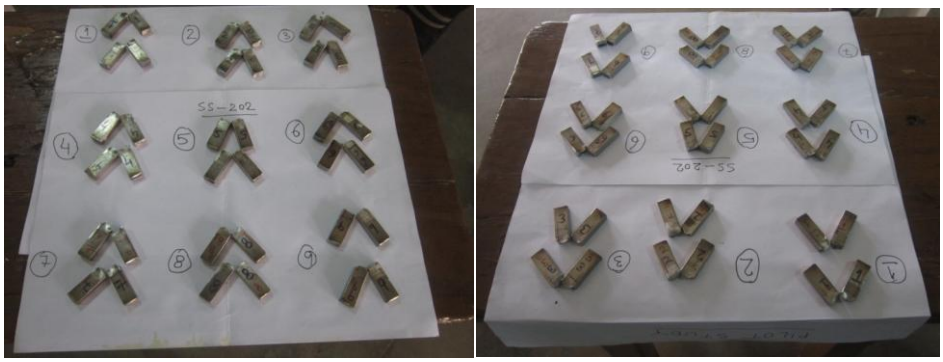

Figure 7.1: Specimens of SS 202 grade stainless steel after toughness test

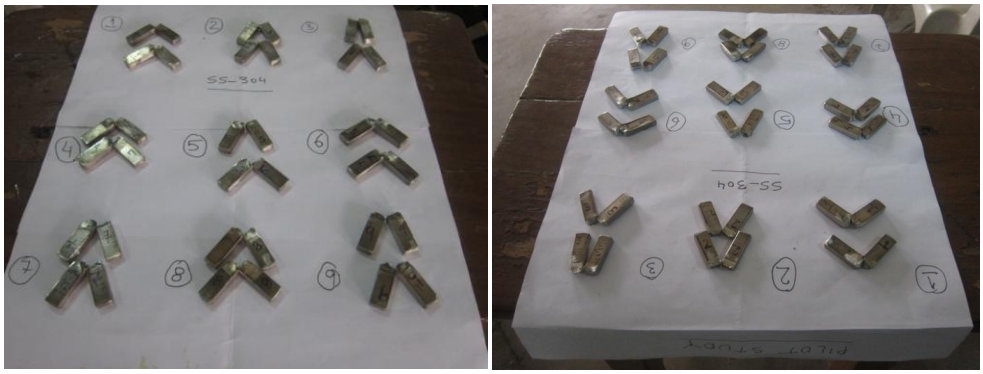

Figure 7.2: Specimens of SS 304 grade stainless steel after toughness test

Figure 7.3: Specimens after impact test at -20^0 C

The toughness test details for base metal are shown in the table 7.1.

Table 7.1: Toughness test values of base metal

Base metal	Charpy Test results at room temperature (18^0 C) (Joule)	Charpy Test results at -20^0 C (Joule)
SS 202	29.43	0.0
SS 304	83.385	63.765

For all nine set of experiments, the toughness test summary for both the metals are shown in the table 7.2 and 7.3. It is to be noted here that all experiments were repeated two times and the average values are shown.

7.1. TOUGHNESS TEST RESULTS FOR SS202 GRADE STEEL

Results of toughness test carried out on various experimental specimens of SS202 are shown in the table 7.2. It is clear from table 7.2 that SS202 grade steel specimens have almost zero strength at -20 ^{0}C so results of this are not analyzed by ANOVA.

Table 7.2: Charpy impact test results for SS 202 grade test samples

Experiment no.	Contributing factors	Charpy Test results at room temperature (18^0 C) (Joule)	Charpy Test results at -20^0 C (Joule)
1	I1,G1,F1,Θ1	58.86	4.905
2	I1,G2,F2,Θ2	39.24	4.905
3	I1,G3,F3,Θ3	61.3125	0.0
4	I2,G1,F2,Θ3	71.1225	0.0
5	I2,G2,F3,Θ1	17.1675	4.905
6	I2,G3,F1,Θ2	19.62	0.0
7	I3,G1,F3,Θ2	39.24	0.0
8	I3,G2,F1,Θ3	24.525	0.0
9	I3,G3,F2,Θ1	17.1675	0.0

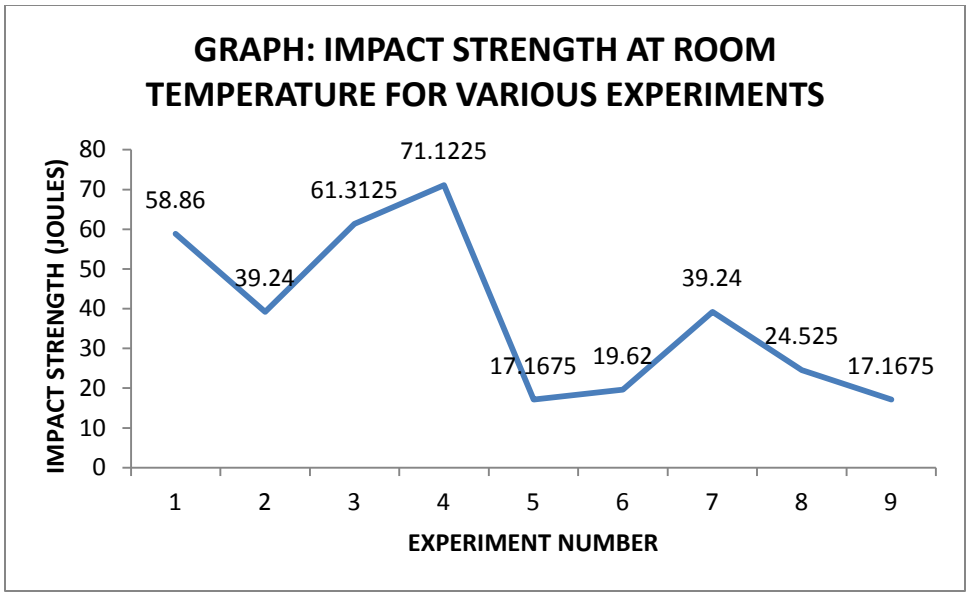

Figure 7.4: Graph showing variation of impact strength of SS 202 grade stainless steel material at room temperature for various experiments

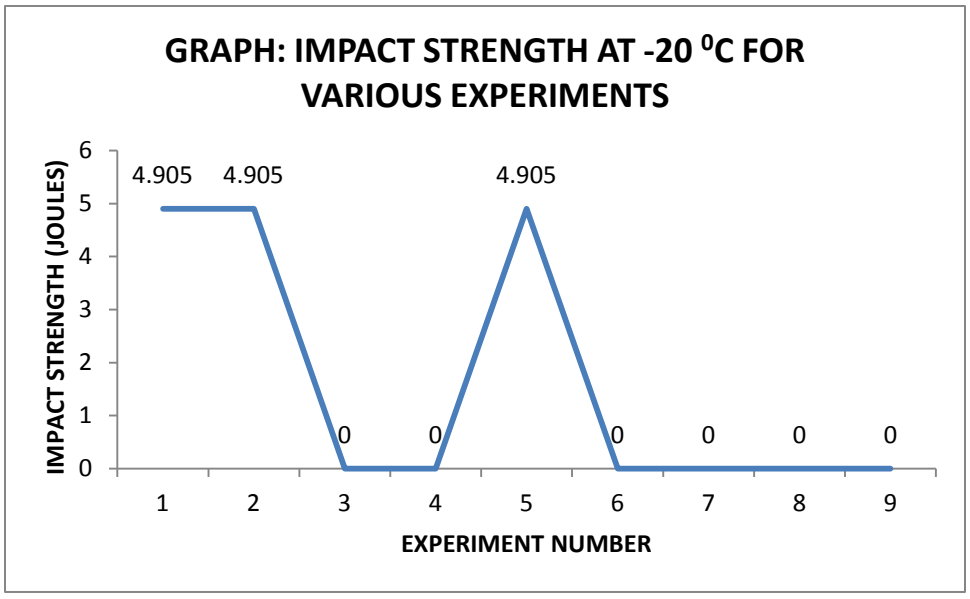

Figure 7.5: Graph showing variation of impact strength of SS 202 grade stainless steel material at -20^0 C temperature for various experiments

7.2. ANOVA FOR TOUGHNESS AT ROOM TEMPERATURE

Table 7.2 column no. 3 consists of the values of toughness at room temperature for the nine experiments of SS202 steel. The experimental results for toughness are analyzed using ANOVA and are given in table no. 7.3 to 7.6. The results show that nature of shielding gas is the most significant factor whereas gas flow rate is the least significant factor in effecting the toughness of SS202 grade stainless steel. Main effects plot for SN ratio and means given in figure 7.6 shows the variation in the toughness at room temperature with the change in the input factors i.e. current, gas, gas flow rate and grove angle. It is quite clear from the figure 7.6 that nature of gas is the most significant figure for toughness as the best results are obtained by using argon as the shielding gas and gas flow rate is the least one. Current and grove angle also affects the toughness considerably as toughness is higher for lower value of current and also higher for the maximum grove angle. From table of ANOVA for means we can see that F value of not even a single factor is greater than its critical counterpart and so we can conclude there is no factor which is significant statistically and hence we cannot optimize the results of the toughness at room temperature. Best value of toughness is obtained in the test results of experiments no. 4, 3 and 1. In general we can conclude that after welding the toughness value of welded joint has increased in comparison to the base metal for all the experiments except experiment nos. 5, 6 and 9.

Table 7.3: Analysis of variance for SN ratio of toughness at room temperature for SS202 material

Source	Units	DOF	SS	Variance	F	F(critical)	PC
Current	Ampere	2	66.3167	33.1584	17.94868	19.0	34.113
Gas	--------	2	80.6890	40.3445	21.83853	19.0	41.505
Gas flow rate	L/min.	2	3.6947	1.8474	1.0	19.0	1.900
Grove angle	Degrees	2	43.7086	21.8543	11.82976	19.0	22.483
Total		8	194.409				100
Pooled Error		2	3.6947	1.8474			1.900

(SS= Sum of Square, F= F factor, PC = percent contribution, factor with least variance value is considered for error pooling)

Table 7.4: Response table for SN ratio of toughness at room temperature for SS202 material

LEVEL	CURRENT	GAS	GAS FLOW RATE	GROVE ANGLE
1	34.34	34.77	29.68	28.26
2	29.20	28.12	31.20	29.87
3	28.12	28.77	30.77	33.53
DELTA	6.22	6.65	1.52	5.27
RANK	2	1	4	3

Table 7.5: Analysis of variance for means toughness at room temperature for SS202 material

Source	Units	DOF	SS	Variance	F	F(critical)	PC
Current	Ampere	2	1059.93	529.967	10.434	19.0	30.62
Gas	--------	2	1460.92	730.459	14.382	19.0	42.201
Gas flow rate	L/min.	2	101.58	50.791	1.0	19.0	2.934
Grove angle	Degrees	2	839.39	419.696	8.263	19.0	24.247
Total		8	3461.83				100
Pooled Error		2	101.58	50.791			2.934

(SS= Sum of Square, F= F factor, PC = percent contribution, factor with least variance value is considered for error pooling)

Table 7.6: Response table for means toughness at room temperature for SS202 material

LEVEL	CURRENT	GAS	GAS FLOW RATE	GROVE ANGLE
1	53.14	56.41	34.34	31.07
2	35.97	26.98	42.51	32.70
3	26.98	32.70	39.24	52.32
DELTA	26.16	29.43	8.18	21.25
RANK	2	1	4	3

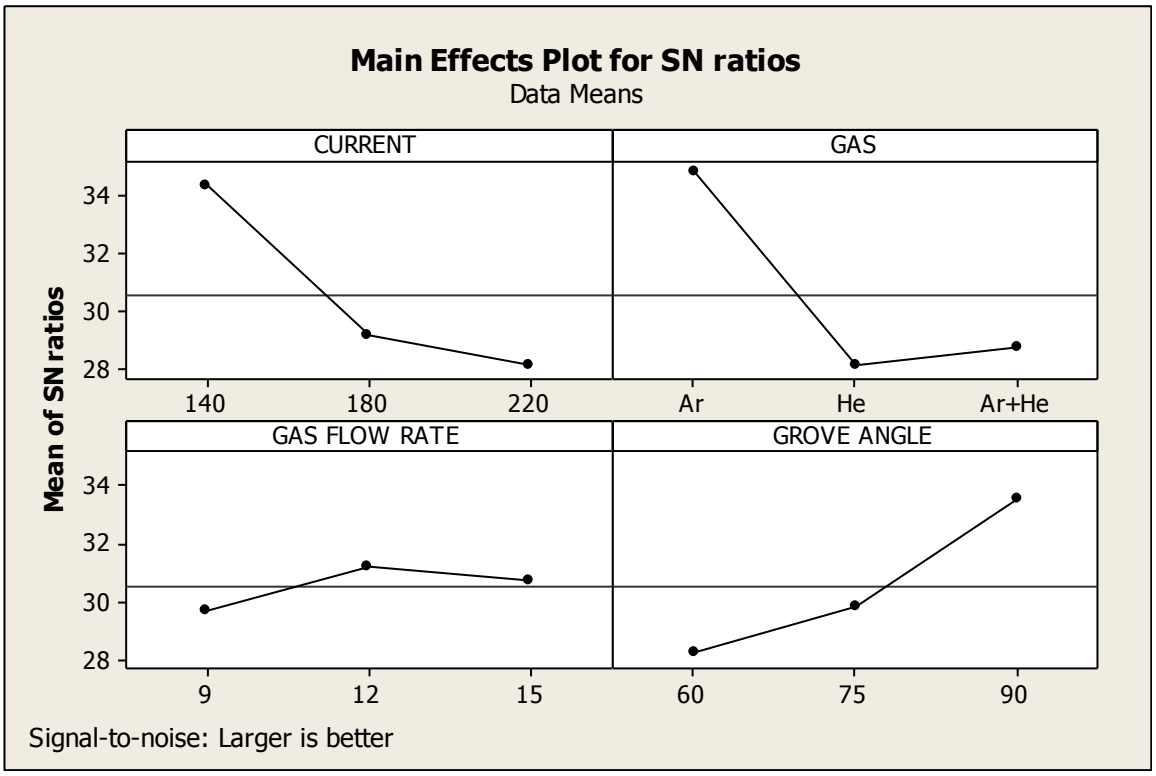

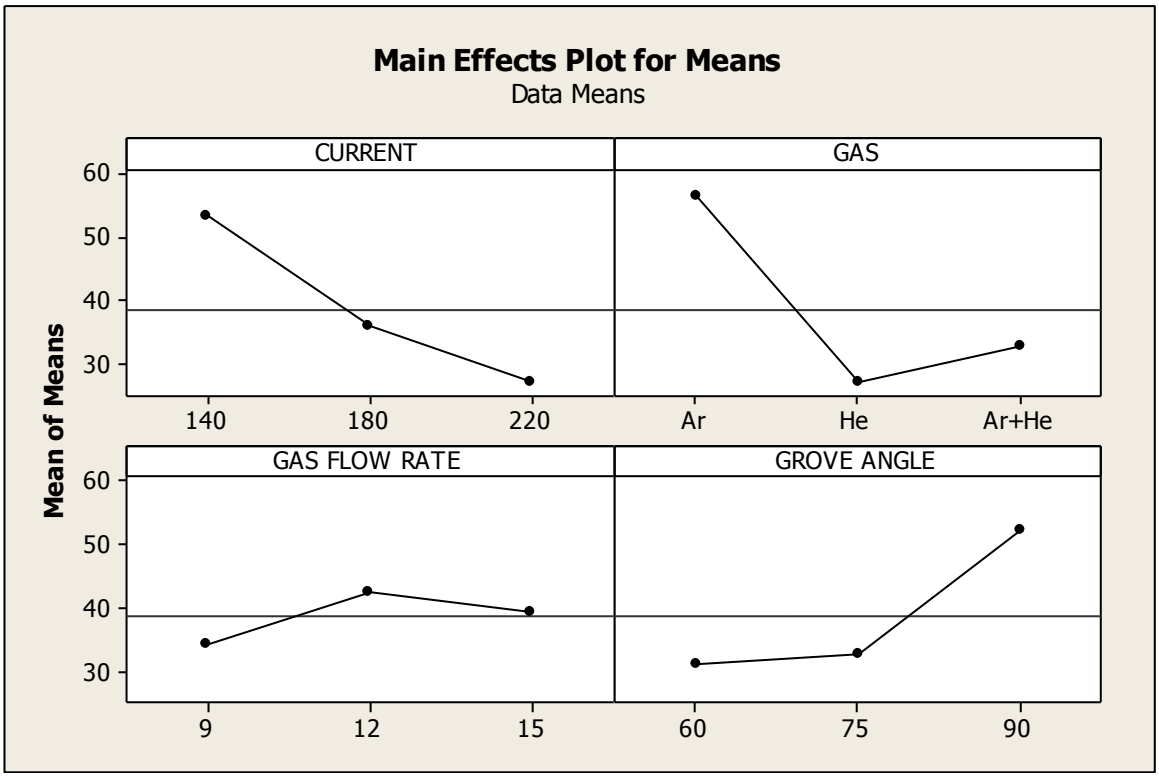

Figure 7.6: Main effects plot for SN ratios and means for toughness of SS202 at room temp.

7.3. RESULTS OF TOUGHNESS TEST PERFORMED ON SS304 GRADE STAINLESS STEEL MATERIAL

Table 7.7 shows the test results of toughness test carried out on SS304 grade steel carried at two different temperatures.

Table 7.7: Impact (Charpy) test results for SS 304 grade test samples

Experiment no.	Contributing factors	Charpy Test results at room temperature (18^0 C) (Joule)	Charpy Test results at -20^0 C (Joule)
1	I1,G1,F1,Θ1	73.575	41.6925
2	I1,G2,F2,Θ2	22.0725	17.1675
3	I1,G3,F3,Θ3	36.7875	31.8825
4	I2,G1,F2,Θ3	73.575	51.5025
5	I2,G2,F3,Θ1	51.5025	53.955
6	I2,G3,F1,Θ2	93.195	58.86
7	I3,G1,F3,Θ2	78.48	56.4075
8	I3,G2,F1,Θ3	66.2175	63.765
9	I3,G3,F2,Θ1	56.4075	44.145

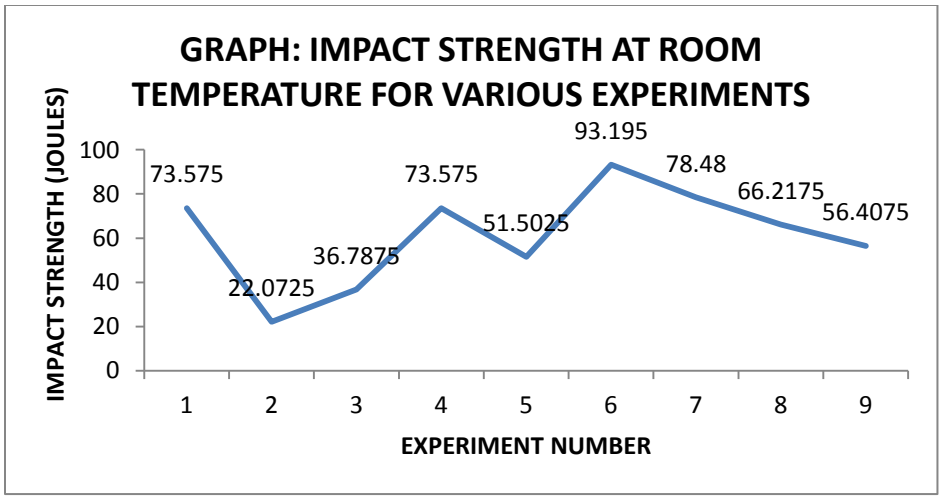

Figure 7.7: Graph showing variation of impact strength of SS 304 grade stainless steel material at room temperature for various experiments

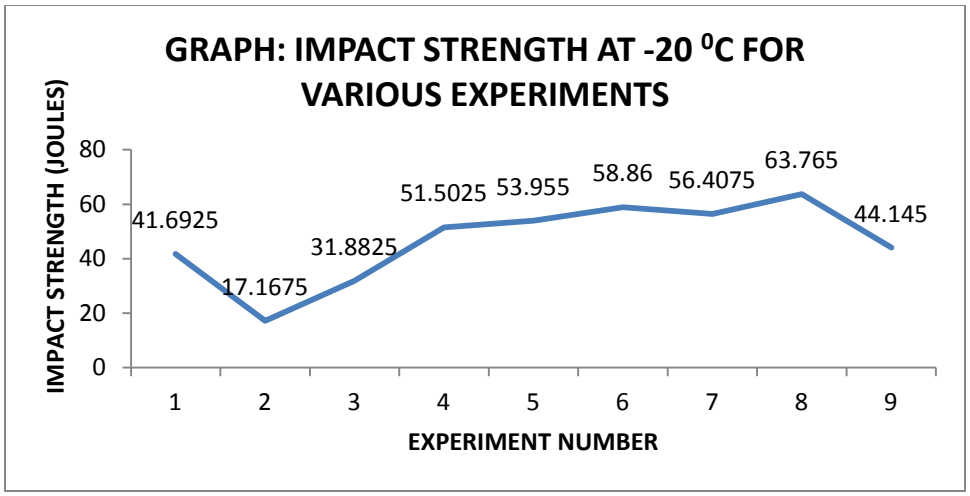

Figure 7.8: Graph showing variation of impact strength of SS 304 grade stainless steel material at -20^0 C temperature for various experiments

7.4. ANOVA FOR SS304 GRADE STAINLESS STEEL AT ROOM TEMPERATURE

Column no. 3 of table 7.7 gives the results of toughness test carried out on experimental specimens of SS304 grade steel. The experimental results are analyzed using ANOVA and the results are shown in the form of tables 7.8 to 7.11. It is clear from tables that current, shielding gas and gas flow rate are the most significant factors, as their F value is greater than F(critical) value, effecting toughness. Best value of toughness is obtained as 93.195 J for experiment no. 6 (180A, Ar-He, 9 l/min. & 75^0). Main effects plot shown in figure 7.9 are self explanatory and indicates that value of toughness first increases with increase in current to 180 A and then decreases somewhat till 220 A. Argon gas results in maximum toughness followed by mixture of argon with helium and pure helium shows the minimum toughness. Small gas flow results in highest toughness and then the toughness decreases to lowest value at 12 l/min. and further rises a bit. Grove angle has no effect on the toughness value.

Table 7.8: ANOVA for SN ratio of toughness at room temperature for SS304 material

Source	Units	DOF	SS	Variance	F	F(critical)	PC
Current	Ampere	2	47.9645	23.9823	47.396	19.0	39.762
Gas	--------	2	37.7596	18.8798	37.312	19.0	31.302
Gas flow rate	L/min.	2	33.8918	16.9459	33.490	19.0	28.096
Grove angle	Degrees	2	1.0120	0.5060	1.0	19.0	0.839
Total		8	120.628				100
Pooled Error		2	1.0120	0.5060			0.839

(SS= Sum of Square, F= F factor, PC = percent contribution, factor with least variance value is considered for error pooling)

Table 7.9: Response table for SN ratio of toughness at room temperature for SS304 material

LEVEL	CURRENT	GAS	GAS FLOW RATE	GROVE ANGLE
1	31.84	37.52	37.71	35.53
2	36.99	32.51	33.08	34.72
3	36.45	35.24	34.48	35.02
DELTA	5.14	5.01	4.63	0.81
RANK	1	2	3	4

Table 7.10: Analysis of variance for means toughness at room temperature for SS304 material

Source	Units	DOF	SS	Variance	F	F(critical)	PC
Current	Ampere	2	1375.37	687.687	26.384	19.0	35.288
Gas	--------	2	1231.02	615.510	23.615	19.0	31.584
Gas flow rate	L/min.	2	1239.04	619.520	23.769	19.0	31.790
Grove angle	Degrees	2	52.13	26.064	1.0	19.0	1.338
Total		8	3897.56				100
Pooled Error		2	52.13	26.064			1.338

(SS= Sum of Square, F= F factor, PC = percent contribution, factor with least variance value is considered for error pooling)

Table 7.11: Response table for means toughness at room temperature for SS304 material

LEVEL	CURRENT	GAS	GAS FLOW RATE	GROVE ANGLE
1	44.15	75.21	77.66	60.49
2	72.76	46.60	50.69	64.58
3	67.03	62.13	55.59	58.86
DELTA	28.61	28.61	26.98	5.72
RANK	2	1	3	4

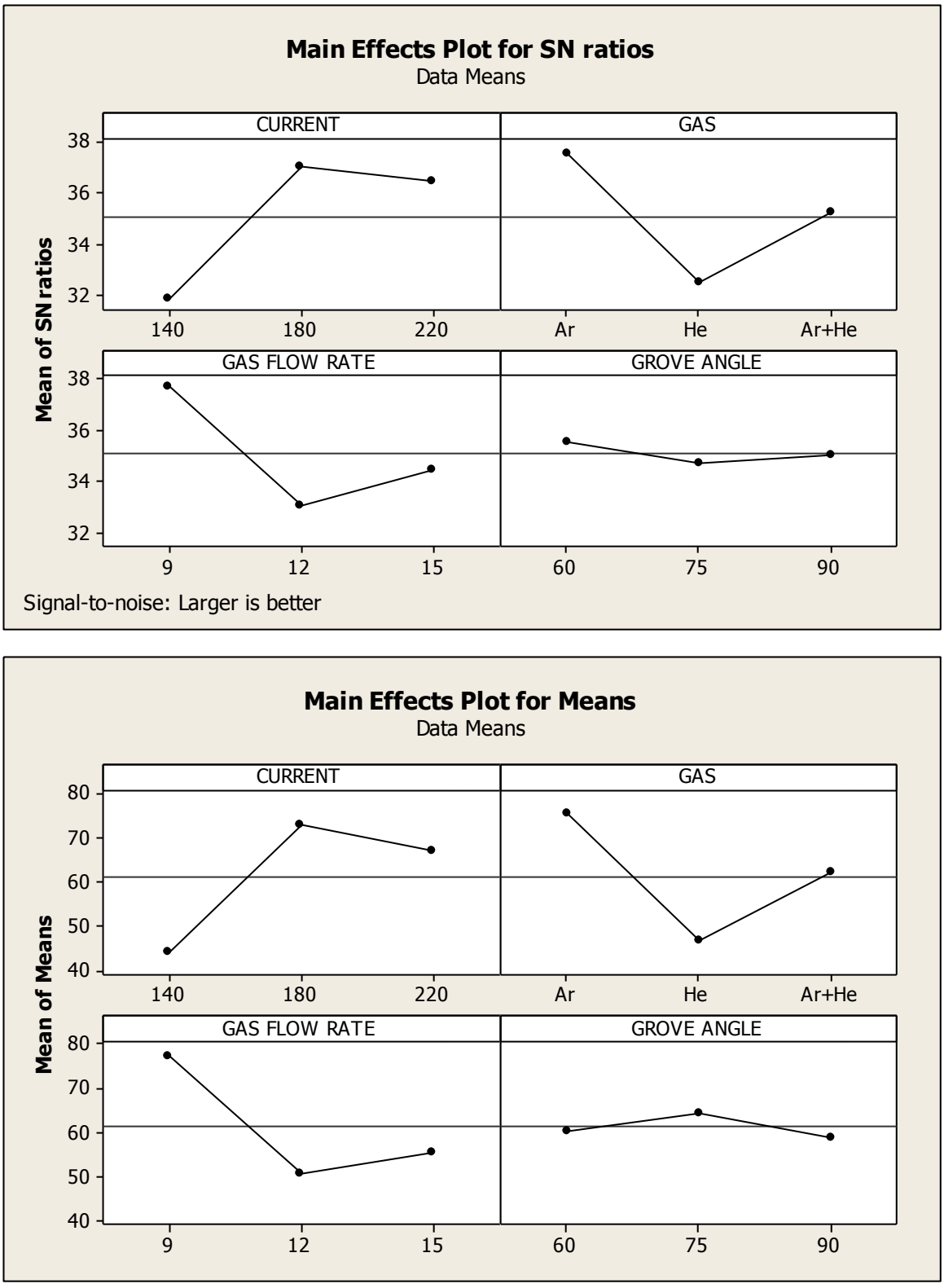

Figure 7.9: Main effects plot for SN ratios and means for toughness of SS304 at room temp.

7.4.1. Optimal design for toughness of SS304 steel at room temperature

It is clear from ANOVA for means (table 7.10) that F value of current, gas flow rate and grove angle is greater than F (critical) and the main effect plot shows that toughness is maximum at 180 A, Argon gas and 9 l/min. Confidence interval predict with 95 % confidence so that value of toughness for SS304 steel at room temperature would be 103.005 ± 19.365 Joules.

Mean value of toughness is given by-

$\mu_{I2G1F1} = \bar{I}_2 + \bar{G}_1 + \bar{F}_1 - 2\bar{T}$

= 72.76 + 75.21 + 77.66 – 2 X 61.3125 (where $\bar{T}$ = average toughness calculated from table)

= 103.005 Joule

Confidence Interval around the estimated mean toughness

$C.I. = \sqrt{\frac{f\alpha:v1:v2 \; X \; Ve}{neff}}$

v2 = DOF for error = 2

Where $f\,\alpha{:}v1{:}v2 = f\,0.05{:}1{:}2 = 18.5$

Variance of error = *Ve* = 26.064

$n_{eff} = \frac{9}{1+DOF_{I2G1F1}} = 1.2857$

C.I. = 19.3658 Joules

So, the confidence interval for bead width is given by 103.005 ± 19.365 Joules.

7.5. ANOVA TABLE FOR SS304 GRADE STAINLESS STEEL AT -20 ^{0}C TEMPERATURE

Table 7.7 column no.4 shows the value of toughness obtained for the specimens of SS304 at -20 ^{0}C. Experimental results are analyzed using ANOVA and results are shown in the form of table from 7.12 to 7.15. It is clear from the table of ANOVA of means that current is the most significant factor among all followed by gas flow rate whereas shielding gas and grove angle are the least significant factors. Graphs for main effects are plotted in figure 7.10 and shows that toughness increases with the increase in the value of the current and it is maximum for a gas flow rate of 9 l/min. and then decreases to a lowest value at 12 l/min. and then again increases for 15

l/min. maximum value of toughness is obtained as 63.765 Joules for experiment no. 8 (220 A, Ar-He, 15 l/min. & 60^0). It is clear from table of ANOVA for means that value of F for current is greater than F (critical) so it is the only significant factor statistically. So we can say from response table for means that the optimal value of toughness at -20 ^{0}C is 54.77 Joules.

Table 7.12: Analysis of variance for SN ratio of toughness at -20 ^{0}C temperature for SS304 material

Source	Units	DOF	SS	Variance	F	F(critical)	PC
Current	Ampere	2	64.0707	32.0353	11.227	19.0	63.248
Gas	--------	2	6.4928	3.2464	1.138	19.0	6.409
Gas flow rate	L/min.	2	25.0292	12.5146	4.386	19.0	24.708
Grove angle	Degrees	2	5.7071	2.8535	1.0	19.0	5.634
Total		8	101.300				100
Pooled Error		2	5.7071	2.8535			5.634

(SS= Sum of Square, F= F factor, PC = percent contribution, factor with least variance value is considered for error pooling)

Table 7.13: Response table for SN ratio of toughness at -20 ^{0}C temperature for SS304 material

LEVEL	CURRENT	GAS	GAS FLOW RATE	GROVE ANGLE
1	29.06	33.89	34.63	33.31
2	34.76	31.81	30.61	31.71
3	34.67	32.79	33.25	33.47
DELTA	5.70	2.08	4.02	1.76
RANK	1	3	2	4

Table 7.14: Analysis of variance for means toughness at -20 ^{0}C temperature for SS304 material

Source	Units	DOF	SS	Variance	F	F(critical)	PC
Current	Ampere	2	1202.95	601.476	33.334	19.0	69.444
Gas	--------	2	48.12	24.059	1.333	19.0	2.778
Gas flow rate	L/min.	2	445.09	222.546	12.334	19.0	25.694
Grove angle	Degrees	2	36.09	18.044	1.0	19.0	2.083
Total		8	1732.25				100
Pooled Error		2	36.09	18.044			2.083

(SS= Sum of Square, F= F factor, PC = percent contribution, factor with least variance value is considered for error pooling)

Table 7.15: Response table for means toughness at -20 ^{0}C temperature for SS304 material

LEVEL	CURRENT	GAS	GAS FLOW RATE	GROVE ANGLE
1	30.25	49.87	54.77	46.60
2	54.77	44.96	37.60	44.15
3	54.77	44.96	47.41	49.05
DELTA	24.53	4.91	17.17	4.90
RANK	1	3	2	4

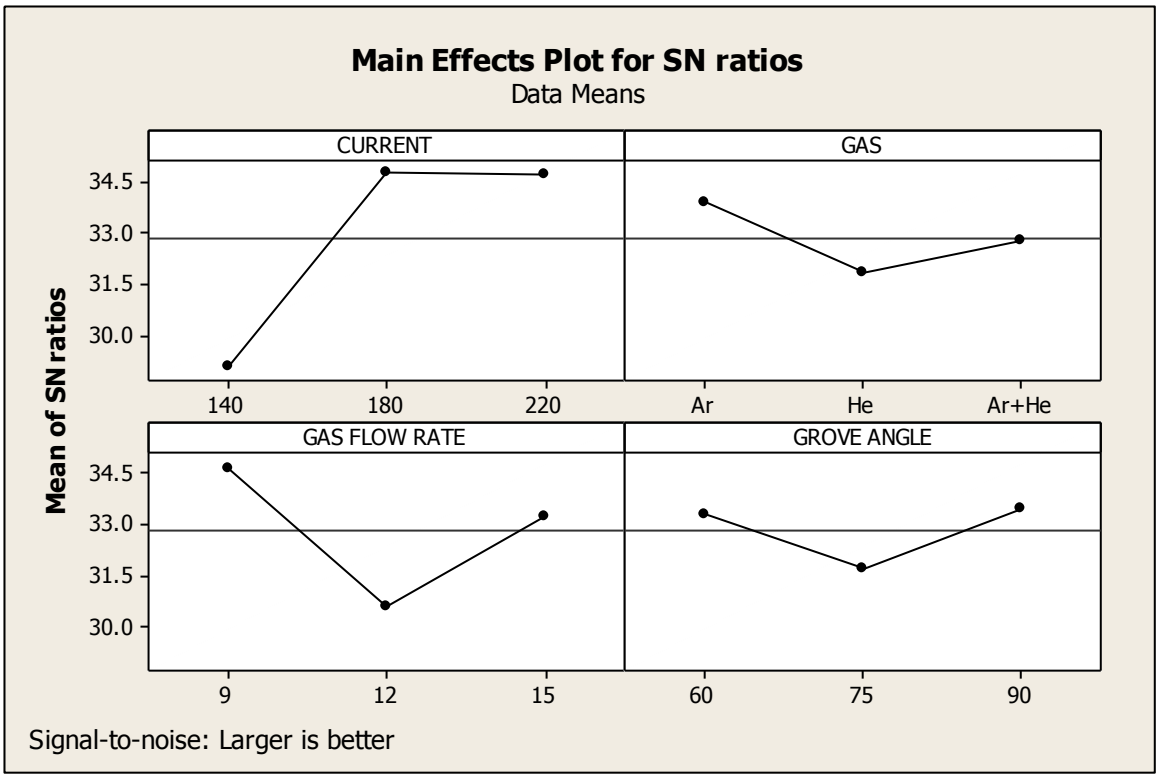

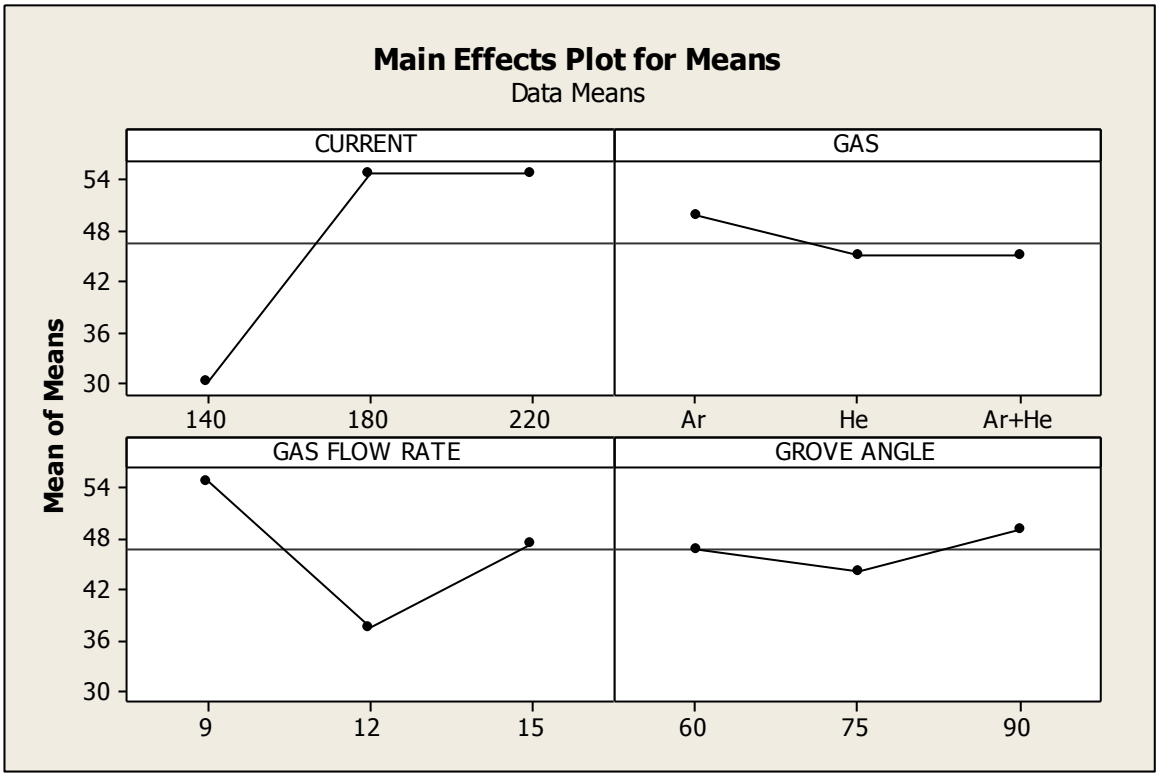

Figure 7.10: Main effects plot for SN ratios and means for toughness of SS304 at -20 ^{0}C temp.

CHAPTER - 8

RESULTS OF MICROHARDNESS (VICKERS) TEST

As discussed earlier Vicker's microhardness test was carried out on all the samples including base metal of both grades of steel. The values of microhardness (HVN) for the two grades are:

Table 8.1: Microhardness (HVN) values for the base metal

S.N.	METAL	MICROHARDNESS (HVN)
1	SS202	77.676
2	SS304	60.653

8.1. RESULTS OF VICKER'S MICROHARDNESS TEST FOR SS202 STAINLESS STEEL

Results for Vicker's Microhardness test for SS202 grade stainless steel are given in the table 8.2 and the figure 8.1 shows the variation of results with the various experiments.

Table 8.2: Microhardness (HVN) for various experiments on SS202 stainless steel

Experiment number	Contributing factors	Microhardness number (HVN)
1	I1,G1,F1,Θ1	77.337
2	I1,G2,F2,Θ2	78.158
3	I1,G3,F3,Θ3	75.579
4	I2,G1,F2,Θ3	75.923
5	I2,G2,F3,Θ1	78.367
6	I2,G3,F1,Θ2	77.310
7	I3,G1,F3,Θ2	78.244
8	I3,G2,F1,Θ3	78.823
9	I3,G3,F2,Θ1	80.474

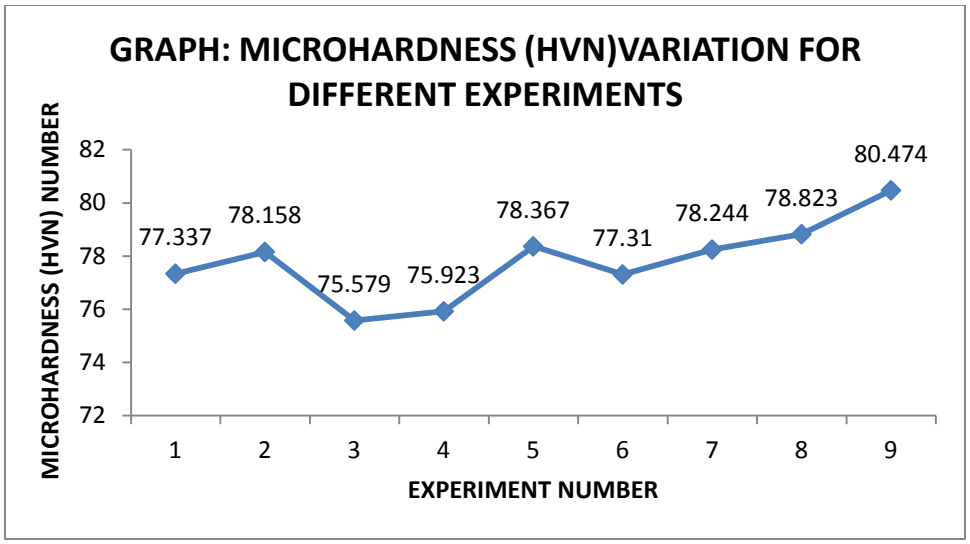

Figure 8.1: Graph showing variation of microhardness (HVN) for SS202 grade stainless steel

8.1.1. ANOVA for microhardness of SS202 steel

Table 8.2 gives all the values of microhardness for various experiments on SS202 steel. The experimental results are analysed using ANOVA and the results are shown from table 8.3 to 8.6. It can be concluded from the ANOVA tables that no factor is significant statistically as the values of F for all factors is less than F (critical) but from percentage contribution we can conclude that current is the most significant factor followed by grove angle. Gas flow rate and shielding gas has almost negligible effect on the value of microhardness. Main effects plot are shown in figure 8.2 and it can be concluded from said figure that the value of microhardness increases as the value of current increases. Microhardness is maximum when He gas is used in comparison to others and it is also maximum when the grove angle is smaller and decreases with increase in angle. Gas flow rate is having almost negligible effect on the microhardness. Maximum value of microhardness is 80.474 VHN for experiment no. 9 (220 A, Ar-He, 12 l/min. & 60^0). Optimal value cannot be given for microhardness as there is no significant factor. So optimization of results is not done.

Table 8.3: Analysis of variance for SN ratio of Microhardness (HVN) for SS202 material

Source	Units	DOF	SS	Variance	F	F(critical)	PC
Current	Ampere	2	0.106438	0.053219	9.378	19.0	48.1598
Gas	--------	2	0.030997	0.015498	2.731	19.0	14.025
Gas flow rate	L/min.	2	0.011350	0.005675	1.0	19.0	5.136
Grove angle	Degrees	2	0.072225	0.036112	6.363	19.0	32.679
Total		8	0.221010				100
Pooled Error		2	0.011350	0.005675			5.136

(SS= Sum of Square, F= F factor, PC = percent contribution, factor with least variance value is considered for error pooling)

Table 8.4: Response table for SN ratio of Microhardness (HVN) for SS202 material

LEVEL	CURRENT	GAS	GAS FLOW RATE	GROVE ANGLE
1	37.73	37.75	37.82	37.92
2	37.75	37.89	37.86	37.83
3	37.97	37.82	37.77	37.70
DELTA	0.24	0.14	0.09	0.22
RANK	1	3	4	2

Table 8.5: Analysis of variance for means Microhardness (HVN) for SS202 material

Source	Units	DOF	SS	Variance	F	F(critical)	PC
Current	Ampere	2	8.59936	4.29968	9.204	19.0	48.436
Gas	--------	2	2.46360	1.23180	2.637	19.0	13.876
Gas flow rate	L/min.	2	0.93432	0.46716	1.0	19.0	5.263
Grove angle	Degrees	2	5.75673	2.87836	6.161	19.0	32.425
Total		8	17.7540				
Pooled Error		2	0.93432	0.46716			5.263

(SS= Sum of Square, F= F factor, PC = percent contribution, factor with least variance value is considered for error pooling)

Table 8.6: Response table for means Microhardness (HVN) for SS202 material

LEVEL	CURRENT	GAS	GAS FLOW RATE	GROVE ANGLE
1	77.02	77.17	77.82	78.73
2	77.20	78.45	78.19	77.90
3	79.18	77.79	77.40	76.78
DELTA	2.16	1.28	0.79	1.95
RANK	1	3	4	2

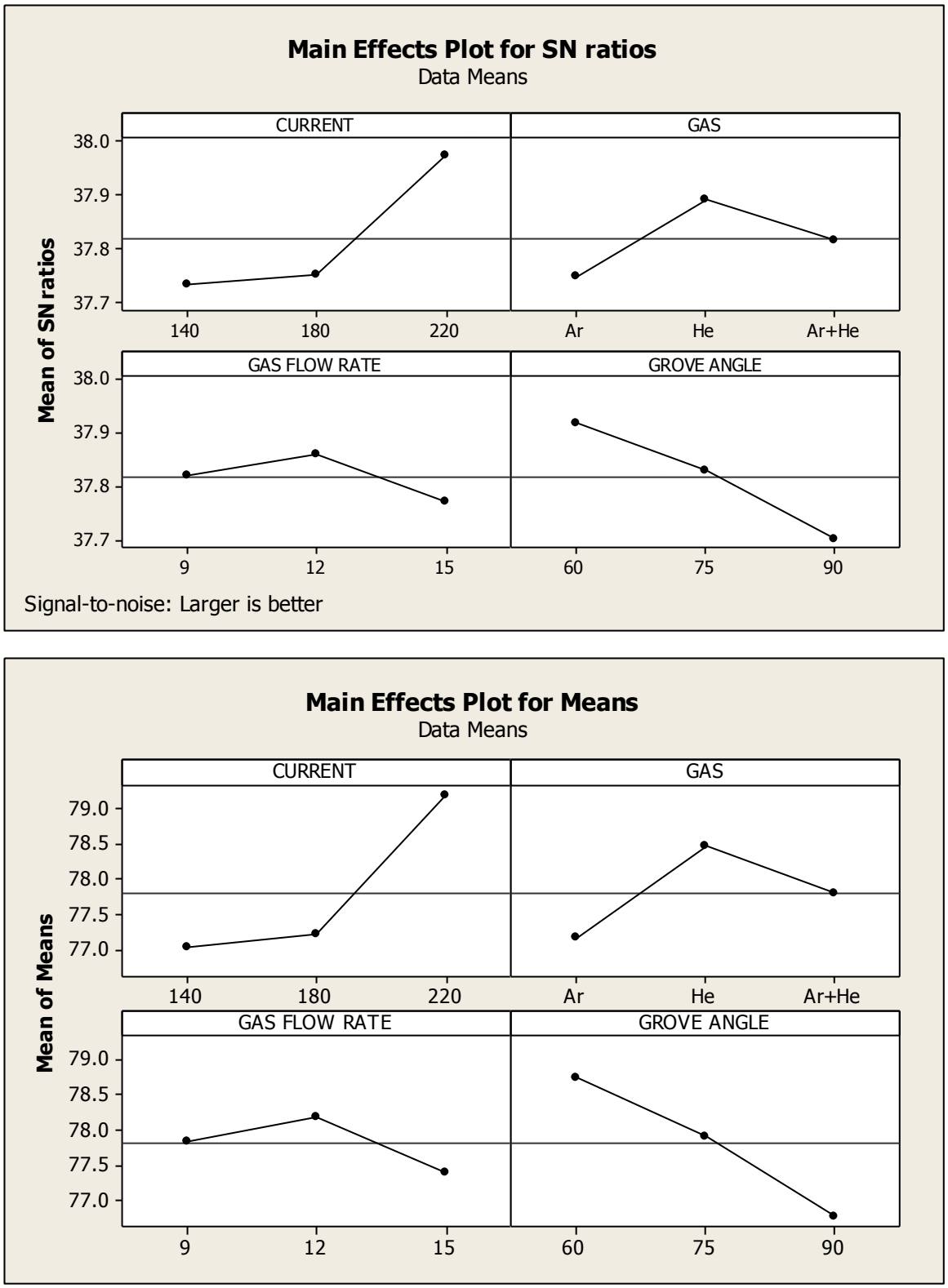

Figure 8.2: Main effects plot for SN ratios and means for Microhardness (HVN) of SS202 specimens

8.2. RESULTS OF VICKER'S MICROHARDNESS TEST FOR SS304 STAINLESS STEEL

Results for Vicker's Microhardness test for SS304 grade stainless steel are given in the table 8.7 and the figure 8.3 shows the variation of results with the various experiments.

Table 8.7: Microhardness (HVN) for various experiments on SS304 stainless steel

Experiment number	Contributing factors	Microhardness number (HVN)
1	I1,G1,F1,Θ1	67.226
2	I1,G2,F2,Θ2	70.139
3	I1,G3,F3,Θ3	70.972
4	I2,G1,F2,Θ3	72.243
5	I2,G2,F3,Θ1	80.031
6	I2,G3,F1,Θ2	71.456
7	I3,G1,F3,Θ2	64.833
8	I3,G2,F1,Θ3	67.523
9	I3,G3,F2,Θ1	64.728

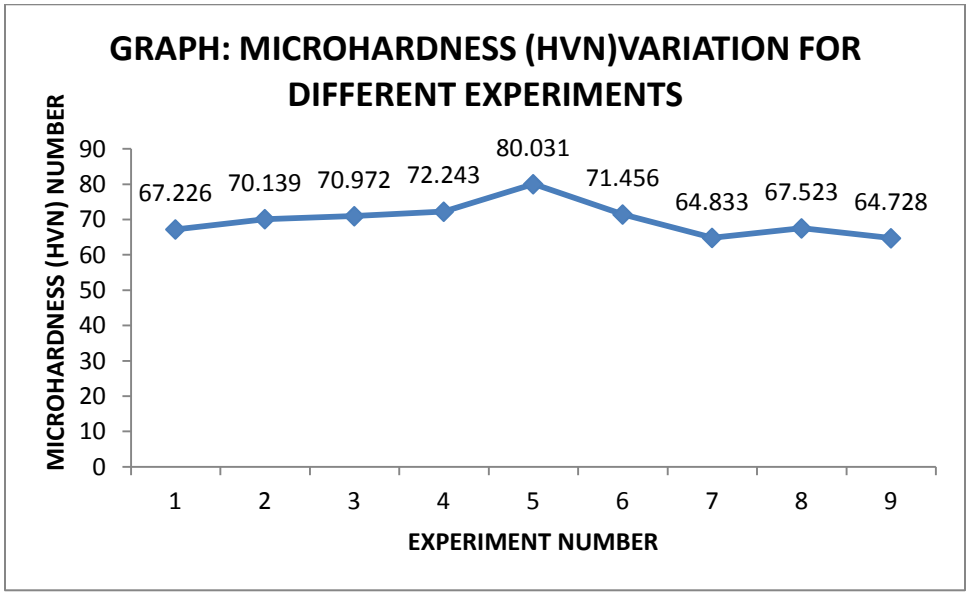

Figure 8.3: Graph showing variation of microhardness (HVN)) on SS304 grade stainless steel

8.2.1. ANOVA for microhardness of SS304 steel

Values of microhardness for SS304 steel are given in table 8.7. The results of measurement are analyzed using ANOVA are shown in the form of tables 8.8 to 8.11. It can be concluded from the tables that current is the most significant factor for microhardness measurement and others factors like shielding gas grove angle have some effect on the said response whereas grove angle is having negligible effect on microhardness. Main effects plot are shown in figure 8.4. It is clear from main effects plot that the value of microhardness is maximum for 180 A and He gas in comparison to other values. It increases with increase in the values of gas flow rate. Maximum value of HVN is 80.031 for experiment no. 5 (220 A, He, 15 l/min. & 60^0). From ANOVA table of means we can see that only current is statistically significant factor for the microhardness results and accordingly from response table for means the optimum value of HVN is 74.58.

Table 8.8: Analysis of variance for SN ratio of Microhardness (HVN) for SS304 material

Source	Units	DOF	SS	Variance	F	F(critical)	P C
Current	Ampere	2	1.79591	0.897955	24.188	19.0	69.212
Gas	--------	2	0.47618	0.238092	6.413	19.0	18.351
Gas flow rate	L/min.	2	0.24845	0.124227	3.346	19.0	9.575
Grove angle	Degrees	2	0.07425	0.037124	1.0	19.0	2.8615
Total		8	2.59480				100
Pooled Error		2	0.07425	0.037124			2.8615

(SS= Sum of Square, F= F factor, PC = percent contribution, factor with least variance value is considered for error pooling)

Table 8.9: Response table for SN ratio of Microhardness (HVN) for SS304 material

LEVEL	CURRENT	GAS	GAS FLOW RATE	GROVE ANGLE
1	36.83	36.65	36.74	36.95
2	37.44	37.19	36.77	36.75
3	36.35	36.77	37.11	36.93
DELTA	1.09	0.54	0.37	0.20
RANK	1	2	3	4

Table 8.10: Analysis of variance for means Microhardness (HVN) for SS304 material

Source	Units	DOF	SS	Variance	F	F(critical)	PC
Current	Ampere	2	119.287	59.6435	21.046	19.0	67.402
Gas	--------	2	33.166	16.5829	5.851	19.0	18.740
Gas flow rate	L/min.	2	18.858	9.4288	3.327	19.0	10.656
Grove angle	Degrees	2	5.668	2.8340	1.0	19.0	3.203
Total		8	176.978				100
Pooled Error		2	5.668	2.8340			3.203

(SS= Sum of Square, F= F factor, PC = percent contribution, factor with least variance value is considered for error pooling)

Table 8.11: Response table for means Microhardness (HVN) for SS304 material

LEVEL	CURRENT	GAS	GAS FLOW RATE	GROVE ANGLE
1	69.45	68.10	68.73	70.66
2	74.58	72.56	69.04	68.81
3	65.69	69.05	71.95	70.25
DELTA	8.88	4.46	3.21	1.85
RANK	1	2	3	4

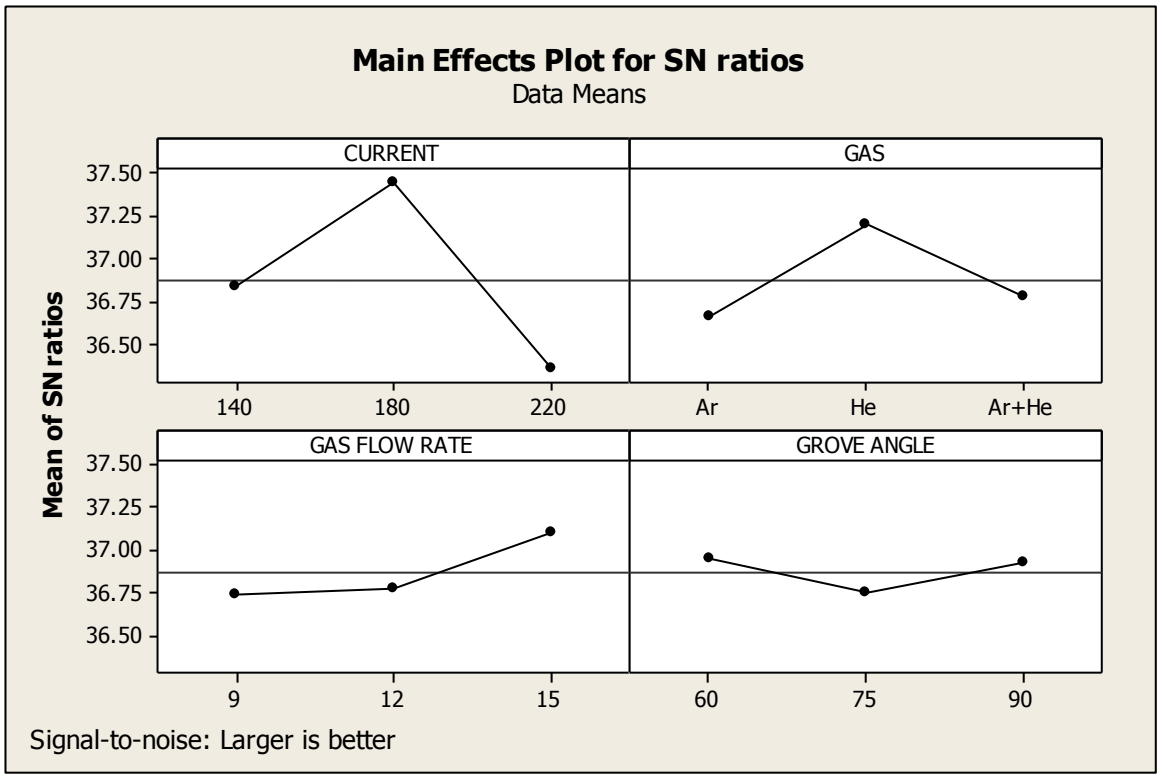

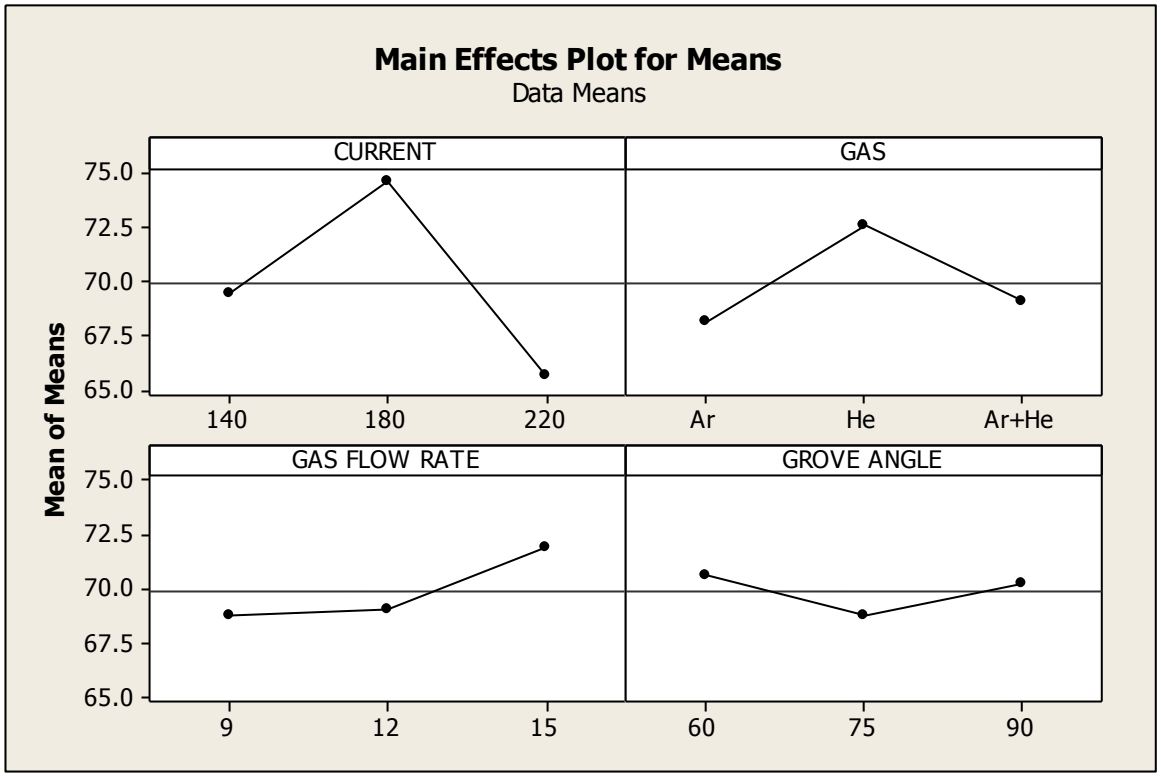

Figure 8.4: Main effects plot for SN ratios and means for Microhardness of SS304 specimens

CHAPTER - 9

RESULT OF JOINT QUALITY

All polished specimens were viewed under Leica Microscope at 100X magnification to detect the presence of internal defects. Figure shows the image of weld region of the polished specimens. By looking at the various specimens we can conclude that there are no major flaws in the specimens except the sample no. 9 (refer to figure 9.9) which has one crack. For better results three different pictures of each sample are taken and shown in the figure 9.1 to 9.9 for SS202 steel.

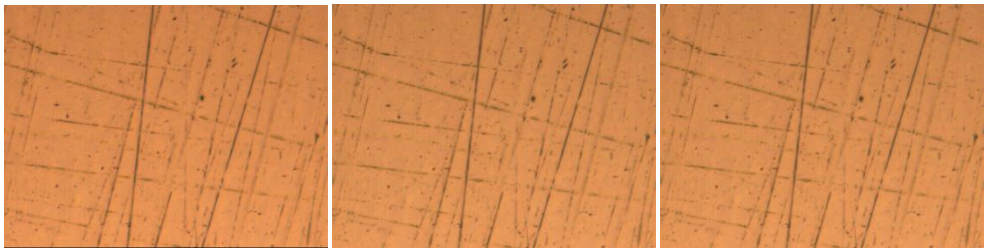

Figure 9.1: Polished welded region of specimen number 1 of SS202 steel

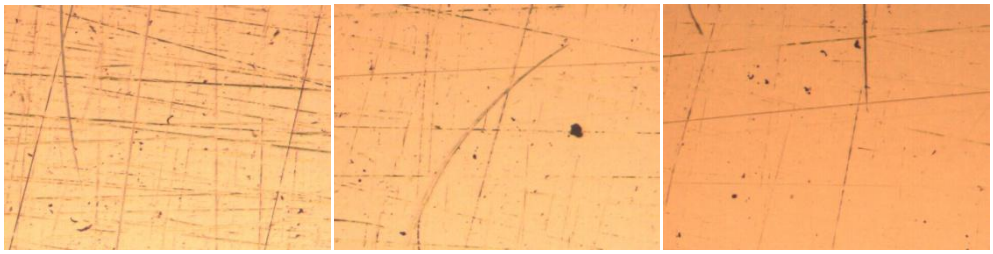

Figure 9.2: Polished welded region of specimen number 2 of SS202 steel

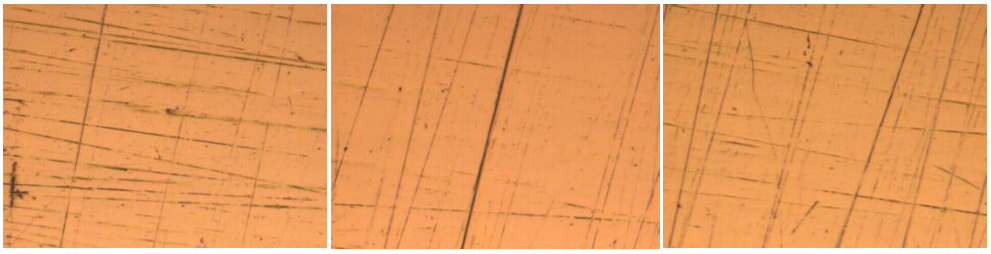

Figure 9.3: Polished welded region of specimen number 3 of SS202 steel

Figure 9.4: Polished welded region of specimen number 4 of SS202 steel

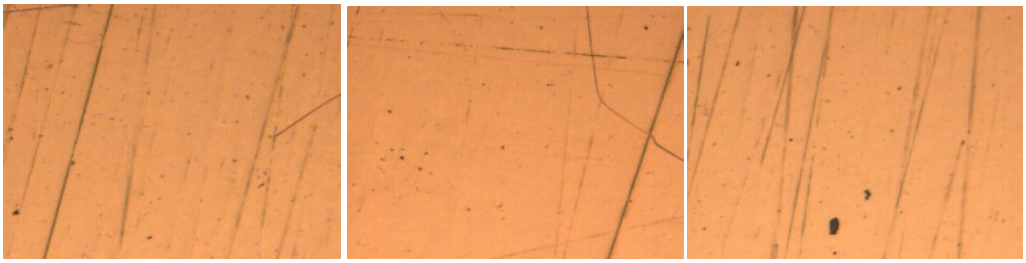

Figure 9.5: Polished welded region of specimen number 5 of SS202 steel

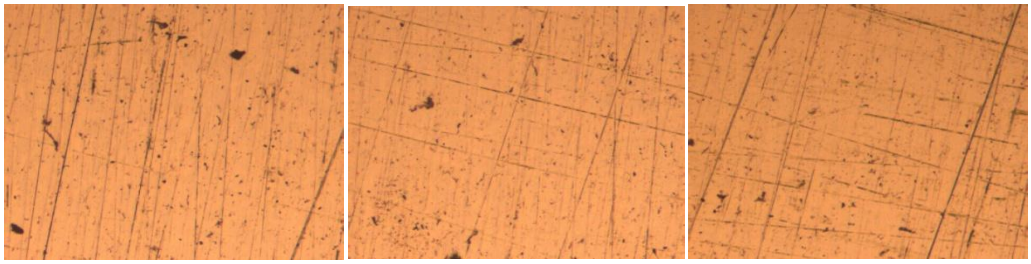

Figure 9.6: Polished welded region of specimen number 6 of SS202 steel

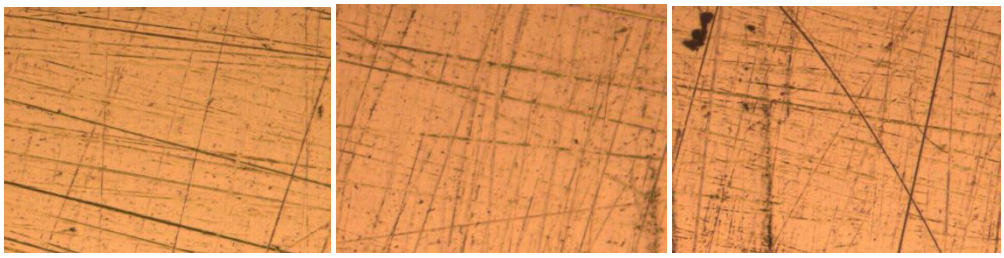

Figure 9.7: Polished welded region of specimen number 7 of SS202 steel

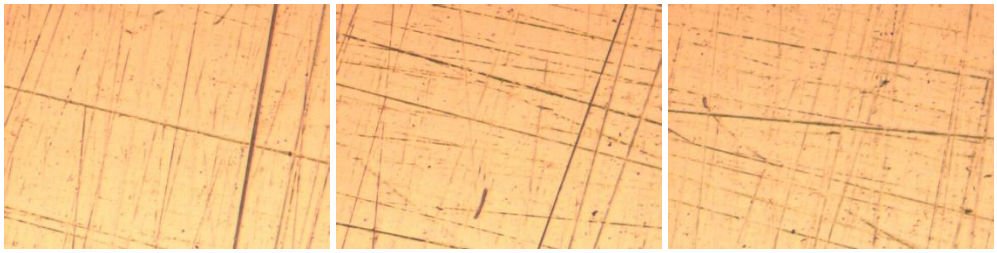

Figure 9.8: Polished welded region of specimen number 8 of SS202 steel

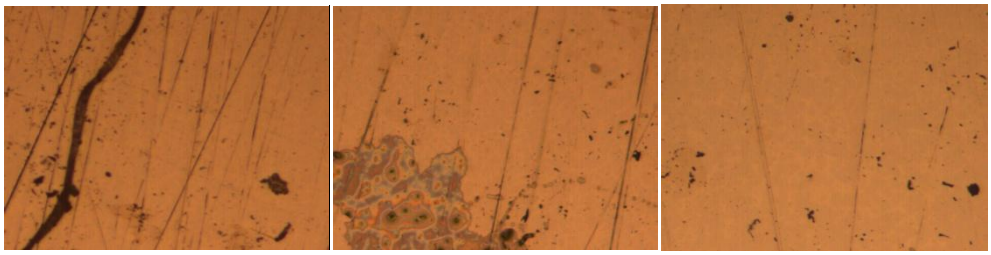

Figure 9.9: Polished welded region of specimen number 9 of SS202 steel

Figure no. 9.10 to 9.18 shows the results of microscopic investigation of all nine samples of SS304 steel for all the nine experiments. It can be concluded from these figures that there are no major flaws and inclusions into the welded region except sample no. 2 which is having small inclusion as shown in the figure 9.11.

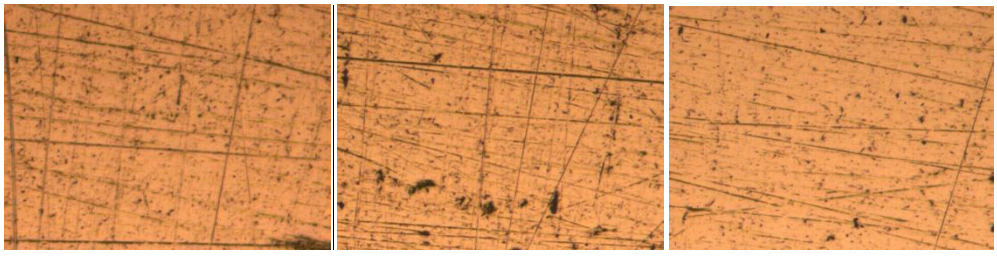

Figure 9.10: Polished welded region of specimen number 1 of SS304 steel

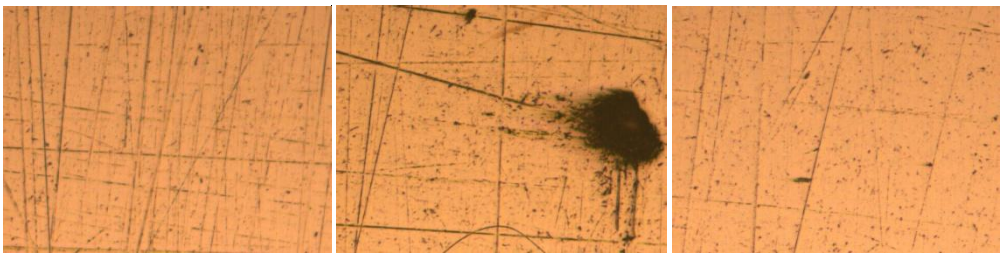

Figure 9.11: Polished welded region of specimen number 2 of SS304 steel

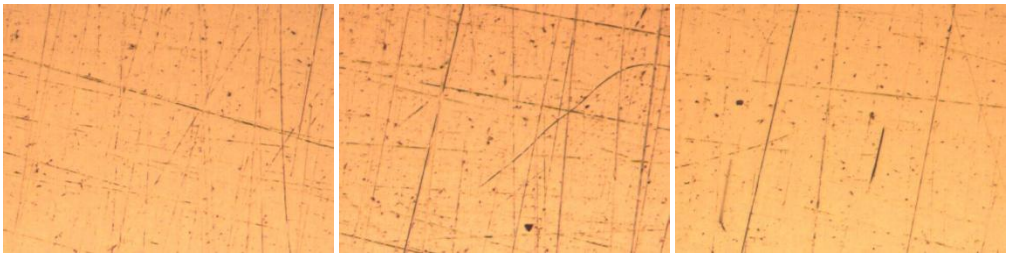

Figure 9.12: Polished welded region of specimen number 3 of SS304 steel

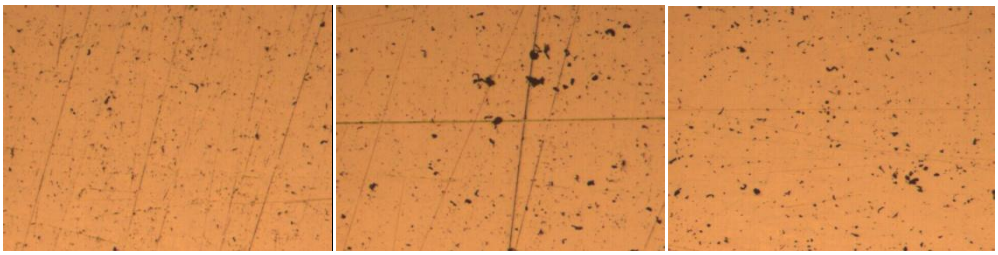

Figure 9.13: Polished welded region of specimen number 4 of SS304 steel

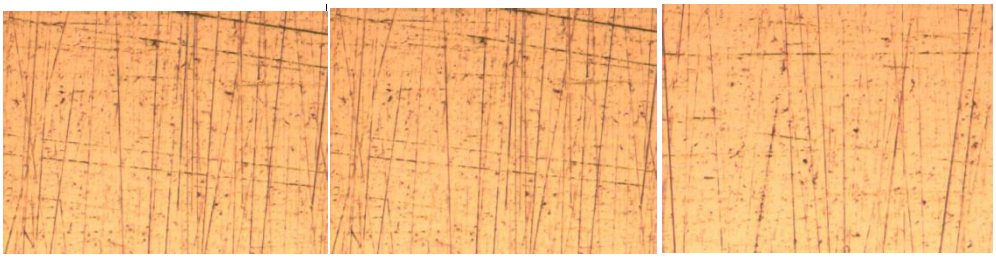

Figure 9.14: Polished welded region of specimen number 5 of SS304 steel

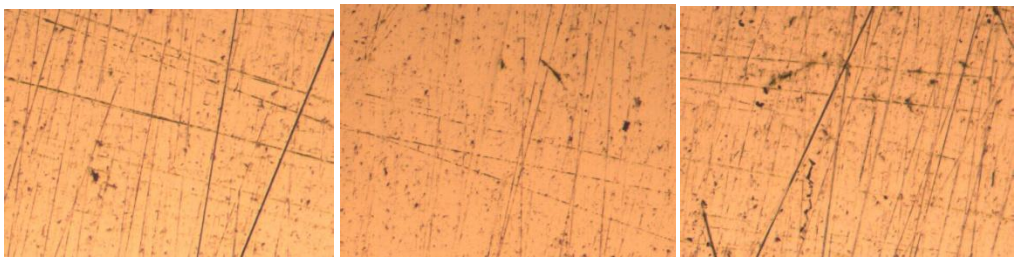

Figure 9.15: Polished welded region of specimen number 6 of SS304 steel

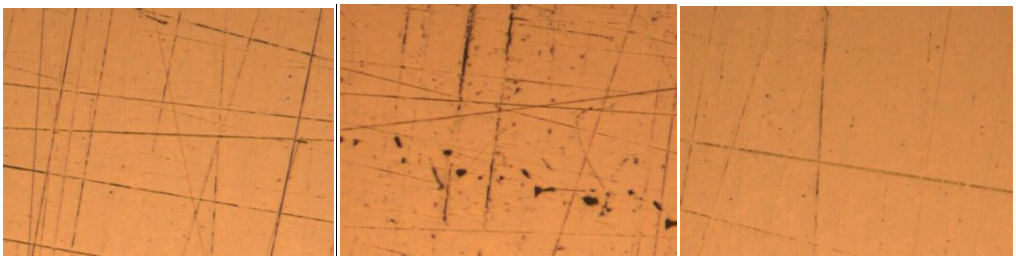

Figure 9.16: Polished welded region of specimen number 7 of SS304 steel

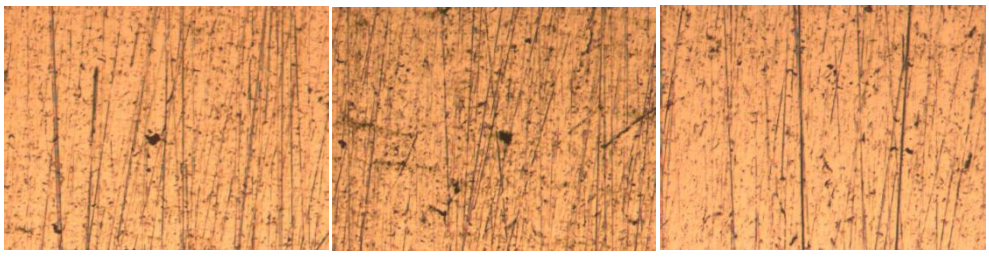

Figure 9.17: Polished welded region of specimen number 8 of SS304 steel

Figure 9.18: Polished welded region of specimen number 9 of SS304 steel

CHAPTER – 10

RESULTS OF CHEMICAL COMPOSITION TESTING

10.1. CHEMICAL COMPOSITION OF WELD METAL

The composition of welded metal was found by using atomic absorption spectrometer. The specimens after spectroscopy are shown in Figure 7.1.

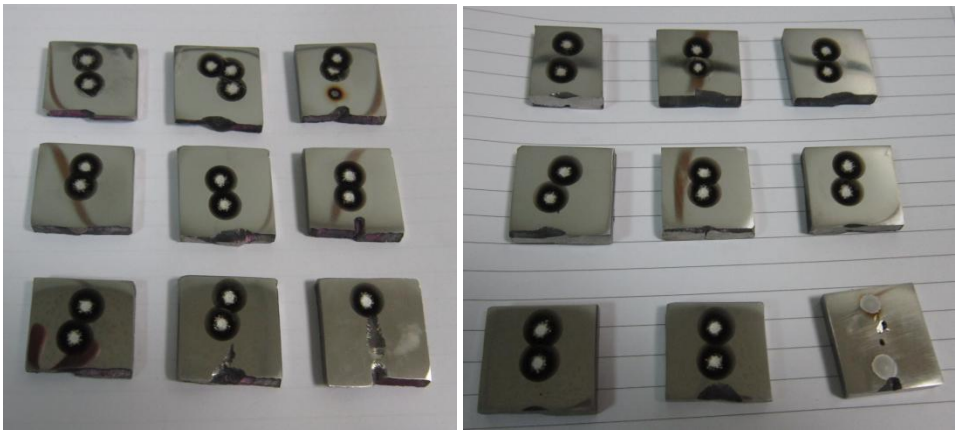

Figure 10.1: Specimen of SS304 and SS202 after checking composition

10.2. RESULTS OF CHEMICAL COMPOSITION OF WELD METAL OF SS202 STEEL

Table shows the main constituent elements of SS202 weld metal and their comparison with base metal is given simultaneously. Figure 7.2 (a-h) shows the variation of various constituents in the welded region from that of base metal. It can be concluded from the given figures that there is small increase in the value of Iron (Fe) and Nickel in the weld region from that of parent metal whereas the composition of Chromium and Carbon decreases in the different welded region from that of parent metal. It may be because of formation of different compounds in the welded region during welding as high heat is generated.

Table 10.1: Chemical composition of base metal SS202 and all the nine specimens

Constituent element → Metal ↓	Fe	C	Si	Mn	P	S	Cr	Ni	Co	Cu
SS202 Base metal	72.6	0.082	0.434	10.7	0.06	0.008	15.0	0.153	0.042	0.707
Sample 1	72.8	0.072	0.496	11.0	0.06	0.005	14.2	0.215	0.045	0.889
Sample 2	72.9	0.074	0.509	10.8	0.06	0.007	14.2	0.210	0.044	0.922
Sample 3	72.4	0.060	0.519	11.1	0.06	0.005	14.3	0.338	0.041	0.974
Sample 4	72.5	0.064	0.523	11.2	0.06	0.005	14.2	0.270	0.041	0.919
Sample 5	73.0	0.075	0.509	10.9	0.06	0.005	14.1	0.231	0.045	0.892
Sample 6	72.9	0.065	0.531	10.8	0.06	0.005	14.0	0.378	0.040	0.974
Sample 7	73.0	0.072	0.497	11.1	0.06	0.005	13.9	0.221	0.046	0.877
Sample 8	73.0	0.066	0.505	11.2	0.06	0.005	13.9	0.202	0.045	0.826
Sample 9	73.1	0.068	0.512	11.2	0.06	0.005	13.9	0.385	0.046	0.884

Figure 7.2 (a-h) shows the variation in %age composition of different elements i.e. iron, carbon, silicon, manganese, phosphorus, sulphur, nickel, copper and chromium.

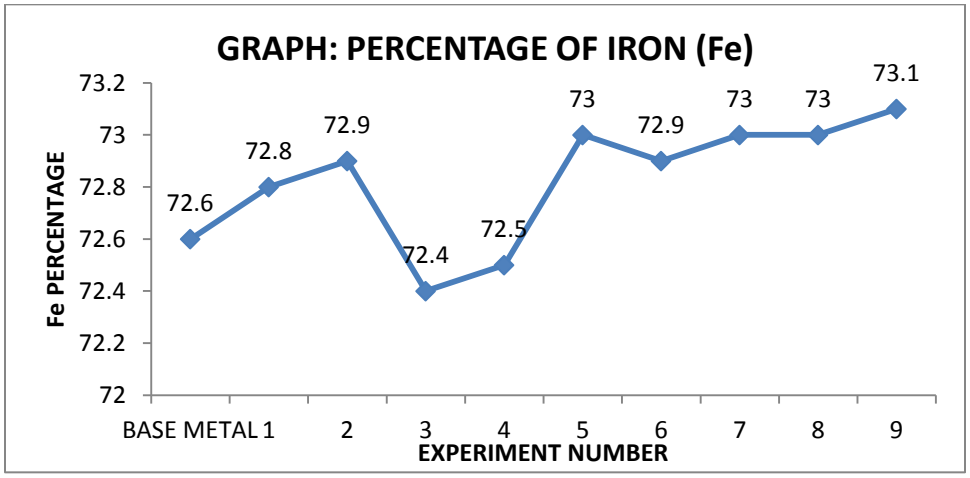

(a): Variations in %age composition of Iron (Fe) at weld centre

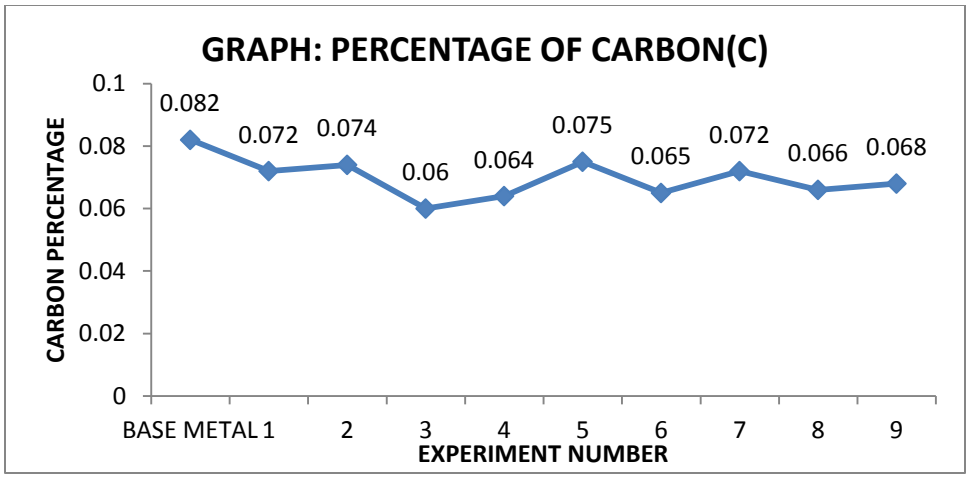

(b): Variations in %age composition of Carbon (C) at weld centre

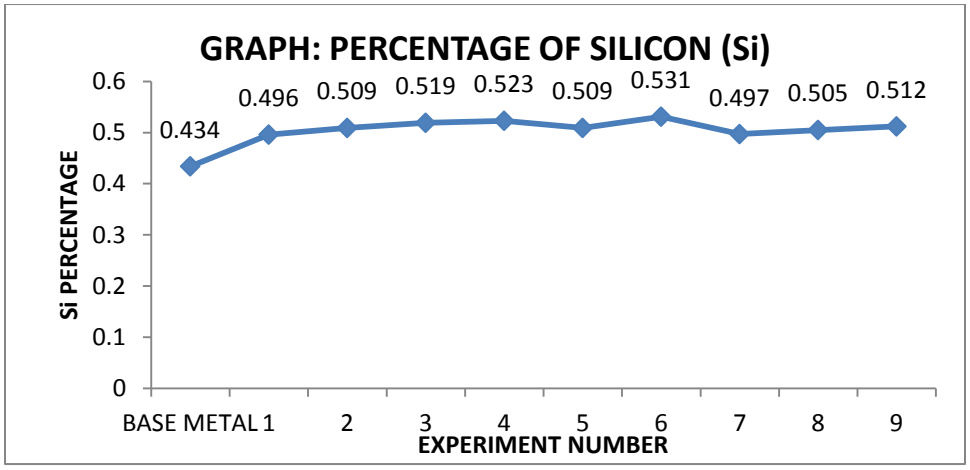

(c): Variations in %age composition of Silicon (Si) at weld centre

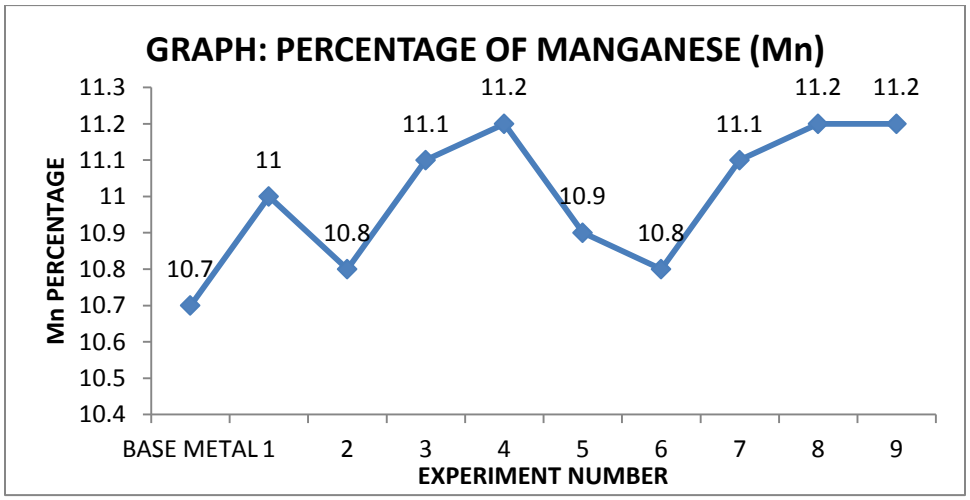

(d): Variations in %age composition of Manganese (Mn) at weld centre

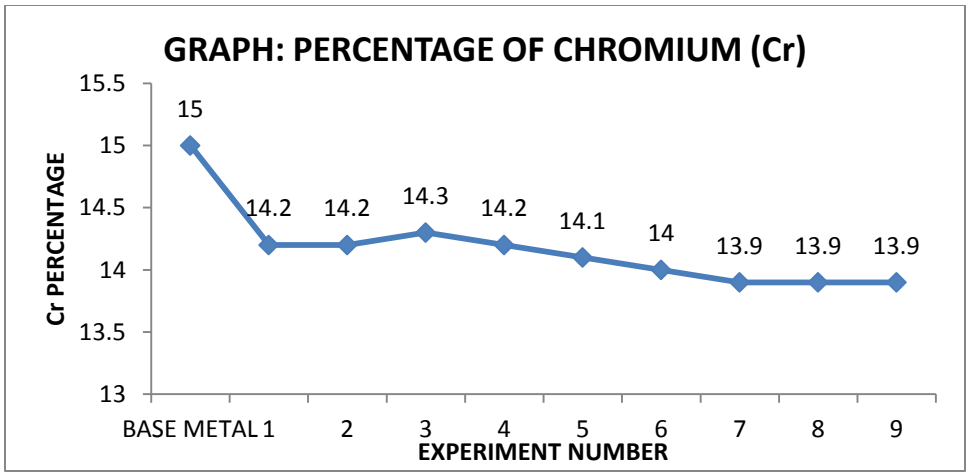

(e): Variations in %age composition of Chromium (Cr) at weld centre

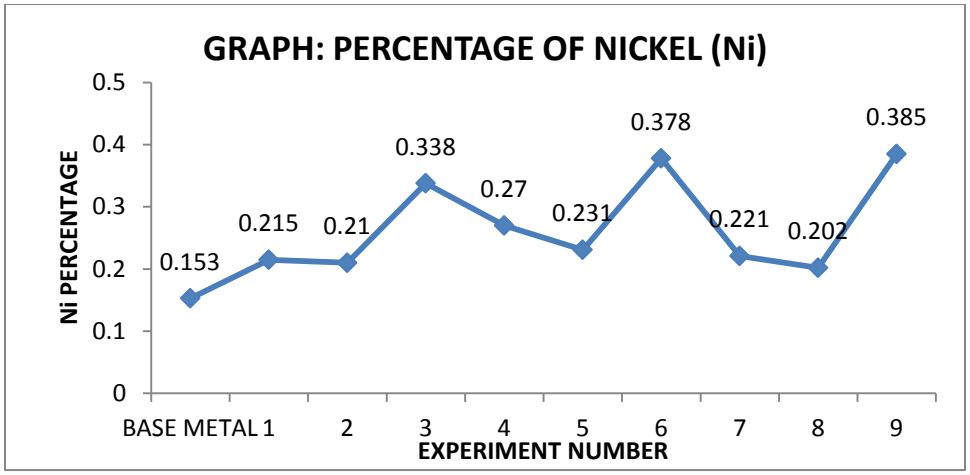

(f): Variations in %age composition of Nickel (Ni) at weld centre

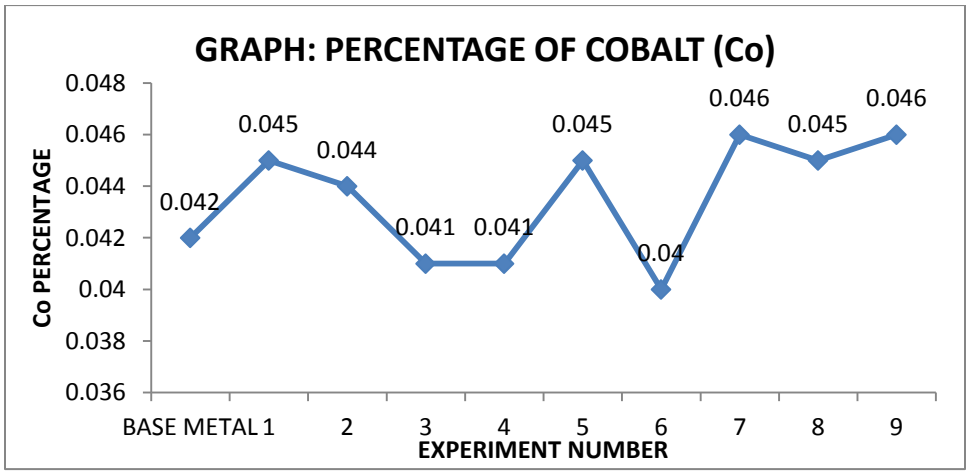

(g): Variations in %age composition of Cobalt (Co) at weld centre

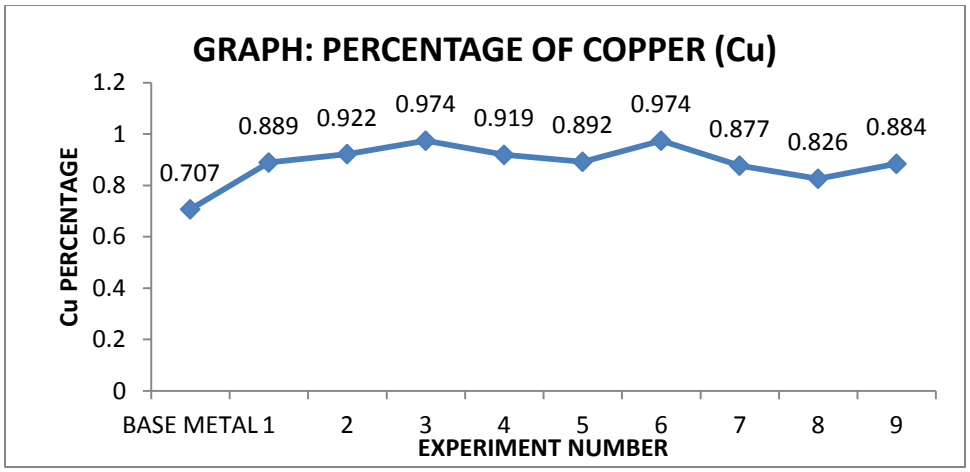

(h): Variations in %age composition of Copper (Cu) at weld centre

Figure 10.2 (a-h): Variation in percentage composition of Fe, C, Si, Mn, Cr, Ni, Co & Cu from base metal to weld metal of different specimens of SS202 steel

10.3. RESULTS OF CHEMICAL COMPOSITION OF WELD METAL OF SS304 STEEL

Table 10.2 shows the main constituent elements of SS304 weld metals and their comparison with base metal is given simultaneously. The variations of different constituent elements in the welded region of different experiments from that of base metal are shown in the figure 10.3 (a-h). It can be concluded from these figures that there is slight increase in the composition of iron and manganese from that of parent metal whereas there is decrease in the composition of chromium, carbon and nickel in the welded region of different experiment from that of base metal.

Table 10.2: Chemical composition of base metal SS304 and all the nine specimens

Constituent element → Metal ↓	Fe	C	Si	Mn	P	S	Cr	Ni	Co	Cu
SS304 Base metal	70.1	0.047	0.272	1.11	0.045	0.005	19.1	8.26	0.194	0.388
Sample 1	69.6	0.047	0.369	3.05	0.049	0.005	18.7	7.31	0.160	0.373
Sample 2	69.7	0.032	0.441	3.51	0.046	0.005	18.0	7.44	0.163	0.376
Sample 3	69.4	0.045	0.382	4.04	0.050	0.005	18.4	6.93	0.146	0.348
Sample 4	70.1	0.037	0.328	2.79	0.047	0.005	18.3	7.53	0.167	0.381
Sample 5	69.9	0.041	0.400	3.96	0.050	0.005	18.0	6.77	0.149	0.369
Sample 6	69.8	0.044	0.405	4.22	0.050	0.005	17.8	6.80	0.148	0.361
Sample 7	70.0	0.039	0.380	3.15	0.046	0.005	18.2	7.32	0.167	0.388
Sample 8	69.9	0.045	0.418	3.34	0.047	0.005	18.1	7.27	0.165	0.363
Sample 9	70.3	0.033	0.388	2.80	0.042	0.005	18.0	7.57	0.173	0.389

Figure 10.3 (a-h) shows the variation in %age composition of different elements i.e. iron, carbon, silicon, manganese, phosphorus, chromium, nickel, cobalt and copper.

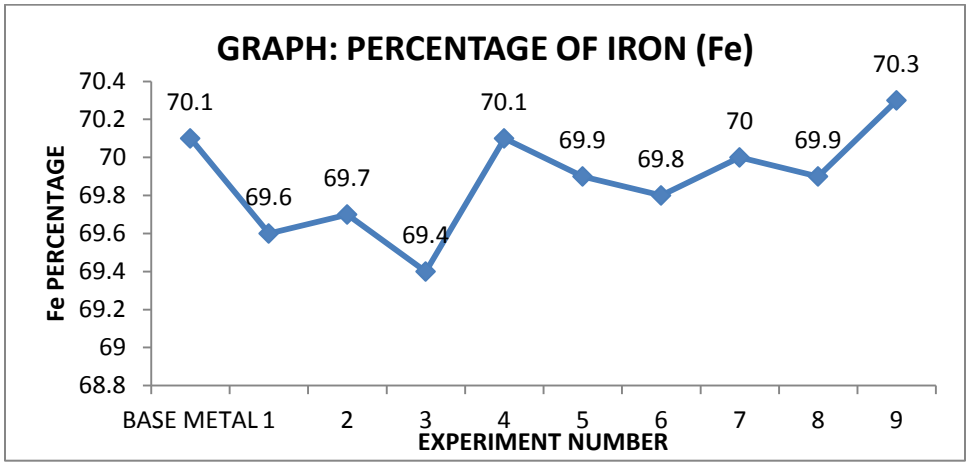

(a): Variations in %age composition of Iron (Fe) at weld centre

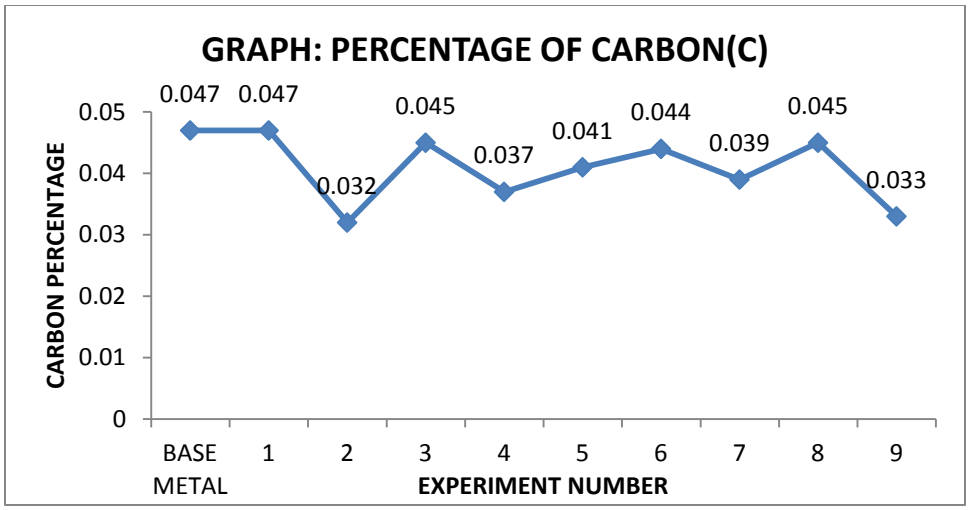

(b): Variations in %age composition of Carbon (C) at weld centre

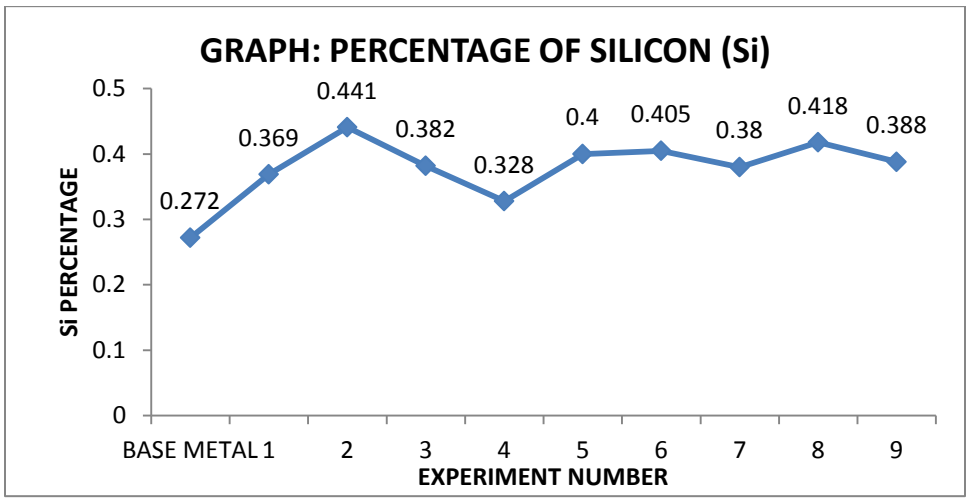

(c): Variations in %age composition of Silicon (Si) at weld centre

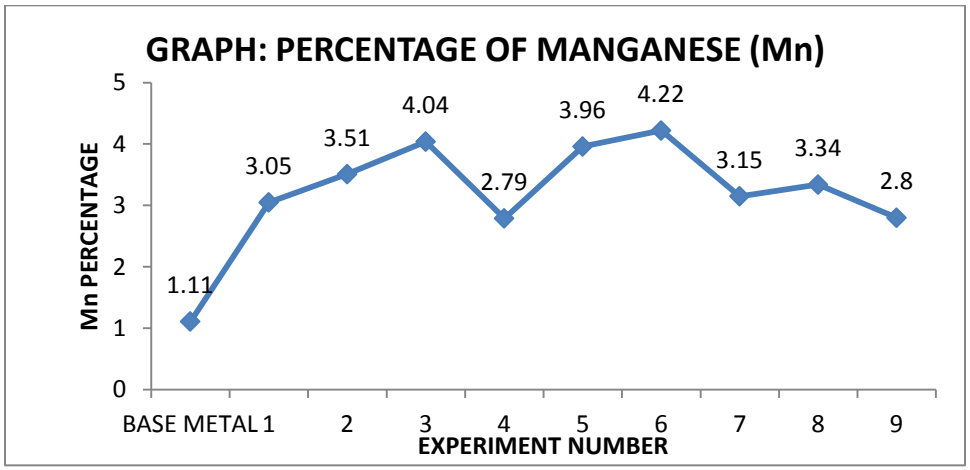

(d): Variations in %age composition of Manganese (Mn) at weld centre

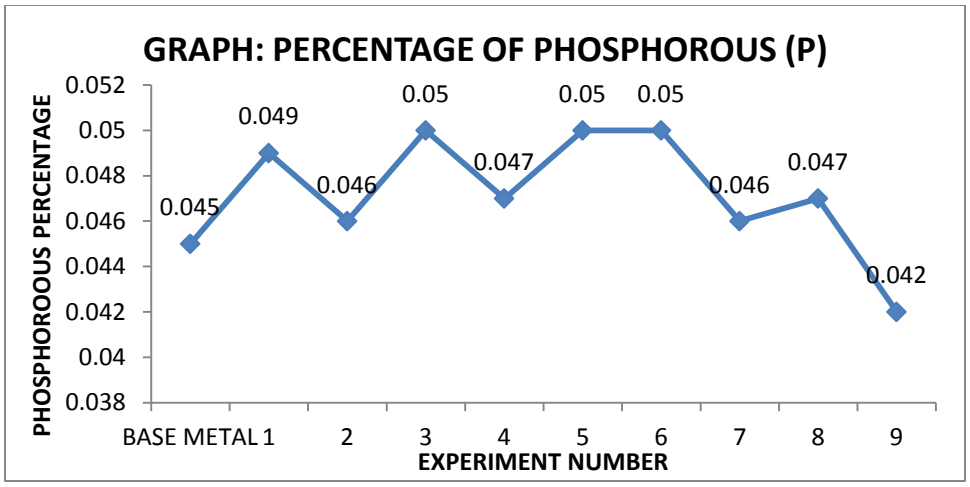

(e): Variations in %age composition of Phosphorous (P) at weld centre

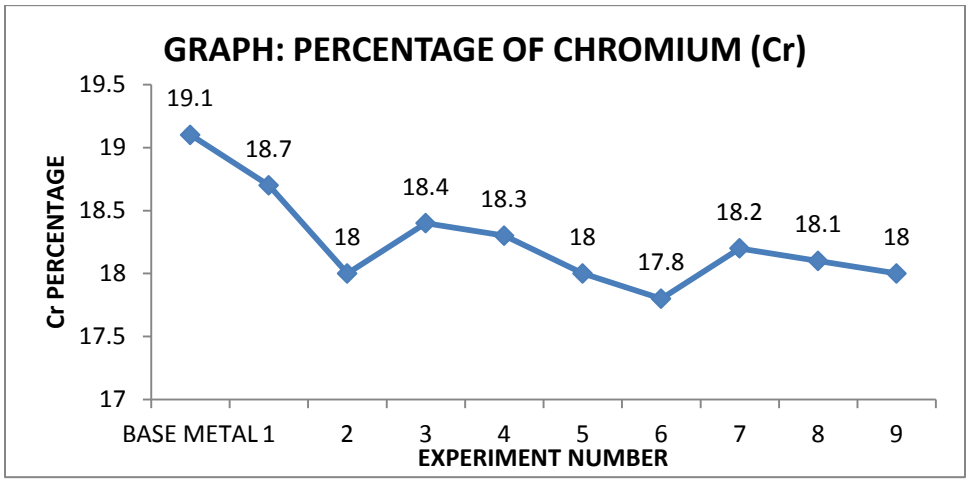

(f): Variations in %age composition of Chromium (Cr) at weld centre

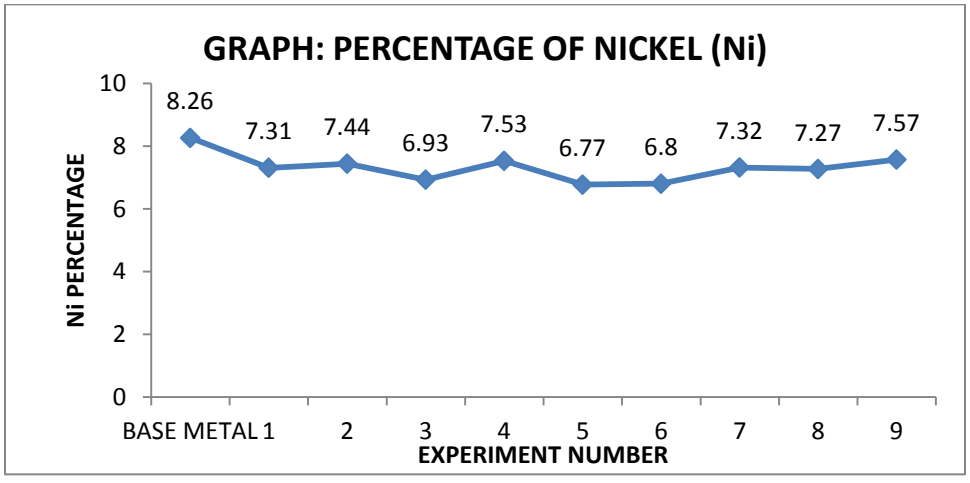

(g) Variations in %age composition of Nickel (Ni) at weld centre

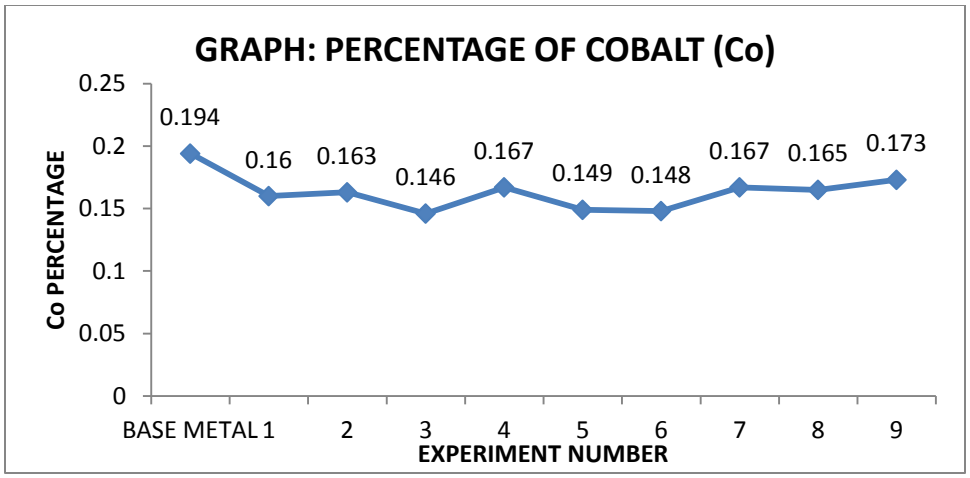

(h): Variations in %age composition of Cobalt (Co) at weld centre

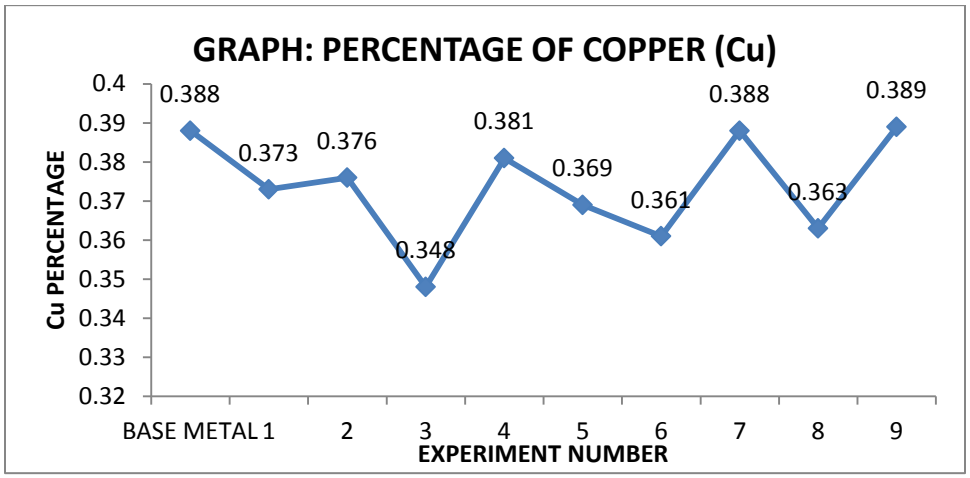

(i): Variations in %age composition of Copper (Cu) at weld centre

Figure 10.3 (a-i): Variation in %age composition of different elements i.e. Fe, C, Si, Mn, P, Cr, Ni, Co and Cu from base metal to weld metal for SS304 steel

CHAPTER – 11

RESULTS, CONCLUSION AND FUTURE SCOPE

For the experimental results and subsequent analysis following conclusions are drawn

- Bead width for SS202 steel depends mainly on the current and nature of shielding gas and the value increases with increase in amount of current and it also increased by using Helium gas. Bead height mainly depends on the shielding gas and gas flow rate and a lower value of gas flow rate is desired.
- Bead width for SS304 steel depends mainly on welding current and shielding gas used. It decreases with increase in the value of current and is minimum when Helium gas was used. Bead height depends on the gas flow rate and grove angle made. Minimum value is for 12 l/min. and with grove angle of 90^0.
- Rockwell hardness test results for both grades steels shows that there is no considerable variation in the results in the weld metal, heat affected zone (HAZ) and base metal.
- Dye penetrant test (DPT) results for SS304 material shows that there is no surface crack in the welded region except for the sample no. 9 (220 A, Ar+He, 12 l/min. & 60^0), at the corner. Similar results are obtained with SS202 material except a few minor defects at the corners which is excluded when cutting out specimens for testing. In general the results show that quality of welding was very good.
- Charpy impact test results for SS202 steel shows that toughness at room temperature mainly depends on the value of current used and shielding gas chosen. Toughness value is higher at lower welding current temperatures and also when Helium is used as shielding gas. Maximum value of toughness (71.1225 Joules) in the welded joint of experiment no. 4 (180 A, Ar, 12 l/min. & 90^0).
- Charpy impact test results for SS202 material shows that this particular grade of material is having zero strength at -20 ^{0}C. It may be because of less amount of nickel.
- Charpy test results for SS304 at room temperature shows that toughness increases as well as decreases in welded specimens. Maximum value of toughness is 93.195 Joule for specimen no. 6 (180 A, Ar+He, 9 l/min. & 75^0). Toughness is higher for 180 A and for shielding gas Ar and also at 9 l/min.

- Charpy test results for SS304 at -20 ^{0}C shows that it mostly depends on the welding current followed by gas flow rate. Highest value of toughness at this temperature is for experiment no. 8 (220 A, He, 9 l/min. & 90^0). Toughness value is maximum on and after 180 A of current and also highest for 9 l/min. Shielding gas has no effect on toughness value at this temperature.
- Microhardness test results for SS202 steel shows that there is slight increase in the value of microhardness for most of the welding combinations. Maximum value of HVN is 80.474 for experiment no. 9 (220 A, Ar + He, 12 l/min. & 60^0). HVN value increases with increase in the value of current and decrease in the value of grove angle. Use of He as shielding gas can provide maximum hardness.
- Microhardness test results for SS304 material show that maximum value of 80.031 HVN is obtained for experiment no. 5 (180 A, He, 15 l/min. & 60^0). Welding current is the most important parameter in effecting the value of said response and the maximum value of HVN is obtained for 180 A current.
- Joint quality results for SS202 material shows that joint quality is very good in general and the polished welded region is almost free of flaws and inclusions except for specimen no. 9 (220 A, Ar + He, 12 l/min. & 60^0) which is having one crack and blow hole in between.
- Joint quality for SS304 also shows that there are no major flaws and inclusions in the welded region and overall welded joints are of good quality.
- Chemical analysis results for SS202 material shows that the value of chromium decreases slightly after welding and the value of manganese and nickel increases to some extent. It might be because of formation of any compound in the welded region.
- Chemical analysis results for SS304 material shows that there is a slight increase in the composition of manganese after welding whereas there is decrease in the composition of chromium and nickel after welding.
- Use of pure helium and a mixture of argon-helium has resulted in increasing the welding speed by 27% and 12.5% approximately in comparison to that of pure argon which is quite significant.
- SS202 being quite cheaper as compared to SS304 may be used for frames and covering portion various machines and containers.

11.1. FUTURE SCOPE

Following are some of the future recommendations:

- Effect of hydrogen has been studied by many researchers on various grades of steels. Same may also be carried out for SS202 grade.
- Welding speed may be an important parameter in GTAW process and may be studied in fully/semi automatic TIG welding machines.
- Effect of different grades of filler wire on the mechanical properties and chemical composition of welded joints may be carried out.
- Shielding gas composition may be carried to study its effect on various properties of the steel.
- Tensile test, bending and reverse bending test etc. may also be carried along with other non-destructive tests like radiography, ultrasonic testing etc.
- Microstructure analysis may be carried on the welded joints by using SEM, XRD etc. to study the various grains.

CHAPTER – 12

REFERENCES

[1] "A Course in Workshop Technology", B.S.Raghuwanshi, Dhanpat Rai & Co.2008 Editon.

[2] http://en.wikipedia.org/wiki/Gas_tungsten_arc_welding.

[3] "A Text book of Welding Technology", O.P.Khanna, Dhanpat Rai Publications, Edition 2005.

[4] "Welding processes and technology", R. S. Parmar, Khanna Publishers, ISBN No. 81-7409-126-2.

[5] "Manufacturing Technology", P. N. Rao, Tata mc-graw hill publishers, ISBN-1: 978-0-07-008798-9.

[6] "Welding Technology & Design", V.M. Radhakrishnan, New Age International publishers, ISBN: 81-224-1672-1.

[7] http://www.chasealloys.co.uk/steel/alloying-elements-in-steel/, downloaded on Dated-May 13, 2012.

[8] Kumar S. and Shahi A.S. (2011) "Effect of heat input on the microstructure and mechanical properties of gas tungsten arc welded AISI 304 stainless steel joints", Materials and Design, vol. 32, pp. 3617-3623.

[9] Choi B.H. and Choi B.K. (2008) "The effect of welding conditions according to mechanical properties of pure titanium", Journal of Materials Processing Technology", vol.201, pp. 526-530.

[10] Sivashanmugam M., Shanmugam C., Kumar. T and Kumar M. (2010), "Investigation of Microstructure and Mechanical properties of GTAW and GMAW Joints on AA7075 Aluminum Alloy", IEEE (978-1-4244-9082-0), pp. 241-246.

[11] Wang Q., Sun D. L., Na Y., Zhou Y., Han X. L., Wang J. (2011), "Effects of TIG welding parameters on Morphology and Mechanical properties of welded joint of Ni-base Superalloy", Procedia Engineering, vol.10, pp. 37-41.

[12] Gulnec B., Develi K., Kahraman N., Durgutlu A. (2005), "Experimental study of the effect of hydrogen in argon as a shielding gas in MIG welding of austenitic stainless steel", International Journal of Hydrogen Energy, vol. 30, pp. 1475-1481.

[13] Bang Hee Seon, Bang Han Sur, Kim You chul and Oh Ik Hyun (2011), "A study on mechanical and microstructure characteristics of the STS304L butt joints using hybrid CO_2 laser-gas metal arc welding", Materials and Design, vol.32, pp. 2328-2333.

[14] Cao R., Zhu S.S., Feng W., Peng Y., Jiang F., DU W.S., Tian Z.L. and Chen J.H. (2011), " Effects of weld metal property and fraction on the toughness of welding joints of a 8% Ni 980 MPa high strength steel", Journal of Materials Processing Technology, vol. 211, pp. 759-772.

[15] Chenbin Li & Liming Liu (2012), "Investigation on weldability of magnesium alloy thin sheet T-joints: arc welding, laser welding, and laser-arc hybrid welding", International Journal of Advanced Manufacturing Technology, ref. no. DOI 10.1007/s00170-012-4145-9.

[16] Balasubramanian V., Ravisankar V. and Reddy G. Madhusudhan (2008), "Effect of pulsed current welding on mechanical properties of high strength aluminum alloy", International Journal of Advanced Manufacturing Technology, vol. 36, pp. 254-262.

[17] Lakshminarayanan A. K., Balasubramanian V. and Elangovan K. (2009), "Effect of welding processes on tensile properties of AA6061 aluminium alloy joints", International Journal of Advanced Manufacturing Technology, vol. 40, pp. 286-296.

[18] Lee Hwa Teng, Chen Chun Te, Wu Jia Lin (2010), "Numerical and experimental investigation into effect of temperature field on sensitization of Alloy 690 butt welds fabricated

by gas tungsten arc welding and laser beam welding", Journal of materials processing Technology, vol. 210, pp. 1636-1645.

[19] Durgutlu Ahmet (2004) "Experimental investigation of the effect of hydrogen in argon as a shielding gas on TIG welding of austenitic stainless steel", Materials and Design, vol. 25, pp. 19–23.

[20] Sittichai K., Santirat N., and Sompong P. (2012), "A Study of Gas Metal Arc Welding Affecting Mechanical Properties of Austenitic Stainless Steel AISI 304", World Academy of Science, Engineering and Technology, vol. 61, pp. 402-405.

[21] Kumar T. Senthil, Balasubramanian V., Sanavullah M.Y. (2007), "Influences of pulsed current tungsten inert gas welding parameters on the tensile properties of AA 6061 aluminium alloy", Materials and Design, vol. 28, pp. 2080–2092.

[22] Tarng Y.S. and Yang W.H. (1998), "Optimisation of the Weld Bead Geometry in Gas Tungsten Arc Welding by the Taguchi Method", International Journal of Advanced Manufacturing Technology, vol. 14, pp. 549-554.

[23] Giridharan P. K. and Murugan N. (2009), "Optimization of pulsed GTA welding process parameters for the welding of AISI 304L stainless steel sheets, International Journal of Advanced Manufacturing Technology, vol. 40, pp. 478-489.

[24] Kumar A. & Sundarrajan S. (2009), "Effect of welding parameters on mechanical properties and optimization of pulsed TIG welding of Al-Mg-Si alloy", International Journal of Advanced Manufacturing Technology, vol. 42, pp. 118-125.

[25] Nakata K., Oishi M., Koshiishi M., Hashimoto T., Anzai H., Saito Y. and Kono W. (2002), "Re-weldability of neutron-irradiated stainless steels studied by multi-pass TIG welding", Journal of Nuclear Materials, vol. 307-311, pp. 1578-1583.

[26] Gharibshahiyan E., Honarbakhsh A.R., Parvin N., Rehimian M. (2011), "The effect of microstructure on hardness and toughness of low carbon welded steel using inert gas welding", Materials and Design, vol. 32, pp. 2042-48.

[27] Lothongkuma G., Chaumbaib P., Bhandhubanyong P. (1999), "TIG pulse welding of 304L austenitic stainless steel in at, vertical and overhead positions", Journal of Materials Processing Technology, vol. 89-90, pp. 410-414.

[28] ASTM standard A-370 – standard testing methods and definitions for mechanical testing of steel products.

[29] http://www.bocworldofwelding.com.au/media/pdf/WELDING%20CONSUMABLES-Stainless%20Steel.pdf

[30] "Welding and welding technology". Richard L Little, Tata McGraw-Hill Publishing Company limited, ISBN: 0-07-099409-9.